In Vitro Synthesis of the Light-Harvesting

Complex into Artificial Membrane Systems

Shaohua Ding

Geb. am 23. August 1982 in V. R. China

Mainz, 2010

Dekan:

1. Berichterstatter:

2. Berichterstatter:

Tag der mündlichen Prüfung: 17. Dezember 2010

Abstract -Zusammenfassung

In green plants, the function of collecting solar energy for photosynthesis is fulfilled by a series of light-harvesting complexes (LHC). The *light-harvesting chlorophyll a/b protein* (LHCP) is synthesized in the cytosol as a precursor (pLHCP), then imported into chloroplasts and assembled into photosynthetic thylakoid membranes. Knowledge about the regulation of the transport processes of LHCP is rather limited. Closely mimicking the *in vivo* situation, cell-free protein expression system is employed in this dissertation to study the reconstitution of LHCP into artificial membranes. The approach starts merely from the genetic information of the protein, so the difficult and time-consuming procedures of protein expression and purification can be avoided. The LHCP encoding gene from *Pisum sativum* was cloned into a cell-free compatible vector system and the protein was expressed in wheat germ extracts. Vesicles or pigment-containing vesicles were prepared with either synthetic lipid or purified plant leaf lipid to mimic cell membranes. LHCP was synthesized in wheat germ extract systems with or without supplemented lipids. The addition of either synthetic or purified plant leaf lipid was found to be beneficial to the general productivity of the expression system. The lipid membrane insertion of the LHCP was investigated by radioactive labelling, protease digestion, and centrifugation assays. The LHCP is partially protected against protease digestion; however the protection is independent from the supplemented lipids.

Lichtsammelkomplexe (light harvesting complexes, LHCs) sind eine Gruppe von Membranproteinen, die das für die Photosynthese benötigte Sonnenlicht absorbieren und die Energie an ein Reaktionszentrum weiterleiten. In der vorliegenden Arbeit wurde das *light-harvesting chlorophyll a/b-binding protein* (LHCP), ein Apoprotein des photosynthetischen Lichtsammlerkomplexes II in Pflanzen, alternativ mittels zellfreier Expression hergestellt und die Insertion in Lipidmembranen untersucht. Im natürlichen zellulären Kontext wird das LHCP als lösliche Vorstufe im Zytosol (precursor LHCP, pLHCP) synthetisiert, in die Chloroplasten transportiert und anschließend in Thylakoidmembranen eingefügt. Die Details und Regularien des

LHCP Transportprozesses sind bisher wenig verstanden. Zelllfreie Proteinexpressionssysteme erlauben eine Nachbildung der *in vivo* Situation und einen mechanistischen Ansatz zur Untersuchung von Transport- und Insertionsprozessen. Ausgehend von der genetischen Information können Proteine direkt mittels Zelllysaten hergestellt werden, so dass die schwierige und zeitaufwendige Prozedur der konventionellen Proteinexpression und -aufreinigung vermieden werden kann. Dazu wurde das LHCP kodierende Gen aus P*isum sativum* in ein für die zellfreie Expression kompatibles Vektorsystem kloniert und das Protein mittels einem zellfreien Expressionsystem basierend auf Weizenkeimen, hergestellt. Um die Umgebung einer natürlichen Zellmembran nachzubilden wurden aus synthetischen Lipide oder aufgereinigten Pflanzenlipiden Vesikel hergestellt. Dabei wurden sowohl reine Vesikel verwendet, als auch Vesikel, die Pigmente enthielten. Die Zugabe von synthetischen oder aufgereinigten Lipiden hatte einen förderlichen Effekt auf die generelle Proteinausbeute. Untersuchungen der Membraninsertion des LHCPs mittels Radioaktivmarkierung, Proteaseverdau und Zentrifugation ergaben eine teilweise Membraninsertion, wobei diese jedoch unabhängig von den zugesetzten Lipiden war.

Abbreviations

Chls	chlorophylls
Chl a	chlorophyll a
Chl b	chlorophyll b
PS	photosystem
LHCII	light-harvesting complex in photosystem II
LHCIIb	major light-harvesting complex in photosystem II
pLHCP	precursor of light-harvesting chlorophyll a/b-binding protein
mLHCP	mature light-harvesting chlorophyll a/b-binding protein
VSV tag	YTDIEMNRLGK derived from the vesicular stomatitis virus glycoprotein
VSV-mLHCP	LHCP with a VSV tag at amino terminus
mLHCP-VSV	LHCP with a VSV tag at carboxy terminus
VSV-pLHCP	pLHCP with a VSV tag at amino terminus
pLHCP-VSV	pLHCP with a VSV tag at carboxy terminus
cpSRP	chloroplast signal recognition particle
PCR	polymerase chain reaction
SPR	surface plasmon resonance
SPFS	surface plasmon field-enhanced fluorescence spectroscopy
SDS-PAGE	sodium dodecyl sulfate polyacrylamide gel electrophoresis
bp	base pair
aa	amino acids
kDa	kilo Dalton
E. Coli	Escherichia coli
RT	room temperature
GFP	green fluorescent protein
DPPG	1,2-dipalmitoyl-sn-glycero-3-phospho-(1'-rac-glycerol)
PG	phosphatidylglycerol
DGDG	digalactosyldiacylglycerol
MGDG	monogalactosyldiacylglycerol
SQDG	sulfoquinovosyl diacylglycerol
SUVs	smalll unilamellar vesicles
GUVs	giant unilamellar vesicles

PDMS	Poly(dimethylsiloxane)
OG	octylglucoside
DM	dodecylmaltoside

Table of Contents

1 Introduction

1.1 Cell-free protein synthesis: the basics

Cell-free protein synthesis (*in vitro* synthesis) refers to protein production *in vitro*, making use of a cell lysate that contains the cellular machinery required for direct protein synthesis from exogenous genetic information. The lysates can be of prokaryotic or eukaryotic origin, depending on specific requirements. Cell-free protein synthesis has become an attractive alternative to the conventional cell culture-based approaches since it offers an easy, open and flexible approach to protein production and analysis.

1.1.1 History and configurations

The principal breakthrough in the development of cell-free protein synthesis systems was made nearly five decades ago by Nirenberg and Matthaei [1]. To date, a number of cell-free expression systems have been successfully prepared and are commercially available. Proteins can be synthesized either from a suitably constructed DNA template using a coupled system that performs *in vitro* transcription and translation in tandem, or from an uncoupled system which requires mRNA produced from native sources or by *in vitro* transcription. The most straightforward configuration for cell-free synthesis is a one-compartment batch reaction. The typical batch reaction times are limited to few hours due to rapid depletion of precursors and accumulation of inhibitory by-products [2]. The consequences are relatively low protein yields. This problem was addressed by the development of different continuous systems [3,4], in which the reaction is separated by a semipermeable membrane into two compartments. One compartment holds the reaction mixture such as the cell free extract, enzymes, and nucleic acids, while the other compartment provides small molecules like NTPs, energy components, and amino acids. With the continuous supply of fresh substrates and removal of reaction by-products, the reaction time can be significantly extended

and the final protein yields can reach up to several milligram per milliliter reaction mixture.

1.1.2 Sources of lysates

Crude cell extract

Although any organism could potentially be used as a source for the preparation of a cell-free protein expression system, in practice, only a few cell-free systems have been developed for *in vitro* protein synthesis. Generally, these systems are derived from cells engaged in a high rate of protein synthesis. The most frequently used cell-free translation systems are based on extracts of *Escherichia coli* (*E. coli*), wheat germ and rabbit reticulocytes [5 - 7]. All are prepared as crude extracts containing the macromolecular components that are required for protein synthesis from exogenous genetic material. In general, the *E. coli*-based systems provide higher yields and more-homogeneous samples suitable for structural studies. The eukaryotic-based systems, although less productive, provide a suitable platform for post-translationally modified proteins for intrinsic reasons.

Recombinant system

Crude cell extracts are not the only source of cell-free expression system. Schmizu et al. [8] developed a system that was entirely reconstituted from purified components required for the *E. coli* translation reaction. Each component exists in the system with known concentration. This flexible system, designated PURE (protein synthesis using recombinant elements), does not contain cell extract and exhibits high translation efficiency with the advantage of easy purification of untagged protein products. Compared to the crude cell extract, which is more like a 'dark box', the PURE system provides a clearly defined environment for controlling and studying protein synthesis process.

The choice of a system should be determined not just by origin but also by the biological nature of protein of interest and the requirements of downstream applications. The protein yields from an *E. coli* based system can be much higher than

eukaryotic-based systems. However, reticulocyte lysate and wheat germ extract systems are more promising platforms for functional studies as well as post-translational modifications once the protein of interest comes from an eukaryotic source.

1.1.3 Advantages over cell-based protein synthesis

Cell-free protein synthesis offers several advantages over traditional cell-based expression methods.

- **Flexibility.** Cell-free systems can produce proteins that are not physiologically tolerated by living cells, for example toxic, proteolytically sensitive or unstable proteins, providing a platform for generation of 'difficult-to-express' proteins. Also cell-free protein synthesis can start directly from PCR fragments or mRNA templates, allowing the possibility of high throughput applications [9].

- **Improved protein productivity**. Since there are no cellular processes going on so virtually all of the resources available in the extract go towards the production of protein of interest. Improvements in translation efficiency have resulted in yields that exceed a milligram of protein per milliliter of reaction mix.

- **Easy adjustment of reaction conditions.** The intrinsic open nature of the cell-free system allows the supplementation of a variety of reagents to the reaction mixture to expand the possibilities of protein engineering. Besides the 20 naturally-occurring amino acids, various kinds of unnatural amino acids can be site-specifically incorporated into a protein structure for designed purposes [10,12]. For example, mild detergents, synthetic or natural lipids can be added to the reaction to provide a suitable hydrophobic environment for the nascent membrane proteins. Chaperones can be added to aid protein correct folding and post-translational modifications.

1.1.4 Cell-free production of membrane proteins

One of the greatest and potentially most far-reaching impacts of cell-free protein synthesis could be in the area of membrane protein production [11]. Over-expression of membrane proteins *in vivo* frequently results in cell toxicity, protein aggregation and misfolding. Also the low expression levels and tedious isolation and purification procedures hampered the functional and structural analysis of this class of proteins. *In vitro* translation offers promising new perspectives for the efficient production of membranes proteins.

Figure 1.1 shows the versatility of cell-free expression of membrane proteins. A typical cell-free reaction system is normally devoid of meaningful amounts of membranes or lipids as most membrane fragments from cell lysates have been removed during centrifugation steps. The virtual absence of substantial amounts of hydrophobic environments promotes precipitation of membrane proteins (mode a). In contrast to proteins present in inclusion bodies, the precipitates generated by cell-free synthesis can be effectively solubilized with mild detergents by gentle shaking for few hours [12].
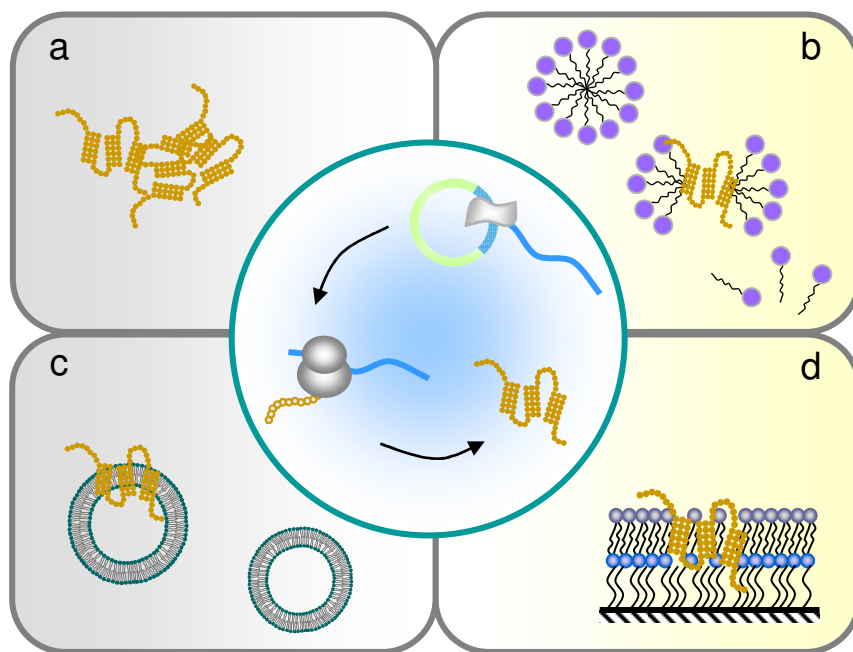

Figure 1.1 Different modes of cell-free production of membrane proteins. Membrane proteins can be expressed in cell-free systems as precipitates (a), detergent-solubilized proteins (b), in the presence of microsomal fractions or defined lipid vesicles (c), or directly into tethered lipid bilayers. Center, *in vitro* transcription and translation.

The open nature of cell-free systems allows the direct supply of artificial hydrophobic environments to the reaction mixture to prevent the precipitation of the synthesized membrane proteins. The addition of certain commonly used detergents (mode b) to the system can notably ease protein insolubility issues and does not apparently inhibit expression efficiency [13]. But the detergents have to be selected in an empirical procedure concerning the critical micelle concentration (CMC) and type of detergents. The protein-micelle complex is formed mainly based on the nonspecific hydrophobic interactions and does not require complex translocation machineries. The major shortcoming of the use of detergents to solubilize membrane proteins is the uncertainty of how micelle structures mimic the natural membrane protein environment [14,15].

The incorporation of membrane proteins into native-like bilayer would extend the accuracy and facility of structural and functional analysis without interference by any other membrane components. Conventionally this can be done with proteoliposomes, formed by reassembly of solubilized or purified membrane protein with liposomes. This reconstitution method is time-consuming and it is difficult to control the directionality of the membrane proteins in the proteoliposomes. Alternatively, the incorporation of membrane proteins into liposomes can be approached by providing the cell-free reaction mixture with either microsomal fractions from lysed cells or preformed liposomes composed of defined lipids or lipid mixtures [16-18] (mode c). In this way problems are circumvented that arise during conventional proteoliposome preparation. Lipid or lipid mixtures are tolerated by cell-free systems at high concentrations and even has slightly beneficial effects on the general expression efficiency [12]. Since the protein synthesis machinery is only present outside of the vesicles, a prevalent inside-out orientation of the membrane protein within the lipid bilayer is expected [16]. The size of the lipid vesicles can vary from the nanometer scale up to micrometer scale. Giant vesicles are also favored as model membranes because protein insertion into the membranes can be directly visualized by optical microscope [19, 20]. Another approach to introduce lipids into cell-free reaction mixture is the so called 'natural swelling method', in which the lipid films are rehydrated directly with the reaction mixture. During incubation, protein synthesis and liposome formation were performed in parallel [21]. In this system, proteins are synthesized probably both inside and outside of the liposomes. Considering the

volume of the formed vesicles, protein synthesis should locate predominantly outside the vesicles.

Robelek et al. [22] present a strategy to perform the *in vitro* reaction in the presence of a solid-supported lipid bilayer (mode d). Vectorial protein insertion into the membrane was verified by immunolabeling in combination with the method of surface plasmon enhanced fluorescence spectroscopy (refer to section 2.4.3). To date, only a handful of membrane proteins have been successfully synthesized *in vitro* and directly integrated into artificial membranes. Without the supplement of required translocation machineries governing the insertion of membrane proteins into membranes, translocation of the synthesized proteins might still be hindered as observed in living cells.

1.2   Protein of interest

1.2.1 Light-harvesting chlorophyll a/b-binding protein

Photosynthesis is the beginning of energy flows and food chains in the living nature. The starting point for the whole photosynthetic process is the capture of sunlight. In green plants, the function of collecting solar energy is fulfilled by a series of light-harvesting complexes (LHC) in the thylakoid membranes of chloroplasts. The most abundant of these pigment-protein complexes is the major light-harvesting chlorophyll a/b complex of photosystem (PS) II (LHCIIb) in chloroplasts, existing as trimers and binding almost 50% of the thylakoid chlorophyll molecules [23].

1.2.2 Structure and functionality

LHCIIb is one of the few membrane proteins for which a high-resolution structure is known (Figure 1.2) [24-26]. The apoprotein, light-harvesting chlorophyll a/b-binding protein (LHCP), contains three transmembrane α-helices. Usually 13-15 chlorophyll a (Chla) and chlorophyll b (Chlb), together with 3-4 carotenoids noncovalently bind to

the protein. The three α-helices serve as a scaffold for packing the pigments into a small volume for efficient energy transfer between the pigments. The chlorophylls are attached to the polypeptide by coordination of the central magnesium atom to polar amino acid side chain or to the main chain carbonyls in the hydrophobic interior of the complex [24]. The N-terminus of mature LHCII is on the stromal side of the thylakoid membrane, while the C-terminus is on the luminal side. The main role of LHCIIb is the absorption and transfer of solar energy to the reaction center. It has also been found to keep the energy balance between PSI and PSII under different light conditions [27], and to maintain the stacking structure of grana [28]. Also LHCIIb is important in the photoprotection of PSII by dissipating excess energy under light stress conditions [26].
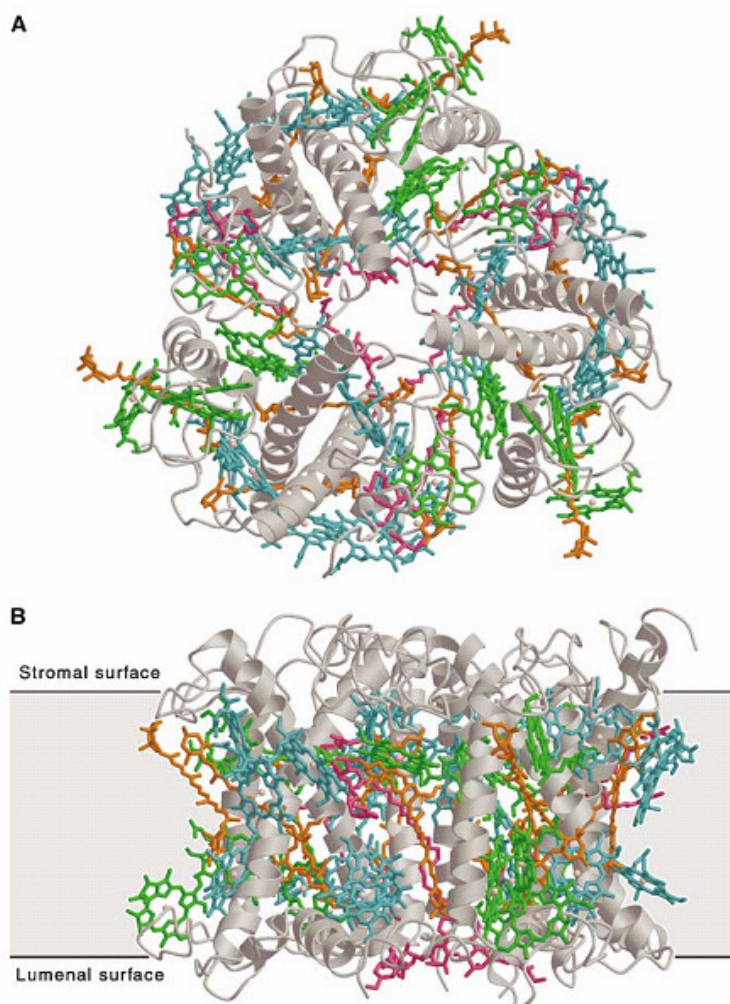

Figure 1.2 The LHC-II trimer. (A) top view from stromal side; (B) side view. LHC-II protrudes from a 35 Å lipid bilayer (black lines) by 13 Å on the stromal side and by 8 Å on the lumenal side. Grey, polypeptide; cyan, Chl a; green, Chl b; orange, carotenoids; pink, lipids [26].

1.2.3 Biogenesis

The chloroplast, best known as the site of photosynthesis, performs a variety of biochemical functions within plant cells. To fulfill these various functions, the chloroplast is equipped with roughly 3000 proteins [29]. Although the chloroplast possesses its own genome, it encodes only a small proportion of the plastid proteins and over 90% of the proteins present in mature chloroplasts are encoded on nuclear DNA, translated in the cytosol [30-32]. The chloroplast is a complex double-membrane organelle that comprises six distinct suborganellar compartments (Figure 1.3). They are three different membranes, namely the outer and inner envelope membranes and the internal thylakoid membrane; three discrete aqueous compartments, namely the intermembrane space of the envelope, the stroma and the thylakoid lumen. Consequently, coordinated and reliable protein transport routes are required to direct these proteins to their final destinations within chloroplasts.
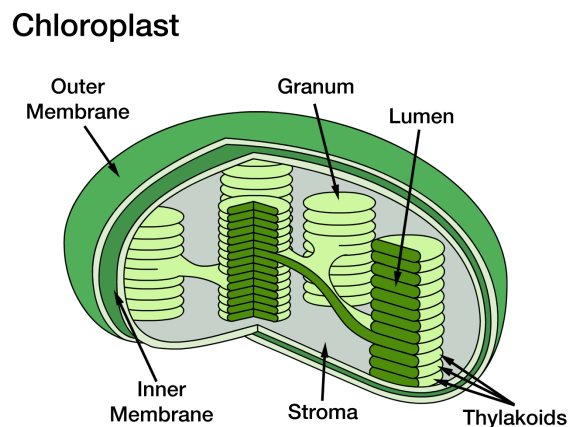

Figure 1.3 The six compartments of chloroplasts: the outer and inner membranes, thylakoid membrane, the aqueous intermembrane space, stroma and thylakoid lumen.

Figure 1.4 shows an overview of the protein import and routing systems of chloroplasts [33]. The first stage for protein transport to the chloroplast is common to all routes. Proteins to be imported into chloroplasts are synthesized in the cytoplasm as precursors or preproteins – each carrying a transit peptide at the amino-terminus (blue bars), which is responsible for directing the precursor across the two chloroplast envelope membranes. Translocation across the chloroplast envelop is medicated by the

Toc/Tic translocase and is energy-dependent. Upon arrival in the stroma, the transit peptide is proteolytically removed and the protein may assume its final conformation or be further targeted to the thylakoids by different pathways.

The photosystem components reside in the thylakoid membranes. After the import into the chloroplasts as described above, the proteins will be further directed to the thylakoids, whose targeting information resides within the mature protein. In the stroma, the chloroplast signal recognition particle (cpSRP), composed of cpSRP54 and cpSRP43 interacts with imported LHCP to form a soluble intermediate termed 'transit complex'. Integration of LHCP into thylakoid membrane also involves GTP, cpFtsY (the chloroplast homolog of the bacterial SRP receptor) and the integral membrane protein Albino3 (Alb3) [34]. This insertion process occurs in a poorly-known way.
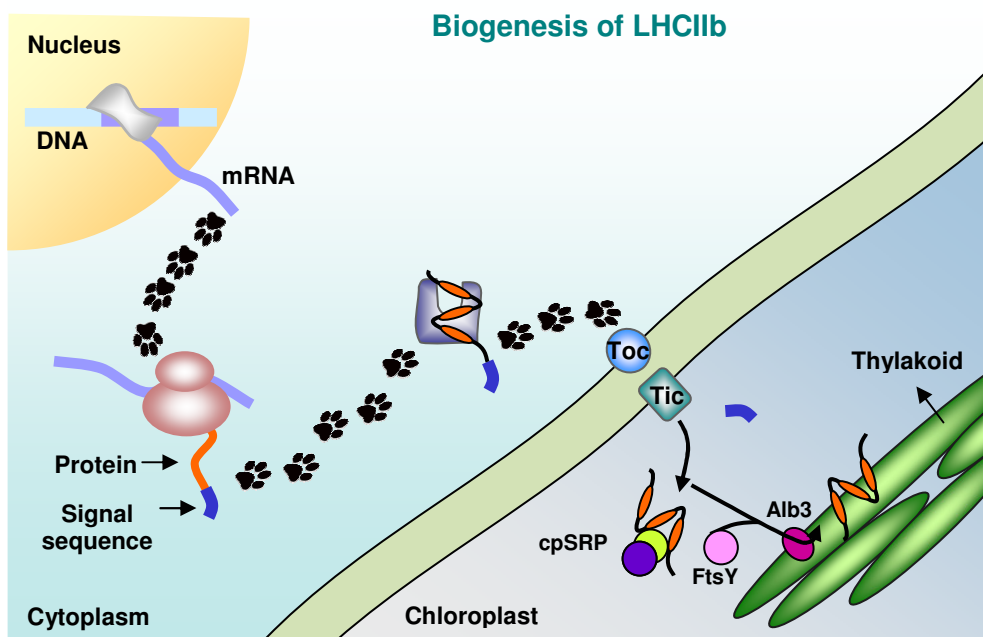
Figure 1.4 Pathways for targeting nuclear-encoded LHCP into thylakoid membranes. The LHCII apoproteins are encoded by nuclear multigene families and cytoplasmically synthesized as soluble precursors that are post-translationally imported into the thylakoid membranes.

1.2.4 *In vitro* reconstitution

In vitro reconstitution is one of the most fundamental and powerful tools to investigate pigment-protein complexes. The method enables the analysis of biogenesis, functions and pigment-protein associations of LHC. Several approaches have been described to assemble structurally and functionally authentic LHCII *in vitro*.

The first *in vitro* reconstitution of LHCII was achieved by Plumley et al [35] using proteins and pigments that were both extracted from pea thylakoids. The method consisted basically of repeated freezing and thawing the pigment-protein mixture in the presence of lithium dodecyl sulfate (LDS), yielding pigment-protein complexes biochemically and spectroscopically similar to the isolated native complexes.

Later on methods were developed to refold LHCII from isolated pigments and recombinant proteins over-expressed in *E. coli* [36]. The assembly is triggered by mixing the recombinant apoprotein solubilized in the ionic detergent dodecyl sulfate with a non-ionic detergent solution of the pigments (Chls and carotenoids). The spontaneous self-organization process can be easily monitored by time-resolved fluorescence spectroscopy using Chls as built-in fluorescence labels. It has been suggested that Chl binding during the assembly happens in two kinetic phases [37], such that Chl a binds predominantly during the first phase, whereas Chl b binds during the later slow phase [38]. Random [39] or site-directed mutations [40,41] were introduced into the apoproteins and the mutants were used for the study of specific pigment-binding properties and protein folding mechanism.

Also, another *in vitro* reconstitution assay system, consisting of cell-free translation products and intact plastids, has been used extensively to investigate the pathways of protein transport into or across isolated thylakoid membranes [42,43]. Most studies with these reconstituted assays have used the full precursors produced by *in vitro* translation as substrates. Analyses haven shown that the transport of LHCP into thylakoid membranes is energy-dependent and requires the coordination of cpSRP and thylakoid integral protein Albio3. LHCP failed to accumulate into thylakoid membranes when Alb3 is blocked by its antibody.

1.3 Aim of this work

Membrane protein studies have mostly to be done in a hydrophobic environment. Conventionally, membrane proteins were bacterially expressed and purified, and reconstituted into preteoliposomes by the detergent-mediated method as shown in Figure 1.5 on the left side. Mimicking nature, a more straightforward method was present for the incorporation of membrane proteins into various artificial membrane systems [16-22]. As depicted in Figure 1.5 on the right side, the membrane proteins are expressed in cell-free protein synthesis systems when hydrophobic environment is around. The open nature of cell-free systems allows the direct addition of artificial membranes to the reaction mixture at anytime. The approach starts merely from the genetic information of the protein, so the difficult and time-consuming procedures of protein expression and purification can be avoided.
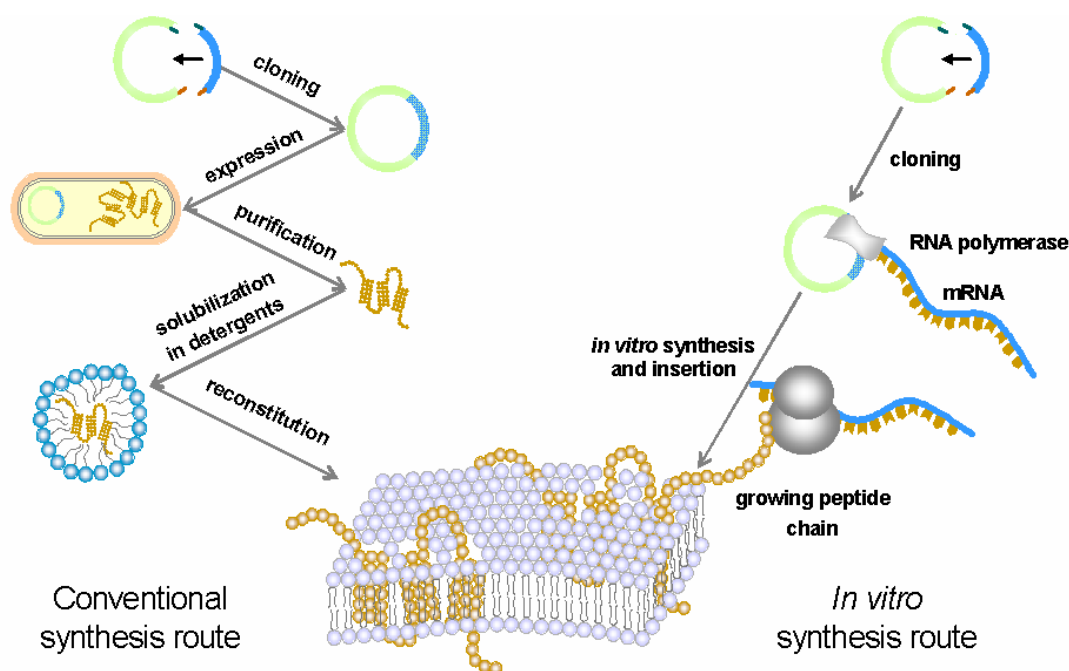
Figure 1.5 Reconstitution of recombinant (left) and cell-free produced membrane proteins (right) into artificial membranes.

In this study, we employed the "*in vitro* synthesis route" as illustrated in Figure 1.5 to study the incorporation of a plant membrane protein into artificial membranes. The main work of the thesis can be divided into following parts:

Plasmid construction. A pea LHCP gene was cloned into a suitable vector backbone for *in vitro* transcription and translation. Three plasmids encoding precursor LHCP and three plasmids encoding mature LHCP were constructed. A commonly used affinity tag was engineered to either amino (N-) or carboxyl (C-) terminus of the protein to facilitate the detection of the protein.

Preparation of artificial membranes. Small unilamellar vesicles and giant unilamellar vesicles prepared from synthetic or isolated plant leaf lipids were used as cell membrane mimics. Chlorophylls were incorporated into the lipid bilayers of both small and giant vesicles prepared from plant lipids. The incorporation of pigments into membranes was characterized by fluorescence microscopy using chlorophylls as built-in fluorescence labels. Biotinylated vesicles were tethered onto gold surface for topological study of proteins in the membranes.

Effect of lipids on cell-free protein synthesis. The addition of small vesicles prepared from either synthetic lipid or purified plant leaf lipid was found to be beneficial to the general productivity of cell-free protein synthesis. The amounts of proteins synthesized in the presence of lipids were promoted to 20%-40% higher than those synthesized in the absence of supplemented lipids. Further increasing the lipid concentration would inhibit the protein expression of the system. Centrifugation assays indicated that the lipid-assisted synthesized proteins formed precipitates in the expression system.

Analysis of *in vitro* translated proteins. Proteins expressed *in vitro* with or without supplemented lipids were treated with thermolysin or trypsin. The digestion products were analyzed by western blotting and autoradiography. The effect of detergents on the digestion products was investigated. The digestion patterns of proteins synthesized in wheat germ extracts and recombinant expression systems were compared.

2 Materials and Methods

2.1 Plasmid construction

To express pLHCP/LHCP in commercial *in vitro* expression systems, we prepared the cDNA of the pLHCP/LHCP equipped with a Kozak consensus sequence and inserted this together with an affinity tag into the expression vector pTNT. Epitope tagging is a widely accepted technique that fuses an epitope peptide to a certain protein as a marker for gene expression [44]. With this technique, gene expression can be easily monitored on western blotting, immunoprecipitation and immunofluorescence utilizing an antibody that recognizes such an epitope. One of the widely used epitope tags is VSV-G [45,46], which represents the amino acid sequence YTDIEMNRLGK derived from the vesicular stomatitis virus glycoprotein. In this work, a VSV tag is engineered onto either the N- or C-terminus of the protein by using recombinant DNA techniques.

2.1.1 pTNT vector backbone

The pTNT[TM] Vector is designed for convenient expression of cloned genes using *in vitro* expression systems [47]. The multiple cloning region is immediately downstream from the T7 and SP6 promoter. Gene of interest is subcloned into restriction sites EcoRI and KpnI.
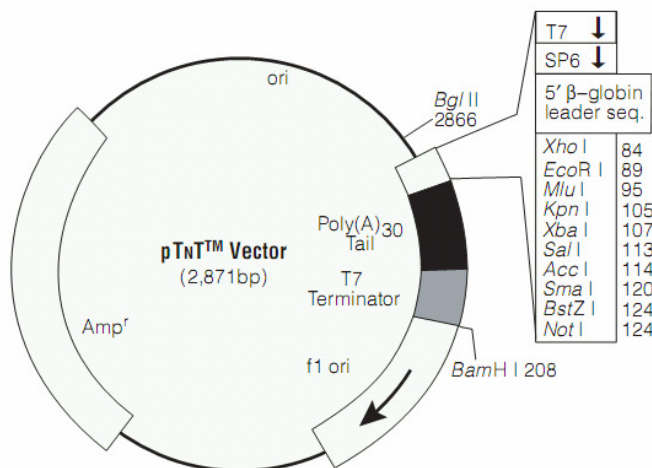
Figure 2.1 pTNT vector circle map [47].

2.1.2 Gene of interest: AB80

AB80 (uniprot accession number: P07371), the gene encoding the entire precursor of an LHCP from *pisum sativum* [48], is 807 base pairs long. The encoded precursor protein – pLHCP is 269 amino acids long, bearing a signal sequence of 36 amino acids at the N-terminus of the protein. Upon arrival into the stroma of chloroplast, the signal sequence is cleaved and the mature protein (mLHCP) is further targeted into the thylakoid membranes. The nucleotide sequence of AB80 and the amino acid sequence of pLHCP are shown in the appendix.

2.1.3 Cloning of AB80 into pTNT vector

2.1.3.1 General cloning procedure

The general cloning procedure is illustrated in Figure 2.2. The construction started out from the plasmid pTZ-AB80-19R, provided by Prof. Harald Paulsen (Universität Mainz). The plasmid harbors the AB80 gene coding for the precursor of pea LHCP. Sequences coding for both pLHCP and mLHCP were amplified by PCR. An EcoRI site and a KpnI site were introduced to the 5' and 3' site of the sequences respectively. In order to prepare tagged protein, coding sequence for the VSV-G tag was also introduced into either upstream or downstream primer. The PCR-amplified products were restricted with *EcoRI* and *KpnI*, and then subcloned into the *EcoRI* and *KpnI* sites of pTNT vector. The Kozak consensus translation initiation sequence, 5'-CCACCATGG-3' [49], was used in place of the ATG start codon to maximize the efficiency of translation in eukaryotic systems. The AB80 gene product is under the control of a T7 promoter, enabling *in vitro* transcription/translation.
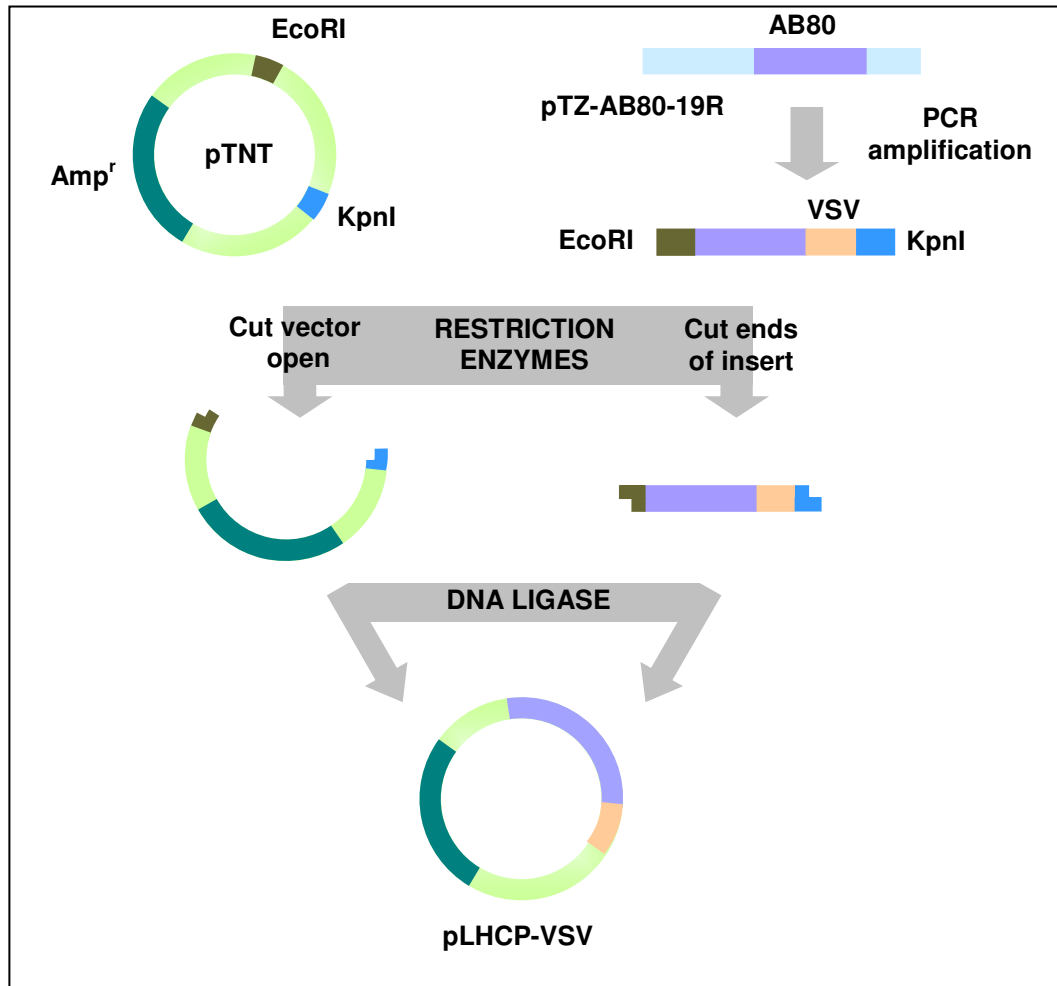
Figure 2.2 Schematic illustration for the construction of LHCP-expression plasmids. AB80, the pea LHCP gene; pLHCP, precursor of light-harvesting chlorophyll a/b-binding protein; Amp[r], ampicillin resistance marker.

2.1.3.2 Primers

Primers used in this study are listed in Tables 2.2-5. EcoRI and KpnI restriction sites are underlined. Kozak sequence is shown in red and sequence coding VSV tag is shown in blue. The primers were purchased from Sigma at a concentration of 100 μM, and were 1:10 diluted with H$_2$O to a final concentration of 10 μM before use. The expected PCR products and their sizes are schematically represented in Table 2.5.

Table 2.1 Forward primers for the construction of pLHCP-expression plasmids.

Name	Orien-tation		Sequence	Total size	3' Homology	Tm* (°C)
	fwd	rev				
P1	✓		ATGGCCGCATCATCATCATC ATCC	24 mer	ATGGCCGCAT CATCATCATC ATCC	62.7
P2	✓		CCGGAATTCATGGCCGCATC ATCATCATCATCC	33 mer	ATGGCCGCAT CATCATCATC ATCC	62.7
P3	✓		CCGGAATTCTTTTTTTTTTA AACCACCATGGCCGCATCAT CATCATCATCC	51 mer	ATGGCCGCAT CATCATCATC ATCC	62.7
P4	✓		CCGGAATTCTTTTTTTTTTA AACCACCATGGGATACACCG ACATCGAGATGAACCGGCTG GGCAAGGCCGCATCATCATC ATCATCCATG	90 mer	GCCGCATCAT CATCATCATC CATG	62.7

*Melting temperature of 3' homology, calculated by MWG Oligo Property Scan (MOPS).

Table 2.2 Forward primers for the construction of LHCP-expression plasmids.

Name	Orien-tation		Sequence	Total size	3' Homology	Tm (°C)
	fwd	rev				
M1	✓		ATGAGGAAGTCTGCTACCAC CAAG	24 mer	ATGAGGAAGT CTGCTACCAC CAAG	62.7
M2	✓		CCGGAATTCATGAGGAAGTC TGCTACCACCAAG	33 mer	ATGAGGAAGT CTGCTACCAC CAAG	62.7
M3	✓		CCGGAATTCTTTTTTTTTTA AACCACCATGGGAAGGAAGT CTGCTACCACCAAGAAAG	58 mer	AGGAAGTCTG CTACCACCAA GAAAG	63.0
M4	✓		CCGGAATTCTTTTTTTTTTA AACCACCATGGGATACACCG ACATCGAGATGAACCGGCTG GGCAAGAGGAAGTCTGCTAC CACCAAGAAAG	91 mer	AGGAAGTCTG CTACCACCAA GAAAG	63.0

Table 2.3 Reverse primers.

Name	Orien-tation		Sequence	Total size	3' Homology	Tm (°C)
	fwd	rev				
R1		✓	TTATTTTCCGGGAACAAAGTTGGTGGC	27 mer	TTATTTTCCGGGAACAAAGTTGGTGGC	63.4
R2		✓	CGGGGTACCTTATTTTCCGGGAACAAAGTTGGTGGC	36 mer	TTATTTTCCGGGAACAAAGTTGGTGGC	63.4
R3		✓	CGGGGTACCTTACTTGCCCAGCCGGTTCATCTCGATGTCGGTGTATTTTCCGGGAACAAAGTTGGTGGCA	70 mer	TTTTCCGGGAACAAAGTTGGTGGCA	63.0

Considering that the long 5' non-complementary sequence of forward primers P4 and M4 might impede the correct PCR amplification, we also designed primers for the 'primary walking' strategy. In the first amplification step, pTZ-AB80-19R was used as DNA template, and the coding sequences for substituting VSV-G tag and a KpnI site were introduced. In the second step, the purified fragments from step 1 were used as template, and the *EcoRI* site and Kozak sequence were introduced (Table 2.5).

Table 2.4 Primers for 'Primer Walking' strategy.

Name	Orien-tation		Sequence	Total size	3' Homology	Tm (°C)
	fwd	rev				
P4W1	✓		TACACCGACATCGAGATGAACCGGCTGGGCAAGGCCGCATCATCATCATCATCCATG	57 mer	GCCGCATCATCATCATCATCCATG	62.7
M4W1	✓		TACACCGACATCGAGATGAACCGGCTGGGCAAGAGGAAGTCTGCTACCACCAAGAAAG	58 mer	AGGAAGTCTGCTACCACCAAGAAAG	63.0
W2	✓		CCGGAATTCTTTTTTTTTTAAACCACCATGGGATACACCGACATCGAGATGAACCG	56 mer	TACACCGACATCGAGATGAACCG	62.4

Table 2.5 Expected PCR fragments. The combinations of forward primers and reverse primers are listed; the expected PCR amplification fragments (F1-10) are shown in colored blocks.

name	fwd/rev	size (bp)	Expected fragments
F1	P1/R1	810	AB80
F2	P2/R2	828	EcoRI — AB80 — KpnI
F3	P3/R2	846	EcoRI — Kozak — AB80 — KpnI
F4	P4/R2	882	EcoRI — Kozak — VSV — AB80 — KpnI
F5	P3/R3	879	EcoRI — Kozak — AB80 — VSV — KpnI

name	fwd/rev	size (bp)	Expected fragments
F6	M1/R1	702	Mature AB80
F7	M2/R2	720	EcoRI — Mature AB80 — KpnI
F8	M3/R2	741	EcoRI — Kozak — Mature AB80 — KpnI
F9	M4/R2	774	EcoRI — Kozak — VSV — Mature AB80 — KpnI
F10	M3/R3	774	EcoRI — Kozak — Mature AB80 — VSV — KpnI

'Primer walking' strategy

Step 1 (DNA template: pTZ-AB80-19R)				
name	fwd	rev	size	Expected fragments
F11	P4W1	R2	849 bp	VSV — AB80 — KpnI
F12	M4W1	R2	741 bp	VSV — Mature AB80 — KpnI
Step 2 (DNA template as indicated)				
F4	W2	R2	882 bp	F4 (fragment 'F11' as DNA template)
F9	W2	R2	774 bp	F9 (fragments 'F12' as DNA template)

2.1.3.3 PCR program

For the first PCR, analytical-scale reactions (20 µL) were set up (Table 2.6) and the amplification fragments were analyzed. Amplification was performed on a thermocycler (Biometra) using the program shown in Table 2.7.

Table 2.6 Assembly of analytical-scale (20 µL) and preparative-scale (3×50 µL) PCR reactions.

Component	Volume (for 20µL reaction)	Volume (for 50-µL reaction)	Final concentration
Nuclease-free H_2O	Add to 20 µL	Add to 50 µL	
5× Phusion HF Buffer	4 µL	10 µL	1×
1 mM dNTPs	4 µL	10 µL	200 µM each
Forward primer (10 µM)	1 µL	2.5 µL	0.5 µM
Reverse primer (10 µM)	1 µL	2.5 µL	0.5 µM
DNA template (pTZ-AB80-19R)	1 µL (4 ng)	2.5 µL (10 ng)	200 µM
Phusion T7 Polymerase	0.2 µL	0.5 µL	0.02 U/µL

Table 2.7 PCR program.

Cycle step	Temperature	Time	Number of cycles
Initial denaturation	98 °C	30 s	1
Denaturation	98 °C	10 s	
Annealing	55 °C	20 s	30
Extension	72 °C	20 s	
Final extension	72 °C 4 °C	10 min Hold	1

The PCR fragments were analyzed with 1% agarose gel/TAE stained with SYBR Safe (Invitrogen). Figure 2.3 shows the result of the first analytical PCR amplification. The expected size of each fragment is labeled below the corresponding band. All of the fragments have the correct sizes except fragment F4, which appears to be smaller than its expected size. As stated above, the 'primary walking' strategy was used to generate

fragment F4. Preparative-scale PCR reactions (3×50 µL) were performed as schemed in Table 2.6 using the same program.
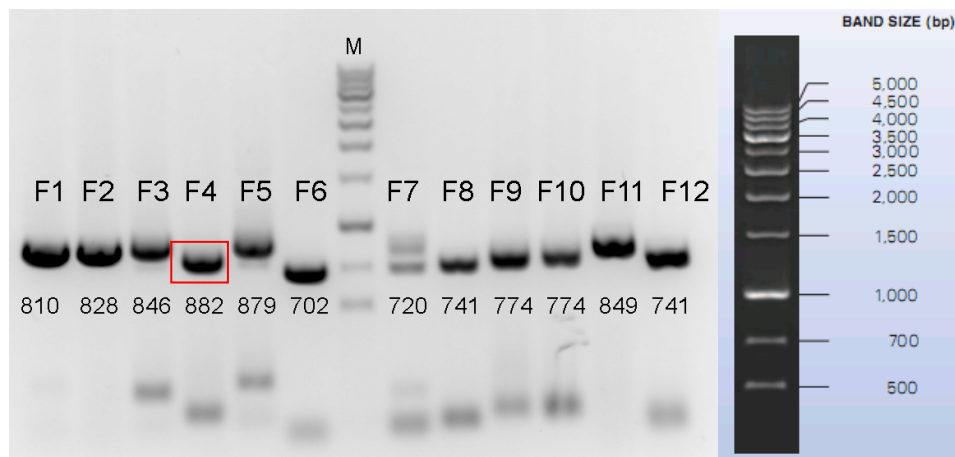
Figure 2.3 Gel electrophoresis of analytical PCR reactions. The names of the fragments and the expected sizes (in base pair) are indicated under the bands. The size of F4 was smaller than expected. The HyperLader III DNA marker is shown in the right (Bioline, BIO-33043).

2.1.3.4 Restriction

The PCR-generated fragments from preparative scale reactions were gel-purified. The recovery of DNA fragments from agarose gel slices was performed with QIAquick PCR Purification Kit (Qiagen, 28104). The pTNT vector and PCR fragments (F2-F5, F7-F10) were sequentially digested with restriction enzymes *EcoRI* and *KpnI* (New England Biolabs) to produce sticky ends. The digestion reactions were incubated at 37 °C for 2 h. The digested fragments were gel-purified.

2.1.3.5 Ligation

The digested pTNT vector and PCR fragments were ligated by Phusion High-Fidelity DNA polymerase (New England Biolabs, F-530S). The molar ratio of insert to vector was set to 3:1. The ligation reactions were incubated at room temperature overnight. The ligation mixture was directly transformed to One Shot TOP10 *E. coli* cells (Invitrogen, C4040-03). After transformation, 50, 100, and 200 µL aliquots were

plated out on selective LB-agar plates (refer to section 2.1.4). The plates were incubated at 37 °C overnight until colonies developed.

2.1.4 Plasmid preparation

Medium

Stock solutions of Ampicillin (50 mg/mL in water) were prepared, sterilized by filtration, aliquoted, and stored at -20°C. Liquid media and solid agar media were prepared according to Table 2.8 and sterilized by autoclaving. The autoclaved medium was cooled to below 50°C before adding heat-sensitive antibiotics. The working concentration of Ampicillin is 100 µg/mL.

Table 2.8 Liquid and solid medium preparation.

LB liquid media	Components per liter	
	Tryptone	10 g
	Yeast extract	5 g
	NaCl	10 g

LB agar	Components per liter	
	Tryptone	10 g
	Yeast extract	5 g
	NaCl	10 g
	Agar (for 1.5% LB agar)	15 g

Bacterial cultures for the plasmid miniprep (1.5 mL) and midiprep (100 mL) were prepared as following:

- A starter culture was prepared by inoculating a single colony from a plate into 2 mL LB medium containing antibiotic. Five different colonies were picked up from each ligation reaction. The culture was incubated at 37 °C for ~8 h with vigorous shaking (~300 rpm).

- The bacterial culture was harvested (keep 200 µL of the culture at 4 °C for starting Midiprep). The plasmid DNA was extracted with QIAprep Spin Miniprep Kit (Qiagen, 27104).

- The extracted DNA was double digested with *EcoRI* and *KpnI*, and analyzed with 1% agarose gels.

- The starter culture (containing plasmids of correct size) was diluted 1/1000 into a larger volume of selective LB medium. The culture was incubated at 37 °C with vigorous shaking (~300 rpm) for 12-16 h. The bacterial culture was harvested and the plasmid DNA was extracted with Qiagen Plasmid Midi Kit (Qiagen, 12143). All of the constructs were verified by DNA sequencing using T7 primer (GENterprise, Mainz, Germany).

2.2 Preparation of vesicles as cell membrane mimics

2.2.1 Lipids

Thylakoid membranes are composed of four major glycerolipid components, among which monogalactosyldiacylglycerol (MGDG) accounts for ~50% of the total lipid content, digalactosyldiacylglycerol (DGDG), ~30%, sulfoquinovosyl diacylglycerol (SQDG), ~5–12%, and phosphatidylglycerol (PG), 5-12% [50]. The structures of the lipids are shown in Figure 2.4 [51]. The three glycolipids comprise more than 90% of thylakoid membrane lipids while PG is the only phospholipids in thylakoid membranes. These lipids support photosynthetic activity by maintaining thylakoid membrane structure or via assembly into photosynthetic machinery. For MGDG and DGDG, the head group is galactose, whereas for SQDG it is sulfoquinovose and for PG it is glycerol phosphate. DGDG is a bilayer-forming lipid, while MGDG is cylindrical and can not be arranged alone in a lamellar structure. It has been demonstrated *in vitro* that association of the two main components of pea thylakoids, the non-bilayer forming lipid MGDG and the chlorophyll-a/b light-harvesting antenna protein of photosysthem II, leads to the formation of large, ordered lamellar structures.

In this study, both synthetic lipid and purified plant leaf lipids were employed to prepare vesicles. Thylakoid lipids, isolated from spinach, were purchased from Lipid Products Company (Redhill, UK). Synthetic DPPG was obtained from Avanti Polar

Lipids (Avanti, 840455). Biotinlated PE (Avanti, 870273) was employed to immobilize vesicles onto gold surfaces (refer to section 2.2.5).
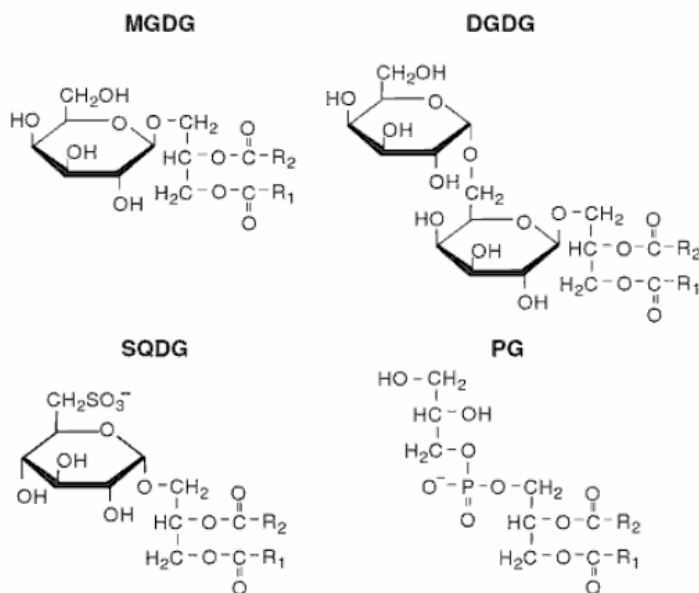
Figure 2.4 Structure of the four major thylakoid glycerolipids [51]. MGDG, monogalactosyldiacylglycerol; DGDG, digalactosyldiacylglycerol; SQDG, sulfoquinovosyl diacylglycerol; PG, phosphatidylglycerol.
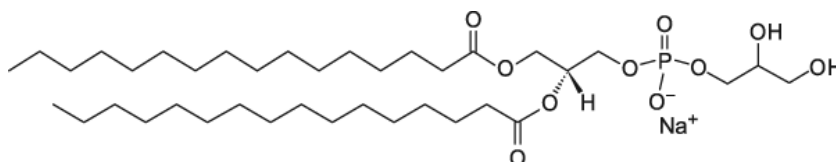
Figure 2.5 Structure of DPPG, 1,2-dipalmitoyl-*sn*-glycero-3-phospho-(1'-*rac*-glycerol) (sodium salt).
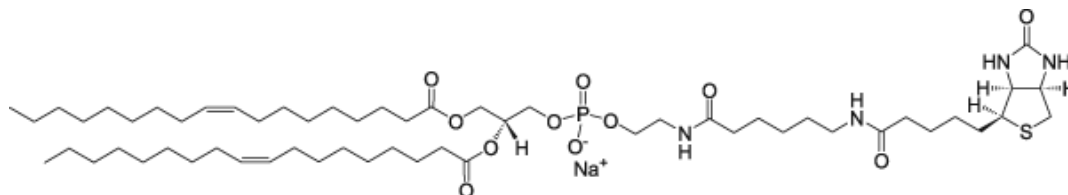
Figure 2.6 Structure of biotinylated PE, 1,2-dioleoyl-*sn*-glycero-3-phosphoethanolamine-N-(cap biotinyl) (sodium salt).

2.2.2 Small unilamellar vesicles

Extrusion technique is used to prepare small unilamellar vesicles (SUVs).

- Thylakod lipid mixture (in chloroform) was dried with a stream of nitrogen and placed in in a desiccator for 2 h to remove residual chloroform.

- The lipid film was hydrated using a suitable buffer, which induces swelling of the film to form multilamellar vesicles (MLVs). Freeze-thaw cycles were repeated five times to break down the MLVs.

- The lipid suspension was passed through a polycarbonate membrane (pore size 50 nm, Avestin Industries) 21 times using the Lipofast extruder (Avestin Industries), to induce SUVs formation. SUVs preparations were stored at 4°C and usually used within 2 days.

Biotinylated SUVs. Phospholipid vesicles were biotinylated by including during their preparation a small amount of phospholipid with biotin covalently attached to the headgroup. Biotin-PE (in chloroform) was added to lipid mixture (in chloroform) to yield 0.3 mol % of biotin-PE. The resulting solution was dried, hydrated and extruded as described above.

DPPG SUVs. The synthetic lipid DPPG has a transition temperature of 41°C. The hydration of the powder was conducted at 70°C for 2 h. The solution was then extruded through 50-nm membrane for 21 times. The size distribution of the as prepared vesicles was characterized with dynamic light scattering.
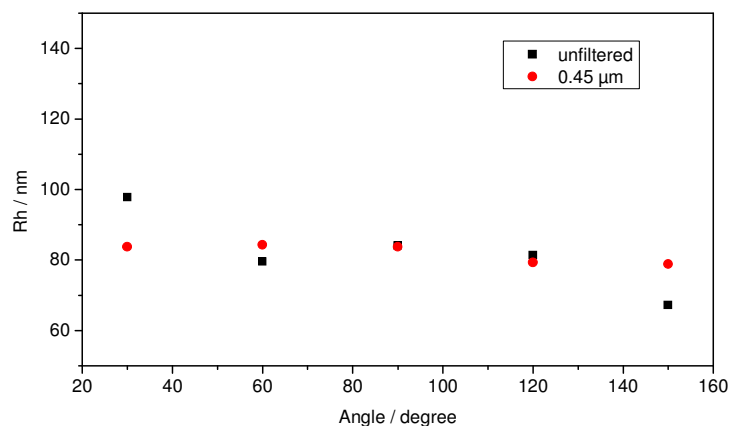
Figure 2.7 Size distribution of DPPG SUVs prepared by extrusion.

2.2.3 Pigment-containing vesicles

Pigment-containing vesicles were prepared by mixing plant lipids and total pigment extracts (provided by Prof. Harald Paulsen, Mainz) in chloroform with a pigment to lipid ratio of 2.5% by molar. The mixture was dried with a stream of nitrogen gas. The dried film was hydrated with Tris-HCl buffer (10 mM NaCl, 10 mM Tris-HCl, pH 7.5) to a final lipid concentration of 1 mg/mL. The mixture was vortexed and sonicated in a water-bath until the cloudiness disappeared. The solution was centrifuged at 14,500 rpm for 15 min on a table-top centrifuge to remove the Chl or Chl/lipid aggregates. Always handle the pigment in the dark or cover the tubes with aluminum foil as pigments are sensitive to light. The vesicles were furthered extruded through 50-nm membrane or directly used for *in vitro* protein synthesis reactions.
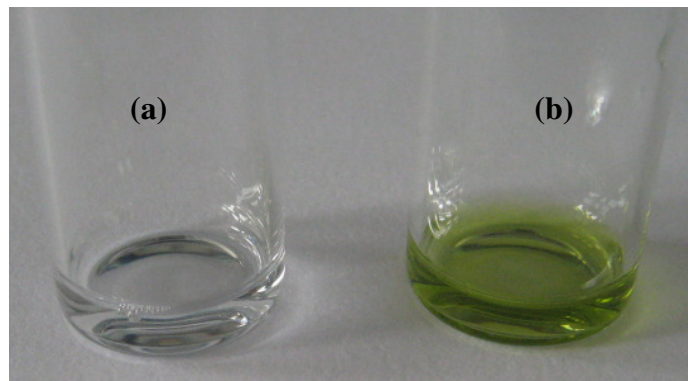
Figure 2.8 Photographic picture of (a) plant PG SUVs and (b) pigment-containing plant PG SUVs prepared by bath sonication.

The physical form of Chl a involved in artificial lipid bilayers has been studied in aqueous dispersions of phosphatidylcholine [52]. These studies suggest that the tetrapyrrole/porphyrin ring of Chl a is located in the polar headgroup layer of the membrane, and the phytol tail is in the hydrophobic core of the hydrocarnon chain of fatty acids. This is compatible with the thermodynamically predicted geography of amphipathic molecules incorporated into the lipid bilayer [53]. The assembly of pigments in the lipid bilayer is schematically illustrated in Figure 2.9. The incorporation of pigments into artificial membranes is further characterized by preparation of pigment-containing giant vesicles. The built-in fluorescence of pigments indicates their successful incorporation into lipid bilayer (refer to chapter 3).
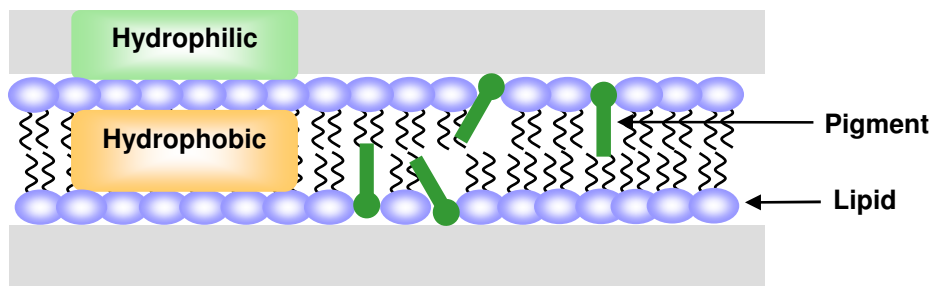
Figure 2.9 Schematic illustration of the assembly of pigments in the artificial lipid membrane.

Figure 2.10 and Figure 2.11 show dynamic light scattering measurement of the pigment-containing PG (PG-Chl) SUVs prepared by bath sonication or first by bath sonication and then extrusion, respectively. The hydrodynamic radius (Rh) of the as prepared PG-Chl vesicles is round 70 nm in both cases. Pigment-containing vesicles prepared by bath sonication were directly used for *in vitro* expression reactions without further extrusion.
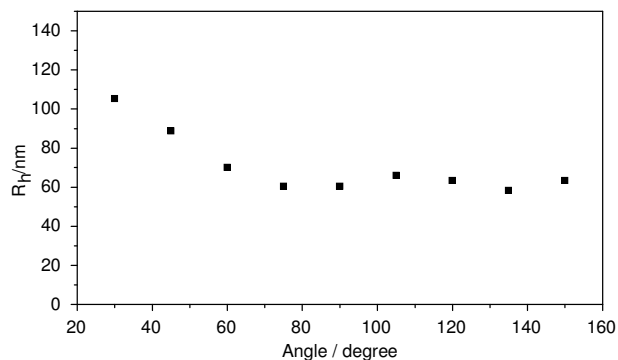
Figure 2.10 Dynamic light scattering. Plant PG-Chl SUVs were prepared by bath sonication, followed by centrifugation to remove aggregates.
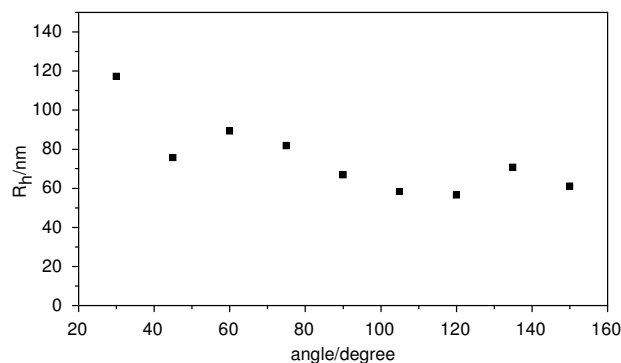
Figure 2.11 Dynamic light scattering. Plant PG-Chl SUVs were prepared by bath sonication, followed by centrifugation at 14,500 rpm for 15 min. The supernatant was extruded through 50 nm-membrane.

2.2.4 Giant vesicles

Giant unilamellar vesicles, or GUVs, have in the past 10 years become extremely attractive systems in the study of membrane model systems, particularly because of their compatibility with optical methods such as light and fluorescence microscopy, and because of the large unperturbed areas of free-standing membranes that they provide [54,55]. Giant unilamellar vesicles (diameter of a few tens of micrometers) are commonly produced by hydration of a dried lipidic film. After addition of the aqueous solution, two major protocols are used: (i) the gentle hydration method where the vesicles spontaneously form and (ii) the electroformation method where an AC electric field is applied. Electroformation is known to improve the rate of unilamellarity of the vesicles though it imposes more restricting conditions for the lipidic composition of the vesicles [56]. This technique allows to form giant vesicles (from 1 to 100 um) in a couple hours with a good yield and few multilamellar ones. It relies on the hydration of dry films of lipids under an oscillating electric field.

Electroformation of GUVs

- The ITO slides (5 cm × 5 cm) were cleaned by 15 min bath sonication in 2% Hellmanex, then 15 min in water and 15 min in absolute ethanol. The slides were dried with nitrogen gas.

- Using a glass syringe apply droplets of the lipid or lipid/pigment solution over an area of about 1 to 2 cm diameter of both ITO slides (typically 50 µL for each slide). The layer must be as thin and as homogeneous as possible. Hence the need for a slow deposition. Vacuum dry the slides for at least 1.5 h to remove all of the chloroform from the film.

- Remove the slides from the desiccator and make a little chamber by placing a PDMS spacer around the lipid area in between the two ITO slides. The gap of the chamber is 1 to 2 mm. Hold the two slides together with binder clips.

- The chamber was filled with ~800 µL sucrose (200 mM) by using a syringe.

- Attach the connector to the chamber. Set the voltage amplitude to 1 V, the driving frequency to 10 Hz for 2 h.

- To detach the vesicles from the surface apply 1 V, 5 Hz for 30 min.

The vesicles were slowly taken out of the chamber using a syringe and kept at 4°C for further use. 5 µL of the prepared vesicles was diluted with 200 µL PBS in a hrdrophobic chamber (ibidi, 80821) for the observation under the microscope.
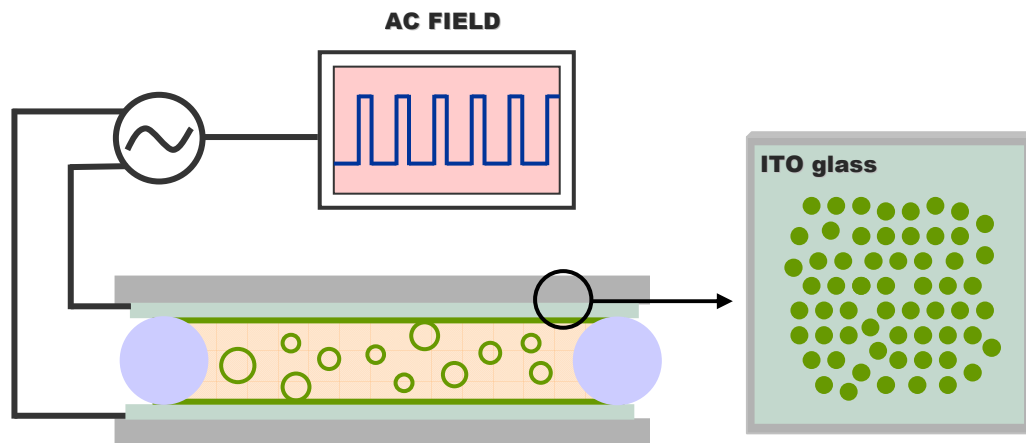
Figure 2.12 A rough sketch of the electroformation chamber. The green coating on the ITO glass represents the lipid film. A PDMS spacer is put around the lipids to form a chamber. Electrical contacts are attached to the conductive substrate on both sides of the chamber filled with 200 mM sucrose.

Spontaneous formation of GUVs

For the spontaneous formation of giant vesicles, the chamber is put in an incubator (Hera Cell) at 30°C for 3 h.

2.2.5 Immobilization of vesicles onto surface

The vesicles were immobilized onto gold or glass surfaces using an immobilization strategy based on the biotin-streptavidin bridge [57-59]. Biotinylated vesicles were prepared as described in section 2.2.2.

Preparation of gold slides

The LaSFN9 glass substrates (Schott, 25×25×2.5 mm, n = 1.85 @ λ = 632.8 nm) were put in the Färber box and cleaned according to the following procedure: Bath sonication in 2% Hellmanex (Hellma GmbH) for 15 min; then the slides were rinsed 15 times with MilliQ water. Put the slides in Bath sonication in 2% Hellmanex for 15 min yet again; Rinse 20 times with MilliQ water; Rinse 2 times with ethanol.

The glass slides were then dried with a stream of nitrogen gas and mounted in the thermal evaporation apparatus (Edwards, FL400) for gold evaporation. A 50 nm gold film was deposited at a rate of ~2 Å/s under vacuum condition (5×10^{-6} mbar). The gold slides were used directly or stored under Argon.

Self-assembled monolayers on gold

Formation of mixed (binary) self-assembled monolayers (SAMs) is a strategy to build sensor surfaces as it has been reported extensively [60,61]. Practically, two different kinds of thiols, with one carrying a functional group, the other with a passive end group, are mixed together before being chemisorbed onto the gold surfaces. In this study, a thiol couple, i.e., a biotinylated thiol and a spacer thiol is utilized for the fabrication of functional SAMs (Figure 2.13). The gold-coated glass substrates were then placed in a mixture of biotinylated thiol and spacer thiol in absolute ethanol and incubated overnight. The molar ratio of biotinylated thiol to passive spacer thiol has been set to 1:9, with a net thiol concentration of 500 µM based on the optimized surface by Spinke et al [60]. The slides were then removed and rinsed thoroughly with absolute ethanol and dried in a N_2 gas stream.
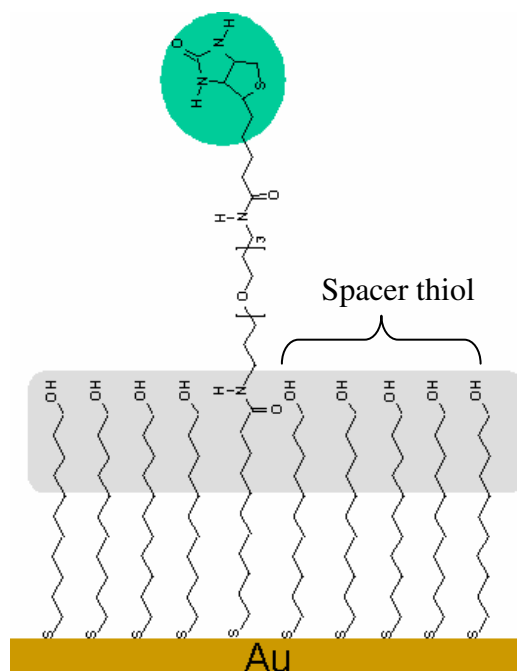
Figure 2.13 Schematic representation of a self-assembled monolayer of biotinylated thiol and spacer thiol. The functional thiol and spacer thiol were mixed in a 1:9 molar ratio, with a net thiol concentration of 500 µM. The biotin group was depicted in a green circle.

Immobilization of biotinylated SUVs onto gold surface. The SAMs-coated gold slide was then mounted to form the flow cell (refer to section 2.4.3). Streptavidin (0.025 mg/mL) in PBS was injected and incubated until the adsorption appeared to reach a saturation coverage of streptavidin. After being rinsed with PBS to remove any physisorbed streptavidin, the biotinylated vesicles were injected and bind to the immobilized streptavidin until equilibrated. A schematic representation of the immobilization technique is shown in Figure 2.14.
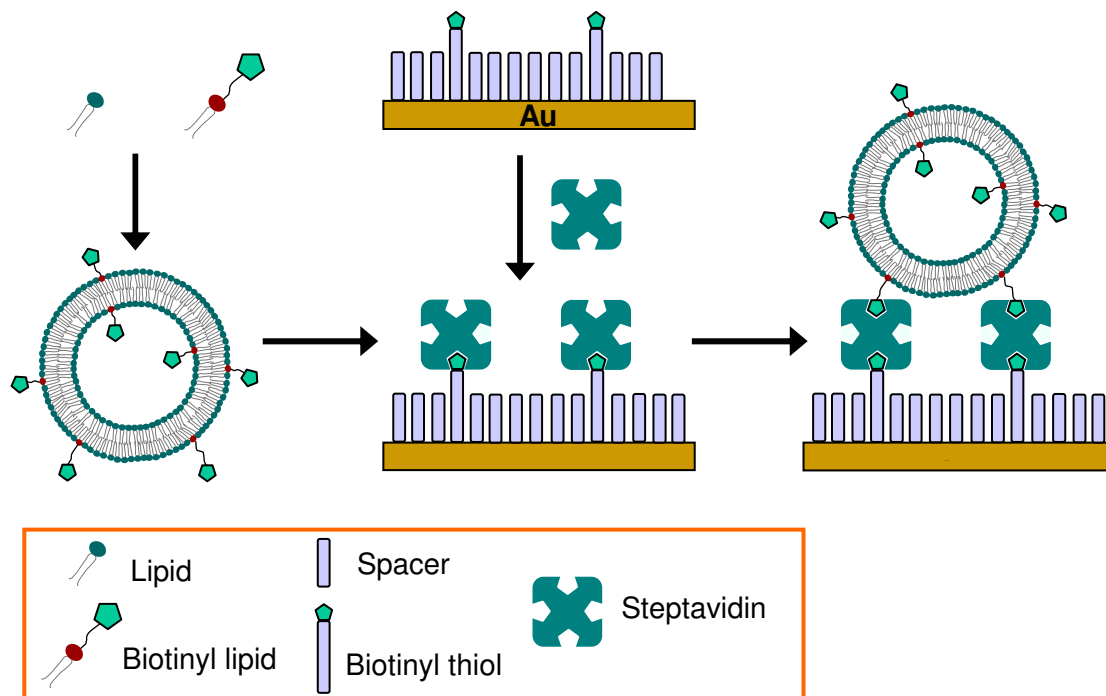
Figure 2.14 The immobilization technique for tethered biotinzlated SUVs onto gold surface. Streptavidin molecules bind to biotin groups on the gold surface. The remaining free pockets of the streptavidin can bind biotinylated SUVs providing a simple and reliable immobilization protocol for vesicles.

Immobilization of biotinylated GUVs onto glass surface

The biotinylated GUVs were immobilized onto glass surfaces via biotin-streptavidin interaction. The cover glass slides (170 +/- 10 µm) were cleaned by first bath sonication in 2% (v/v) Hellmanex for 10 min. The slides were then flushed with MilliQ water for 5 times, and bath-sonicated in MilliQ water for 15 min. Finally the slides were bath-sonicated in methanol for 15 min. The slides were stored in methanol until use.

Poly(dimethylsiloxane) stamps were washed with phosphate-buffered saline. The residual buffer was removed under a nitrogen stream. For printing, the stamps were inked with BSA–biotin (0.1 mg/mL). The stamp was flushed with buffer and the BSA–biotin was then printed onto a clean glass substrate. The stamp was removed from glass slide and mounted to the sticky bottom of sticky-Slide (ibidi, 80828) to form a chamber with a volume of ~800 µL. The substrate was then functionalized by incubation with streptavidin (0.025 mg/mL) for 10 min.

2.3 Assembly of *in vitro* protein synthesis reactions

2.3.1 Coupled wheat germ extract system

In this study, cell-free synthesizing system based on wheat germ extracts (Promega, L4140) was mainly used to carry out protein synthesis, as it provides a homologous system for plant protein LHCP. The open nature of *in vitro* synthesis systems allows the direct addition of lipids and radioactively labeled amino acids (Easytag [^{35}S]-Methionine, PerkinElmer) to the reaction mixture. Typical 50-µL nonradioactive and radioactive reactions were assembled as in Table 2.9.

Table 2.9 Assembly of *in vitro* synthesis using wheat germ extract systems.

	Non-radioactive reactions		Radioactive reactions	
Component	Sample	No DNA control	Sample	No DNA control
Wheat Germ Extract	25 µL	25 µL	25 µL	25 µL
Reaction Buffer	2 µL	2 µL	2 µL	2 µL
Amino acid mixture minus Methionine	0.5 µL	0.5 µL	1 µL	1 µL
Amino acid mixture minus Leucine	0.5 µL	0.5 µL	-	-
[^{35}S]Methionine	-	-	0.5 µL	0.5 µL
RNasin ribonuclease inhibitor (40 U/µL)	1 µL	1 µL	1 µL	1 µL
T7-WG Polymerase	1 µL	1 µL	1 µL	1 µL
Liposomes	x µL	x µL	x µL	x µL
DNA(500 ng/µL, 1µg)	2 µL	-	2 µL	-
RNase-Free H$_2$O to	50 µL	50 µL	50 µL	50 µL
Reactions were incubated at 30°C for 90 min.				

2.3.2 Coupled reticulocyte lysate system

Other than the wheat germ extracts, the reticulocyte lysates (Promega, L1170) and the reconstituted system were also employed for protein synthesis. The digestion patterns of proteins expressed in these different systems were compared.

Table 2.10 Assembly of in vitro synthesis using reticulocyte lysate systems

	Non-radioactive reactions		Radioactive reactions	
Component (Promega, L1170)	Sample	No DNA control	Sample	No DNA control
T7 Quick Master Mix	40 µL	40 µL	40 µL	40 µL
Methionine, 1mM	1 µL	1 µL	-	-
[^{35}S]Methionine	-	-	1 µL	1 µL
Liposomes	x µL	x µL	x µL	x µL
DNA template (500 ng/µL, 1 µg)	2 µL	-	2 µL	-
RNase-Free H$_2$O to	50 µL	50 µL	50 µL	50 µL
Reactions were incubated at 30°C for 90 min.				

2.3.3 Recombinant expression system

The recombinant expression system, PURExpress *in vitro* protein synthesis kit (NEB, E6800S), is based on the PURE system technology originally developed by Shimizu et al [8]. Assemble the reactions on ice in new 0.5 mL-tubes according to Table 2.11.

Table 2.11 Assembly of *in vitro* synthesis using PURExpress system [62].

	Non-radioactive reactions		Radioactive reactions	
Component (NEB, E6800S)	Sample	No DNA control	Sample	No DNA control
Nuclease-free H$_2$O to	25 µL	25 µL	25 µL	25 µL
Solution A	12.5 µL	12.5 µL	12.5 µL	12.5 µL
Solution B	5 µL	5 µL	5 µL	5 µL
[^{35}S]Methionine	1 µL	1 µL	1 µL	1 µL
Vesicles	x µL	x µL	x µL	x µL
DNA template (500 ng/µL, 250 ng)	0.5 µL	-	0.5 µL	-
Reactions were incubated at 37°C for 2 h.				

2.4   Analysis of *in vitro* translated proteins

2.4.1 Western blotting

After *in vitro* translation, the expressed protein was analyzed by SDS-PAGE (sodium dodecyl sulfate-polyacrylamide gel electrophoresis) followed by western blotting or autoradiography (for radiolabeled proteins). The reaction mixture was amenable to direct analysis, with no need for protein precipitation prior to analysis.

(a)   Protein separation by SDS-PAGE

   Materials:

   - Precast gels: NuPAGE Novex 10% Bis-Tris Gel 1.0 mm, 12 well (Invitrogen, NP0302BOX)
   - Protein standards: MagicMark^{TM} XP Western Protein Standard (Invitrogen, LC5602); SeeBlue Plus2 (Invitrogen, LC5925)
   - Running Buffer: NuPAGE MES-SDS Running Buffer (Invitrogen, NP0002)
   - Apparatus: XCell SureLock Mini-Cell Electrophoresis System (Invitrogen)

Table 2.12 Preparation of protein samples for gel electrophoresis

Components	Volume
In vitro reaction mixture	5 µL
10×Sample Reducing Agent (Invitrogen, NP0009)	1 µL
4×LDS Buffer (Invitrogen, NP0008)	2.5 µL
MilliQ H$_2$O	1.5 µL

Samples were heated at 70°C for 10 min. The gel is run at 200 V for 35 min.

(b)   Transfer of proteins to PVDF membrane

Kit: iBlot Gel Transfer Stacks, PVDF Mini (Invtrogen, IB4010-02)

Device: iBlot™ Dry Blotting System (Invitrogen)

At the end of electrophoresis, turn off the power supply, disassemble the gel apparatus, and carefully pry open the two glass plates with a plastic spatula. Using the iBlot Gel Transfer Device to perform dry blotting of proteins as described in the supplied manual.

(c) Immunodetection

Kit: WesternBreeze® Chemiluminescent Kit (Invitrogen, WB7104/WB7106)

The primary antibody used in western blotting detection was monoclonal anti-VSV-G (Roche, 11667351001) against the VSV-G epitope tag or polyclonal anti-LHC against LHCP. Anti-LHC was provided by Prof. Harald Paulsen (Universität Mainz).

Table 2.13 Solutions for PVDF membrane according to manufacturer's protocol.

Blocking Solution	MilliQ H_2O	5 mL
	Blocker / Diluent (Part A)	2 mL
	Blocker / Diluent (Part B)	3 mL
Primary Antibody Diluent	MilliQ H_2O	7 mL
	Blocker/Diluent (Part A)	2 mL
	Blocker/Diluent (Part B)	1 mL
	The primary antibody was diluted into this diluent according to the manufacturer's recommendations.	
Antibody Wash	MilliQ H_2O	150 mL
	Antibody Wash Solution (16x)	10 mL

Procedure was carried according to manufacturer's manual. Chemiluminescent images of western blotting were taken with LAS 3000 Imaging System (Fujifilm).

2.4.2 Autoradiography

Labelling the sample with radioisotope offers the double advantages of specific labelling and extremely sensitive detection [63]. Autoradiography detects the distribution of radioactivity on gels or filters by producing permanent images on photographic film. It is frequently used in a variety of experimental techniques ranging from Southern and Northern blot analysis, to visualization of radioactive protein separated by SDS-PAGE [64]. Autoradiographic images are formed when particles emitted by radioactive isotopes encounter the emulsion of an X-ray film and cause the emission of electrons from silver halide crystals that, in turn, react with positively

charged silver ions, resulting in the precipitation of silver atoms and the formation of an image. ^{3}H, ^{14}C, ^{35}S and ^{32}P isotopes are the most commonly used isotopes for autoradiography. In this study, [^{35}S]-methionine was incorporated into synthesized proteins.

1. Refer to 2.4.1 for protein separation by SDS-PAGE.
2. At the end of electrophoresis, turn off the power supply, disassemble the gel apparatus, and carefully pry open the two glass plates with a plastic spatula.
3. Place the gel into a shallow tray containing a volume of fixing solution () sufficient to cover the gels, and fix for 30 min.
4. After fixation, carefully remove the gel from the tray, and place it onto a wet piece of 3mm Whatman paper, being careful to avoid formation of bubbles and folding of the gel.
5. Carefully cover the gel with plastic wrap, avoiding folding, and then dry the gel in a slab gel vacuum dryer for 2 h at 80°C.
6. When the gel is dry, remove the plastic wrap. In a dark room, place the gel in direct contact with the X-ray film (Kodak BioMax MR Film, 8701302) in a tight Kodak cassette.
7. After expose for an appropriate length of time at room temperature, develop the film using an automatic X-ray processor (Amersham Hyperprocessor).

2.4.3 Surface plasmon resonance spectroscopy

The principle

Surface plasmon resonance (SPR) spectroscopy has been well accepted as an analytical tool for biosensing as well as for characterizing interfaces and thin films [65-67]. Surface plasmons are transverse electromagnetic oscillations along the interface of two media with different reflective index, e.g. a metal and a dielectric. Excitation of surface plasmons by photons requires the use of a coupling medium such as a prism as the propagation constant of a surface plasmon at a metal-dielectric interface is larger than the wave number of the light wave in the dielectric. Figure 2.15 shows a sketch for the prism coupling, also known as Kretschmann configuration. The

coupling wave to excite the surface plasmons is generated by a light wave that passes through a high refractive prism where it is totally reflected at the prism base. The created evanescent wave propagates along the metal-dielectric interface with a propagation constant that can be adjusted to match that of the surface plasmon by tuning the angle of incidence θ. If parallel monochromatic light is used, reflection under certain incident angles is strongly decreased because the surface plasmons adsorb the irradiated energy. Hence the SPR signal can be derived by monitoring the changes of reflectivity R, i.e. the reflected light intensity, scaled to the incoming intensity, as a function of the incident angle θ. The binding interaction at the surface will induce a angle shift, which can be used to calculate the optical thickness of the deposited layer, detect the changes in the local index of refraction. Changes in the reflected intensity are measured as a function of the scattering angle, also, we can monitor real-time by using the kinetic mode, monitoring changes at a fixed angle as a function of time.
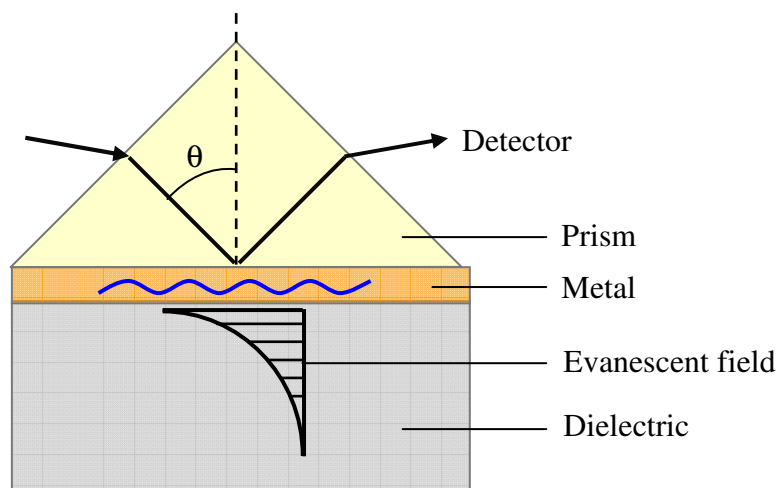
Figure 2.15 Prism coupling sketch.

One of its major advantages is that it allows for real-time, label-free analysis of binding events. Problems arise if only a very diluted lateral packing can be achieved or if very small analytes of low molecular mass are to be detected. The relatively low limit of detection based on the angular shift hinders its further use as a very sensitive technique. As a consequence, fluorescence spectroscopy is combined to SPR by taking advantage of the fact that fluorescent dyes, in close proximity to the metal/dielectric interface, can be excited by the enhanced electromagnetic field [68]. This is the so

called surface-plasmon field-enhanced fluorescence spectroscopy, SPFS. For that, the fluorophores should be placed within the decay length of the evanescent field for excitation, which is typically several tens to hundreds of nanometers for applicable wavelength [68,69].

The setup
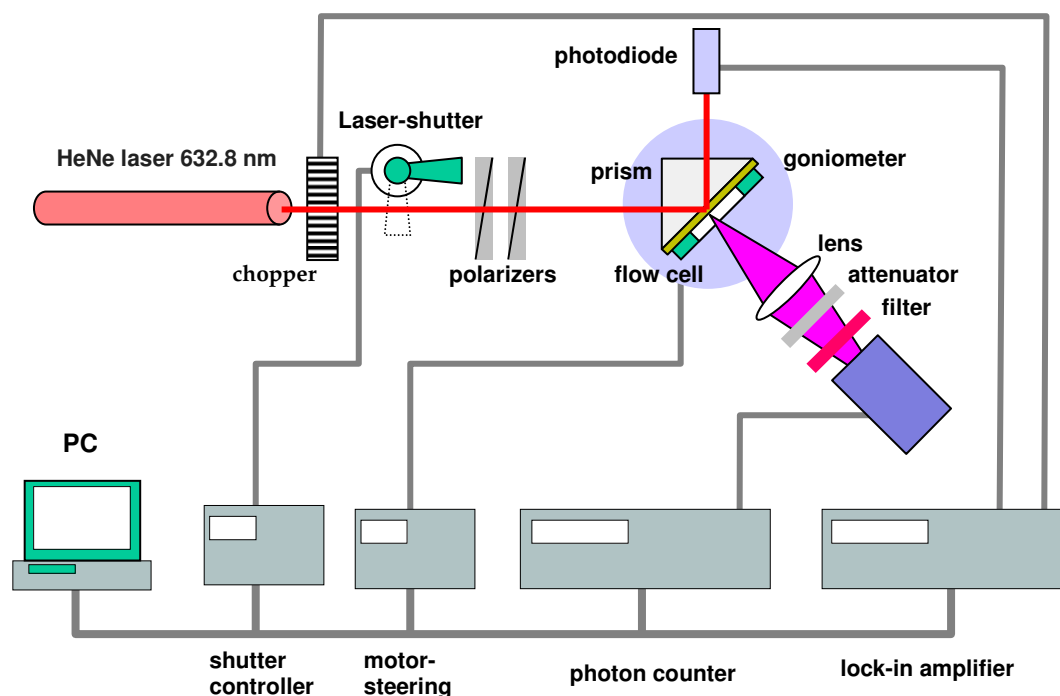
Figure 2.16 Schematic view of the employed SPR/SPFS setup [61].

In this work the immmobilization of vesicles on gold surafce and topological organization of proteins in membranes were studied with a lab-built surface plasmon spectrometer based on the Kretschmann-Reather configuration. The setup is schematically depicted in Figure 2.16. It allows for simultaneous recording of reflectivity and fluorescence intensity. The He/Ne laser beam (Uniphase, 5 mW, $\lambda =$ 632.8 nm) first passes a chopper that is connected to a lock-in amplifier, and then passes two polarizers (for attenuation and polarization, respectively). Next, the beam is reflected at the base of the coupling prism (Schott, LASFN9, n = 1.85 @ 632.8 nm). Coupled to the prism is a gold substrate (see chapter 3.2) index-matched by an immersion oil (n=1.7) with the prism. The reflected light is focused by a lens onto a

photodiode, which is connected to the lock-in amplifier. The prism/sample and the photodiode are mounted on two co-axial goniometers, allowing different operation modes such as an angular scan in a θ-2θ reflection geometry or a kinetic mode at a fixed angle of incidence as a function of time. The fluorescence emission from the sample is focused onto a photomultiplier after passing an interference filter ($\lambda = 670$ nm) that discriminates between excitation and emission wavelength. A programmable shutter is employed to minimize photobleaching of the fluorophore.

Flow cell and liquid handling system

A sketch for the homemade flow cell is shown in Figure 2.17. It consists of a thin polydimethylsiloxane (PDMS) spacer (300 µm in thickness, with a 5 mm × 7 mm ellipse hole in the middle). It is sandwiched in between a quartz slide with two holes and the gold-coated LaSFN9 glass slides. The PDMS O-ring provides a reservoir volume of ~50 µL. Two steel needles are glued to the holes in the quartz slide, serving as inlet and outlet, respectively. The flow cell is connected to a peristaltic pump and the sample tube via Tygon® tubing with an inner diameter of 0.76 mm. Buffer and sample solutions can be manually exchanged. The prism is coupled to the glass by adding one drop of index matching oil in between. Be careful to avoid any air bubbles. The flow cell is then fixed to a holder which then is mounted to the SPR setup for SPR/SPFS measurements.
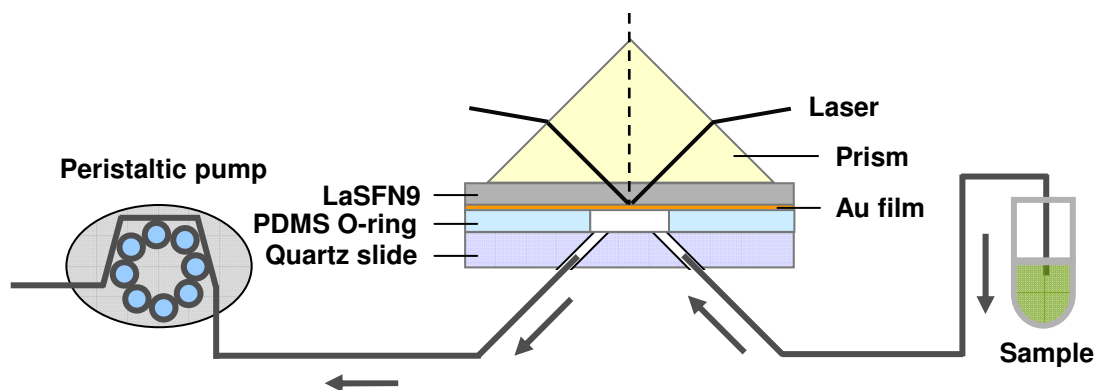
Figure 2.17 Sketch of a home-made flow cell.

3 Results and Discussion

3.1 pLHCP/LHCP-expression plasmids

To express proteins in commercial cell-free expression systems, the gene encoding precursor LHCP or mature LHCP was cloned into a suitable vector backbone as described in section 2.1. The three precursor LHCP-expression plasmids are: pLHCP, encoding precursor LHCP (pLHCP); K-VSV-pLHCP, encoding precursor LHCP carrying a VSV tag at the amino terminus (VSV-pLHCP); K-pLHCP-VSV, encoding precursor LHCP carrying a VSV tag at carboxyl terminus (pLHCP-VSV). The three mature LHCP-expression plasmids are: mLHCP, encoding mature LHCP (mLHCP); K-VSV-mLHCP, encoding mature LHCP carrying a VSV tag at the amino terminus (VSV-mLHCP); K-mLHCP-VSV, encoding mature LHCP carrying a VSV tag at carboxyl terminus (mLHCP-VSV). Each plasmid contains a selection marker Amp^r. The vector NTI maps of the plasmids are shown in the appendix. The nomenclature of the six plasmids is describeded in Table 3.1. K stands for a Kozak sequence being used in place of the ATG start codon. Plasmids constructed for this study and the encoded proteins are schematically represented in Figure 3.1.

Table 3.1 Nomenclature of the constructed plasmids.

Name of plasmid	Encoding protein (pLHCP/mLHCP)	VSV-G tag (VSV)	Kozak sequence (K)
pLHCP	precursor LHCP	No	No
mLHCP	mature LHCP	No	No
K-VSV-pLHCP	precursor LHCP	at N-terminus	Yes
K-pLHCP-VSV	precursor LHCP	at C-terminus	Yes
K-VSV-mLHCP	mature LHCP	at N-terminus	Yes
K-mLHCP-VSV	mature LHCP	at C-terminus	Yes
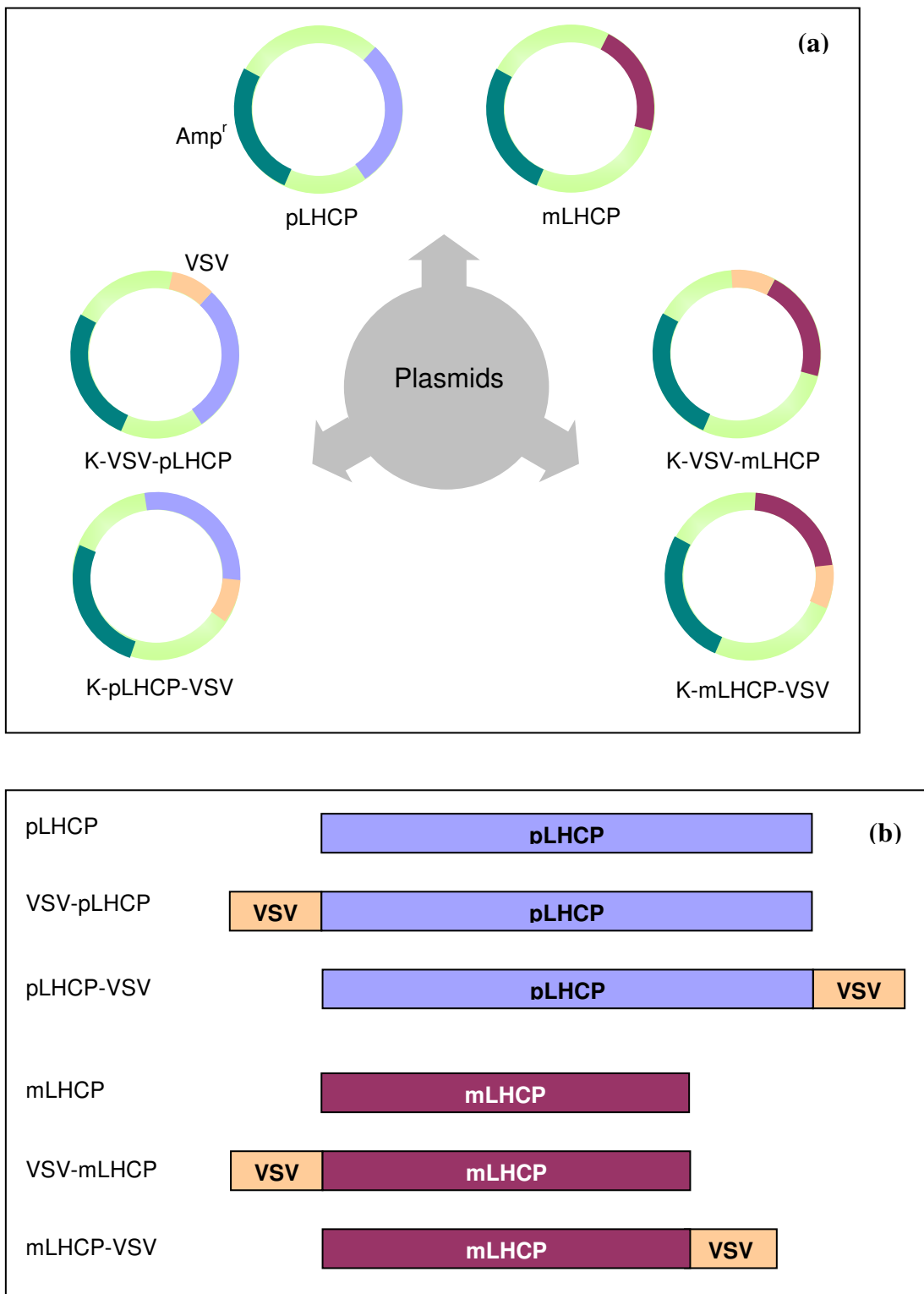
Figure 3.1 Schematic representations of the plasmids constructed for the studies (a) and the encoded proteins (b). pLHCP, precursor of pea LHCP; mLHCP, mature LHCP; K, kozak sequence; VSV, 11 amino acids derived from the vesicular stomatitis virus glycoprotein; Amp^r, ampicillin resistance marker.

3.2   Artificial membranes

The artificial membranes were prepared as cell membrane mimics to provide hydrophobic environment for the nascent membrane proteins. The artificial membranes involved in this study were either small unilamellar vesicles prepared by extrusion or giant vesicles formed by electroformation method or spontaneous swelling. Pigments were incorporated into the lipid bilayers during vesicle preparation, simply by mixing lipid and pigment chloroform solution before the lipid film formation. The small unilamellar vesicles were characterized by dynamic light scattering for their size distribution (refer to section 2.2.2). Giant vesicles were directly observed with optical microscopy. The incorporation of pigments into the lipid bilayer was verified by fluorescence microscopy using the built-in fluorescence of pigments.

3.2.1 Giant vesicles prepared from plant lipids

Giant vesicles were employed as model membranes because protein insertion into the membranes could be directly visualized by optical microscope. Fluorescent tags like green fluorescent protein (GFP) can be fused to the N- or C-terminus of target proteins. The localization of the protein in the membranes can be directly visualized by the built-in fluorescence of GFP [19]. Alternatively, the immunofluorescence technique can be used to detect the presence of target proteins in the membranes. A commonly used tag is placed to either terminus of the protein, and the antibody that recognizes the tag sequence will then be applied to visualize the presence of the target protein.

Both spontaneous swelling method and electroformation method were tried for the preparation of giant vesicles. Vesicles were prepared either from plant lipid PG or from a mixture of DG, MG and PG. Both methods allow the formation of giant vesicles in a couple of hours with a good yield. The microscopy images of the as prepared giant vesicles are shown in Figure 3.2. Giant vesicles were prepared in 200 mM sucrose in order to facilitate observation under microscope. The vesicles formed

from both methods had a broad size distribution, ranging from 1-10 µm in diameter, and were stable up to few weeks when stored at 4°C.
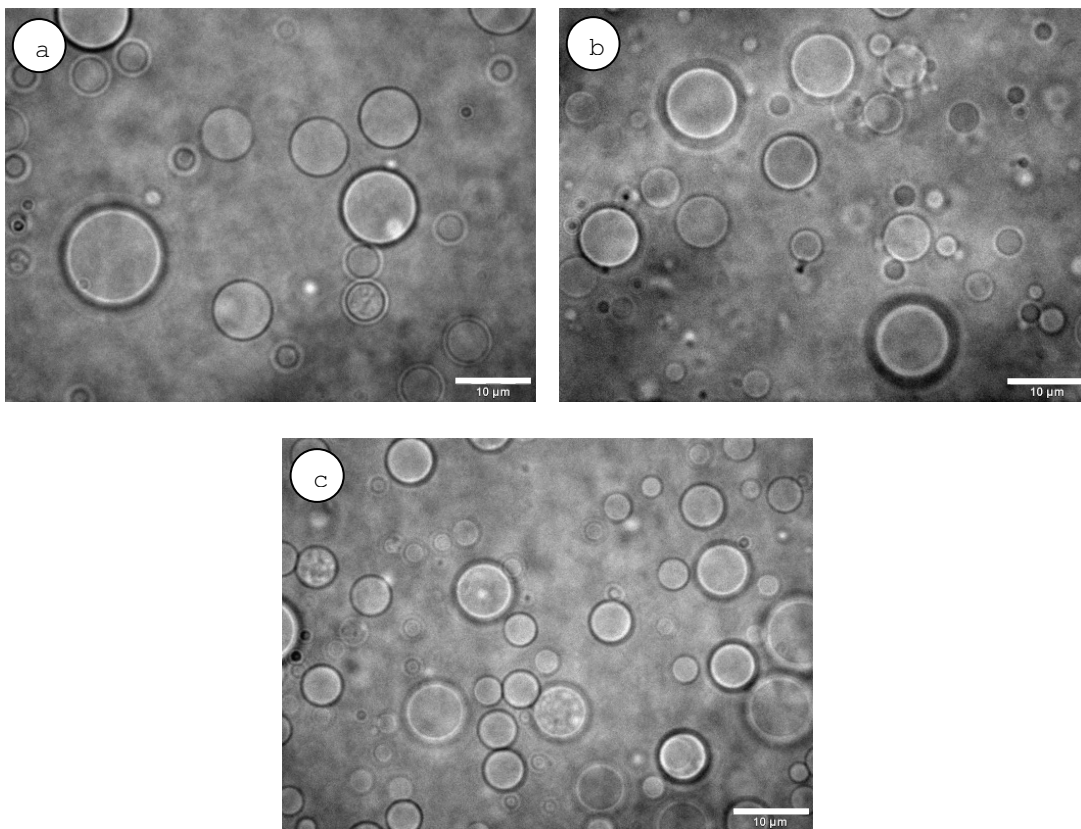
Figure 3.2 Phase contrast microscopy images of giant vesicles prepared from plant lipid PG (a and c), mixture of DG/MG/PG (b, 3:3:4, mol%). Vesicles in (a) and (b) were formed by electroformation method; vesicles in (c) were formed by spontaneous swelling method. Scale bar, 10 µm.

A solid substrate is a well-suited platform for the assembly and characterization of vesicular system down to the single vesicle level [70]. One of the most common specific tethering methods is based on the biological ligation of biotin and streptavidin [57,70]. Biotinylated giant vesicles were prepared as described in section 2.2.2 and attached to glass slides via streptavidin-biotin interaction according to the procedures in 2.2.5. 100 µL of wheat germ reaction mixture without DNA template was incubated on the surface at 30 °C for 90 min. Then the reaction mixture was rinsed away by buffer exchange. After incubation with the wheat germ extracts, the vesicles were mostly fused onto the glass surfaces probably due to the difference of osmotic pressure between the inside and outside of the vesicles. The vesicle were stained with lipophilic

tracer DiD (Invitrogen) for fluorescence microscopy measurement. The microscopy images of the tethered vesicles before and after incubation with wheat germ extracts are shown in Figure 3.3.

As shown in Figure 3.2c, the spontaneous swelling method also can be employed to produce PG giant vesicles. Then we considered using the *in vitro* reaction mixture as the rehydration buffer for the lipid film. During incubation, the vesicles formed in parallel with the synthesis of proteins. In this case, there is supposed to be no difference in osmotic pressure between the inside and outside of the vesicles. The protein synthesis probably takes place both inside and outside of the vesicles. Considering the volume of the formed vesicles, protein synthesis should locate predominantly outside the vesicles. The result is discussed in section 3.6.
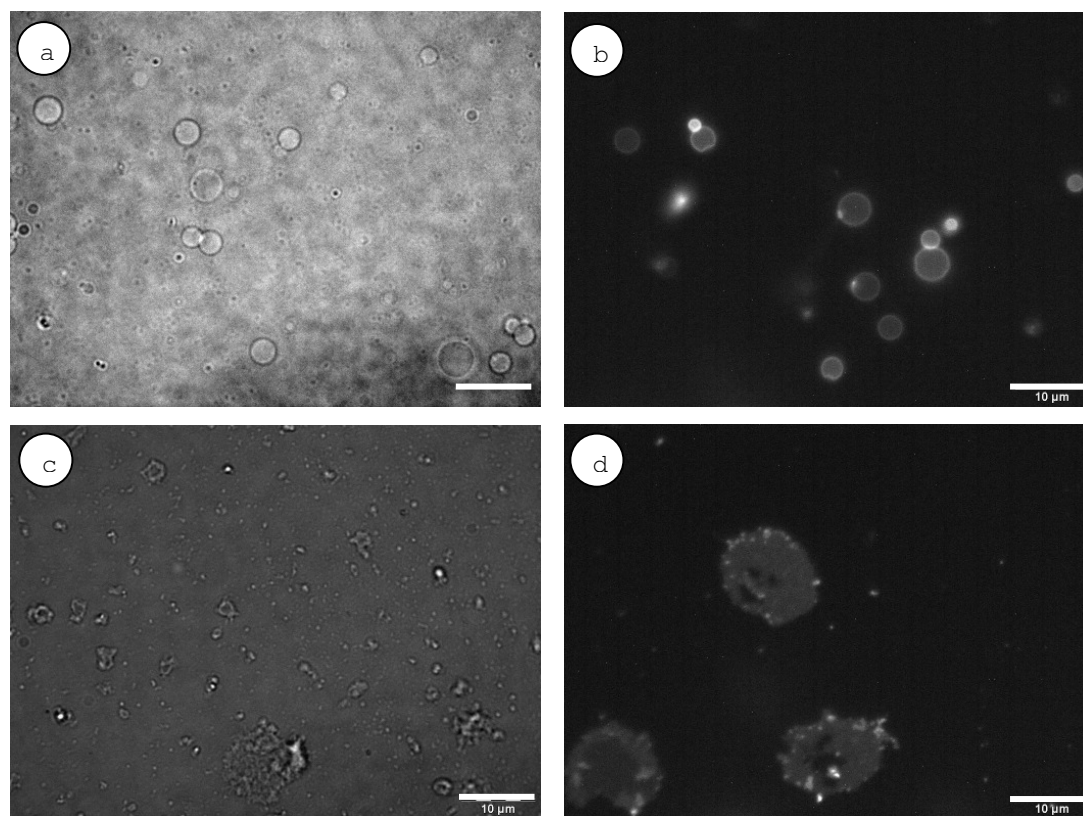
Figure 3.3 Microscopy images of the tethered giant vesicles on the glass slides before (a, b) and after (c, d) incubation with wheat germ extracts. (a) Bright field image of biotylated giant PG vesicles were tethered onto biotinylated glass slides via the streptavidin linker; (b) fluorescence image of the tetherd vesicles; (c) bright filed image of vesicles after incubation with wheat germ extracts; (d) fluorescence image of the giant vesicles fused on surface after incubation with wheat germ extracts. Scale bar, 10 µm.

3.2.2 Pigment-containing giant vesicles

In vivo, the LHCPs are synthesized in their precursor form in the cytoplasm, post-translationally imported into chloroplasts, inserted into the thylakoid membrane and complexed with pigments. The sequence of the later steps is unknown. *In vitro* studies have shown that recombinant LHCP can be inserted into thylakoids and complexed with pigments of other LHCs in the thylakoids. In this study, pigments were supplemented to the cell-free protein synthesis system in the form of pigment-containing vesicles. The total pigment extracts, mainly the lipophilic chlorophylls, were incorporated into the lipid bilayer of both small unilamellar vesicles and giant vesicles. The digital picture and size-distribution of pigment-containing small vesicles prepared by extrusion were shown in section 2.2.3. The microscopy images of pigment-containing giant PG vesicles are shown in Figure 3.4. The morphology of pigment-containing giant vesicles showed no difference to that of the non-pigmented vesicles (Figure 3.2). Both the electroformation method and the spontaneous swelling method can be used to produce the pigment-containing giant vesicles.
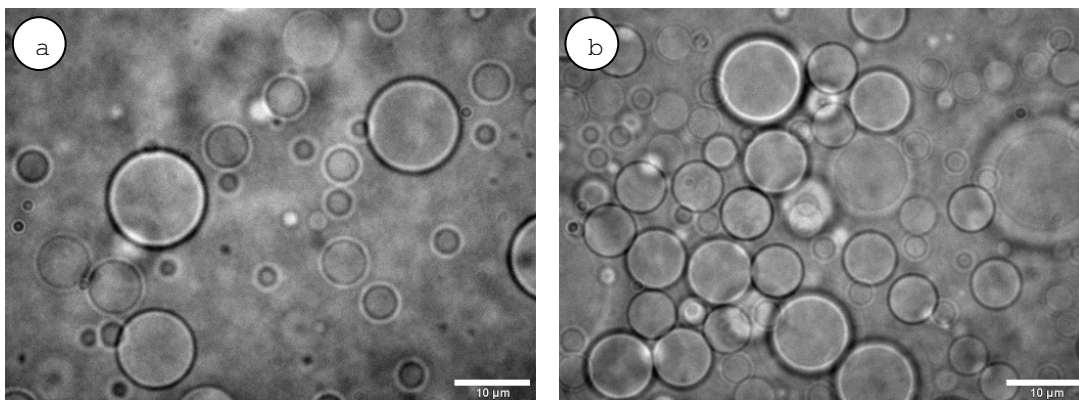
Figure 3.4 Phase contrast microscopy images of pigment-containing giant PG vesicles prepared by electroformation method (a) and spontaneous swelling method (b). Scale bar, 10 μm.

Taking advantage of the built-in fluorescence of the chlorophyll molecules, the assembly of pigments in the lipid bilayer of the pigment-containing giant vesicles were characterized with fluorescence microscope. The pigments can be incorporated into the bilayers of vesicles prepared from either PG (Figure 3.5) or a lipid mixture of

DG/MG/PG (3:3:4, mol%) (Figure 3.6). The incorporation of pigments into the vesicles does not change the morphology of the vesicles. The spontaneous assembly of pigments into the lipid bilayer is compatible with the thermodynamically predicted geography of amphipathic molecules incorporated into the lipid bilayer [53]. The excitation of the chlorophylls-loaded vesicles with high laser intensity of a mercury lamp caused the vesicles to burst in seconds, probably due to the heat dissipation. So care should be taken when characterizing the pigment-containing vesicles using fluorescence microscopy.
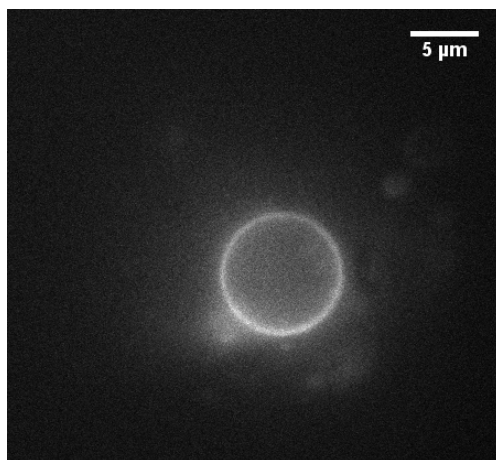
Figure 3.5 Fluorescence microscopy image of pigment-containing giant vesicles prepared from plant lipid PG, excited by an argon laser at 488 nm. Vesicles were prepared in 200 mM sucrose by electroformation method. Scale bar, 5 µm.
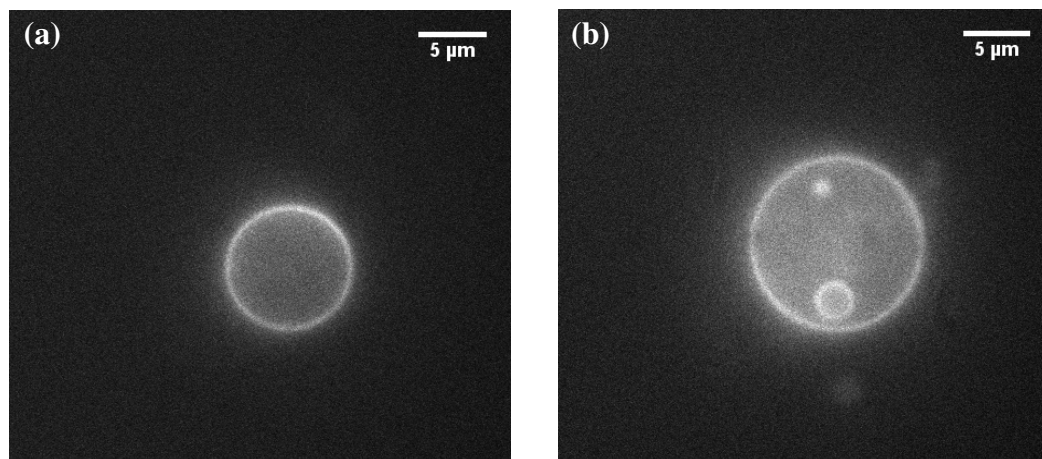
Figure 3.6 Fluorescence microscope images of pigment-containing giant vesicles prepared from lipid mixture of DG/MG/PG (3:3:4, mol%), excited by an argon laser at 488 nm. (a) A single giant vesicle; (b) a smaller vesicle was trapped into a bigger one. Vesicles were prepared in 200 mM sucrose by electroformation method. Scale bar, 5 µm.

3.3 *In vitro* synthesis of LHCP

3.3.1 Standard *in vitro* synthesis of LHCP

A standard *in vitro* synthesis in this work means protein synthesis in the absence of supplemented lipids. In our early study, the coupled wheat germ extract systems from Sigma (TN0100) were used for protein synthesis. Circular plasmid was added and protein synthesis was conducted according to the manufacturer's protocol. Unfortunately no protein band of interest could be detected by western blot analysis. Then BamHI-linearized plasmid or *in vitro*-transcribed mRNA was added to the expression system. Very weak protein bands were detected with anti-VSV antibody in western blotting analysis (Figure 3.7). The size of the protein band was corresponding to the calculated size, indicating that the plasmid construction was successful and the fused VSV tag worked well to facilitate the protein detection. However, the productivity of the system was low.
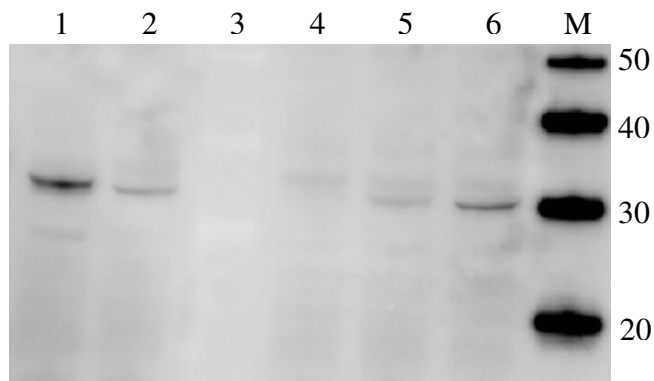
Figure 3.7 Expression of VSV-tagged pLHCP in coupled wheat germ extract systems (Sigma). Linearized plasmid or *in vitro*-transcribed mRNA was used for protein synthesis. M, magic marker XP (kDa); lanes 1-2, synthesis of VSV-pLHCP and pLHCP-VSV from mRNA, respectively; lane 3, SeeBlue maker; lane 4, reaction mixture containing no DNA; lanes5-6, synthesis of VSV-pLHCP and pLHCP-VSV from linearized plasmid, respectively. The blot was probed with anti-VSV antibody.

Later, the coupled wheat germ extract systems from Promega (L4140) were tested. Both circular and linearized DNA template worked for the system. The expression of pLHCP and mLHCP with an N-terminal VSV tag (VSV-pLHCP, VSV-mLHCP) or a C-terminal VSV tag (pLHCP-VSV, mLHCP-VSV) was easily detectable by western blotting (Figure 3.8). For mLHCP, there is a slight difference of protein mass between VSV-mLHCP (lanes 3, 8) and mLHCP-VSV (lanes 4, 9). The mature protein with N-terminal-fused VSV tag runs a little bit slower than protein with C-terminal-fused VSV tag. In the rest of the study, coupled wheat germ extract systems from Promega were used. Circular plasmids served as DNA template for the system.
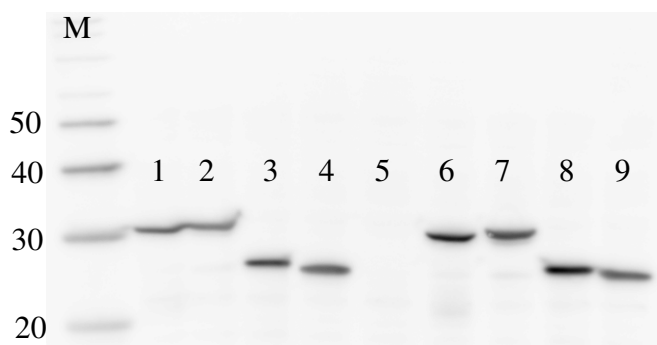
Figure 3.8 Expression of VSV-tagged pLHCP and mLHCP in coupled wheat germ extracts (Promega). BamHI-linearized plasmids or circular plasmids served as template for protein synthesis. Lanes 1-4, proteins synthesized using linearized plasmid as template; lanes 6-9, proteins synthesized using circular plasmid as template; lane 1, VSV-pLHCP; lane 2, pLHCP-VSV; lane 3, VSV-mLHCP; lane 4, mLHCP-VSV; proteins in lanes 6-9 were the same as in lanes 1-4, respectively; Lane 5, reaction mixture without DNA template as a negative control. Protein synthesis was carried out in a 50-µL standard reaction, and samples of 5 µL were analyzed. The blot was probed with anti-VSV antibody.

The cell-free expression of native LHCP and VSV-tagged LHCP was also analyzed on the same blot (Figure 3.9). The pLHCP or mLHCP has an apparent molecular mass of 28 kDa and 25 kDa upon SDS-PAGE analysis (lanes 1 and 4, respectively), corresponding to the calculated values. The VSV tag makes a difference of around 1 kDa (lanes 2 and 5, respectively). The addition of the tag may have some negative effects on the protein expression efficiency, as in both cases, the band intensity is weaker when the protein is attached with a VSV tag.
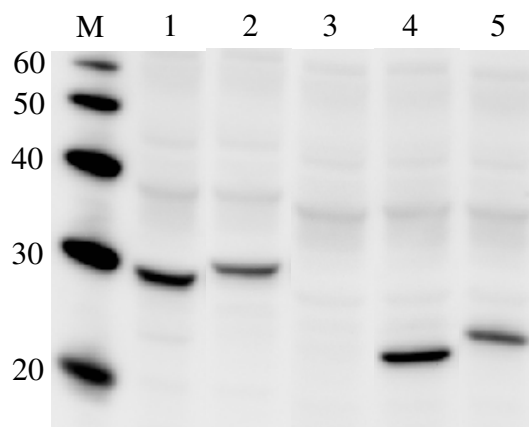
Figure 3.9 Expression of native LHCP and VSV-tagged LHCP. M, magic marker XP (kDa); lane 1, pLHCP; lane 2, pLHCP-VSV; lane 3, reaction mixture without added DNA; lane 4, mLHCP; lane 5, mLHCP-VSV. The proteins were synthesized in standard 50-µL reaction using coupled wheat germ extract systems. Samples of 5 µL were analyzed. The blot was probed with anti-LHC antibody.

3.3.2 Determination of protein yield

Since the cell-free extract itself contains a lot of proteins, there is no real direct method to measure the concentration of target protein. Coomassie staining did not reveal any extrinsic protein band as the amount of the target protein was below the detection limit of this method. In order to determine the productivity of the cell-free wheat germ extract system for our protein, a bacterially-expressed and purified LHCP was used as a standard protein (provided by Prof. Harald Paulsen, Universität Mainz). The so-called C3.2h [71] is a true mature LHCII apoprotein but carrying a His6 tag on the C terminus. A standard cell-free reaction using the coupled wheat germ extract system was incubated at 30°C for 90 min, containing supplemented DNA template encoding untagged mLHCP. Following protein synthesis, portions of the reaction mixture were analyzed on a 10% Bis-Tris gel. Known amounts of C3.2h were also loaded on the same gel. The protein bands were then detected with anti-LHC antibody (Figure 3.10A). The engineered His6 tag on C3.2h lets the protein run a bit slower on the gel than native mature LHCII, which makes a difference of more than 1 kDa – possibly because of the partial positive charge. The intensity of each band was quantified and

plotted as shown in Figure 3.10B, with the intensity of band in lane 8 set to 100%. The amount of *in vitro* synthesized mLHCP was examined by comparing the relative band intensity of the cell-free synthesized mLHCP and the bacterially-expressed LHCP. The yield of mLHCP synthesized in a standard 50-µL reaction is estimated to be ~100-150 ng.
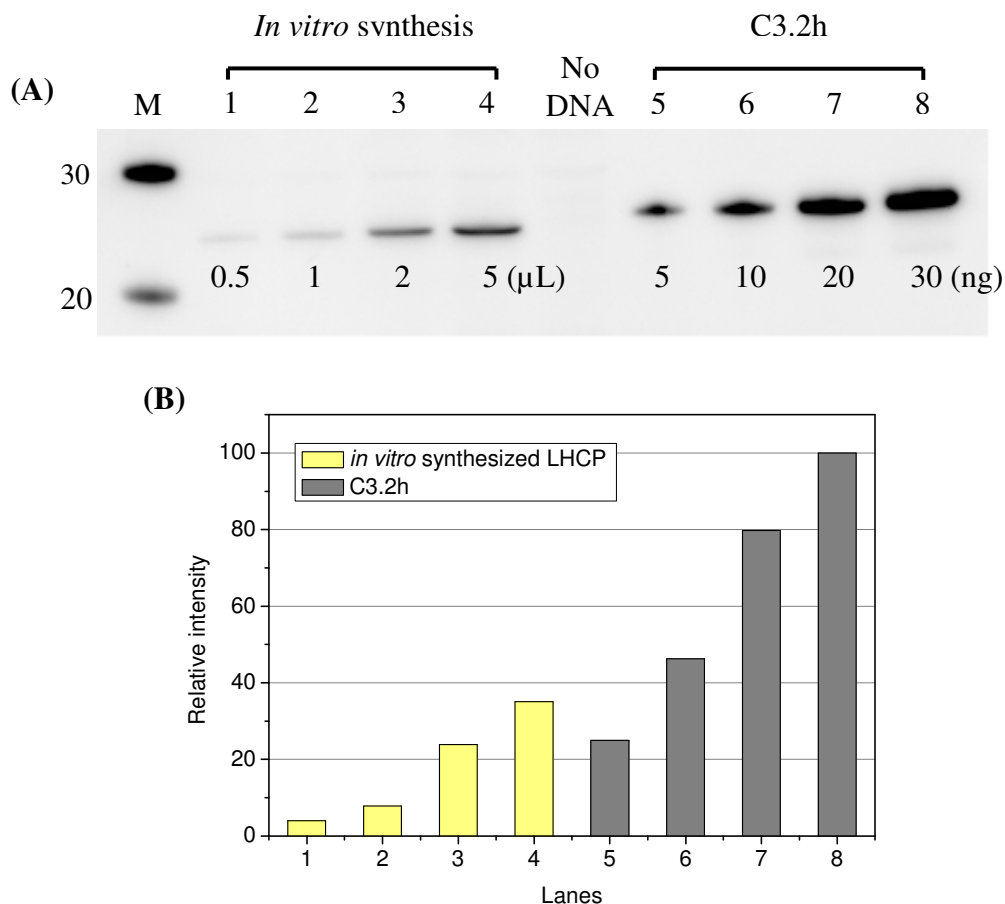
Figure 3.10 Yield determination of *in vitro* synthesized protein. mLHCP was synthesized in a standard cell-free reaction using wheat germ extracts.

(A) Western blotting analysis of in vitro synthesized mLHCP and purified C3.2h. M, magic marker XP (kD), with the molecular weights depicted on the left; lanes 1-4, 0.5 µL, 1 µL, 2µL and 5 µL out of the 50-µL reaction mixture, respectively; lane 5-8, 5, 10, 20 and 30 ng of C3.2h, respectively; No DNA, reaction mixture without added DNA template. The western blot was analyzed with anti-LHC antibody.

(B) The relative intensity of bands in (A) was quantified and plotted. The intensity of band in lane 8, corresponding to 30 ng of C3.2h, was set to 100%. The intensity was quantified using ImageJ software (National Institute of Health).

3.3.3 Lipid-assisted *in vitro* synthesis of LHCP

Unlike living cells, cell-free expression generally provides an open system without membrane barriers. Many additives that could potentially become beneficial for the recombinant protein can be directly added to the system. During the expression of membrane proteins, the addition of lipids to the cell-free expression system would provide hydrophobic environment for the nascent translated protein. Several examples of successful integration of cell-free synthesized membrane proteins into artificial membranes have recently been reported [17,18]. In this study, liposomes prepared from either isolated thylakoid lipids (MGDG, DGDG, PG) or synthetic DPPG were added to cell-free protein synthesis reactions. I started a systematic evaluation of the presence of different concentrations of lipids with respect to (a) their impact on the productivity of the cell-free expression system and (b) their existence to provide suitable hydrophobic environment for protein integration.

3.3.3.1 Impact of DPPG on the expression of VSV-pLHCP and VSV-mLHCP

DPPG was added initially to the cell-free reaction mixture with final concentration ranging from 0.5 to 4 mg/mL. Proteins with N-terminal tag (VSV-pLHCP and VSV-mLHCP) were synthesized in coupled wheat germ extract systems in the presence or absence of DPPG SUVs. The production of proteins was quantified by western blot analysis using specific antibody directed against the terminal VSV tag. The result is shown in Figure 3.11. The densitometry of western blot bands were quantified and plotted, with the band intensity of standard reaction set to 100%. It clearly can be seen that the addition of DPPG at 0.5 and 1 mg/mL was beneficial for the general production of both VSV-pLHCP and VSV-mLHCP. When supplemented with 0.5 mg/mL DPPG, the cell-free expression system yielded 20% more VSV-pLHCP (lane 2) compared with the standard reaction without added lipids (lane 1). The productivity was even slightly higher when DPPG concentration reached 1 mg/mL (lane 3). Similar expression enhancement in the presence of DPPG was also observed with VSV-mLHCP (lanes 5-7). Further increase of DPPG concentration to 4 mg/mL turned out to

have negative effects on the system (lanes 4 and 8). The expression efficiency went down by 10-20%.
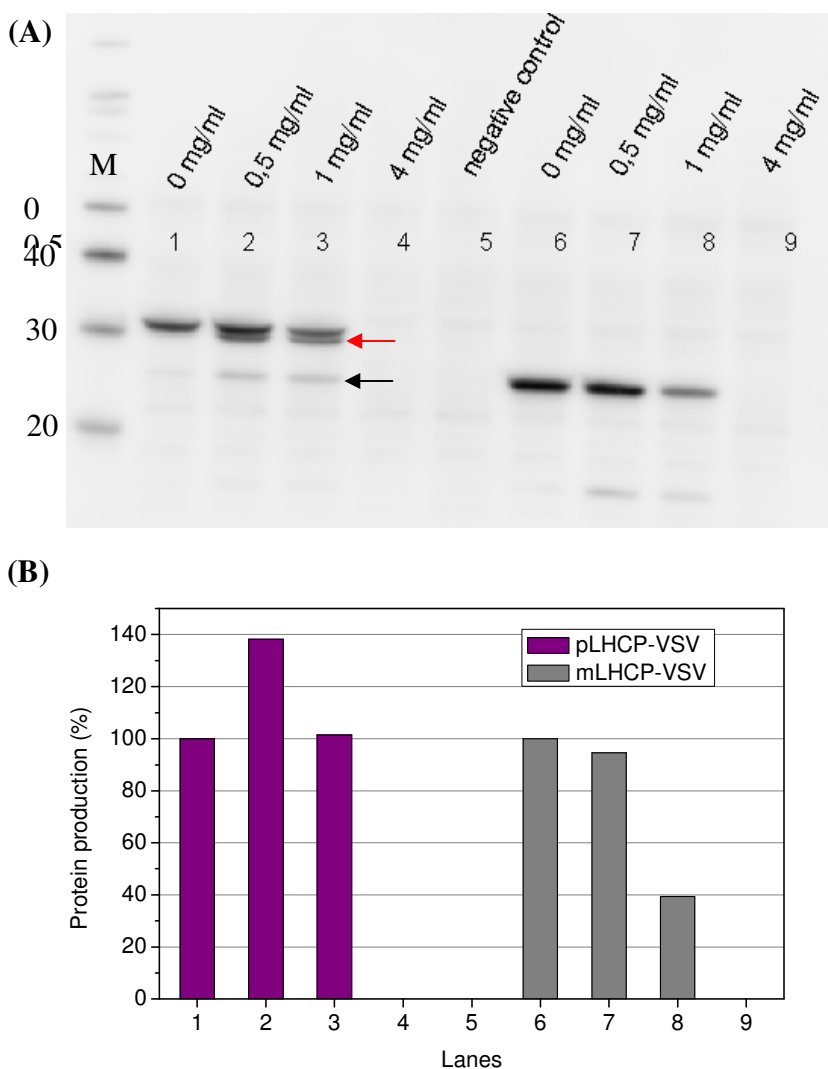
(A)

(B)
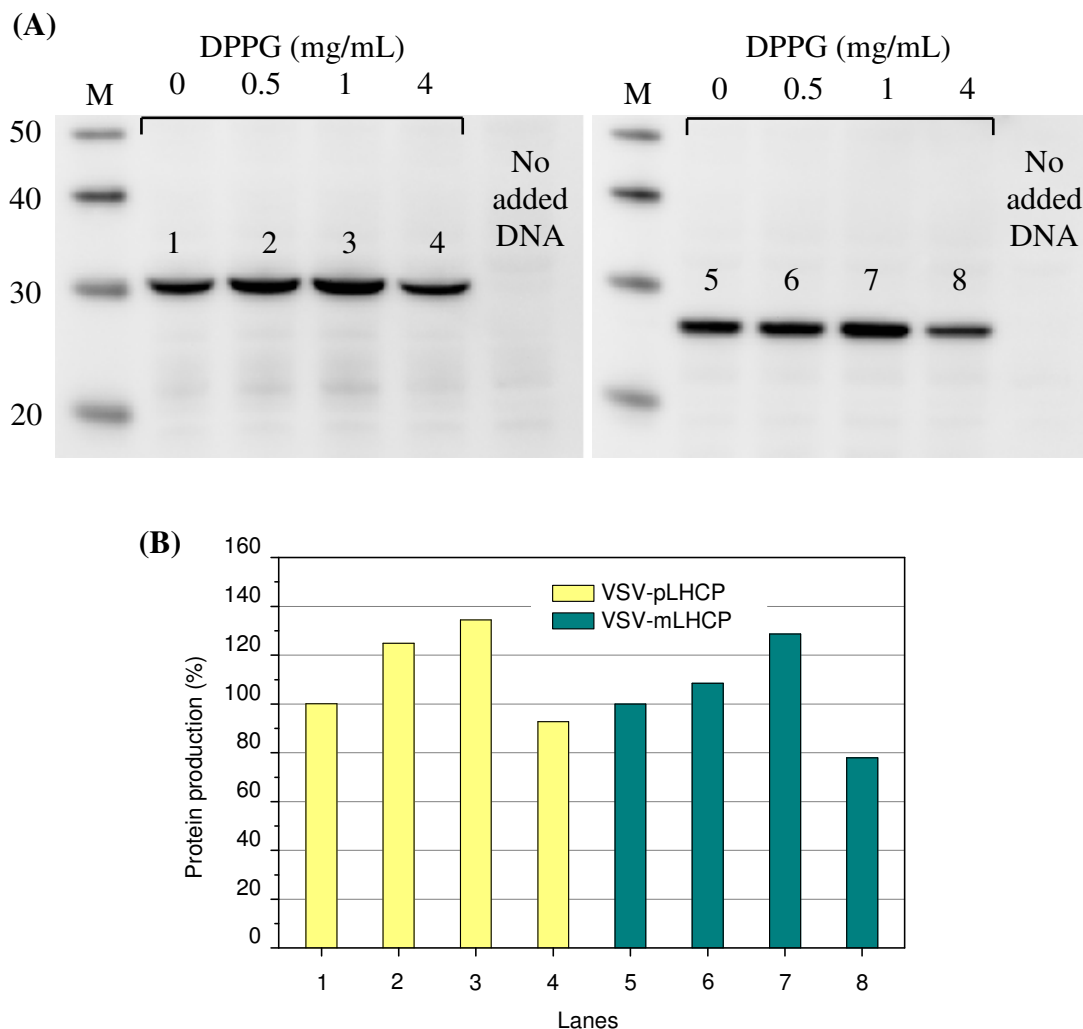
Figure 3.11 Effect of DPPG lipid concentration on the general cell-free expression efficiency.

(A) *In vitro* synthesis of VSV-pLHCP and VSV-mLHCP in wheat germ extracts with or without supplemented lipids. Samples of 5 µL were analyzed. Western blot was detected with anti-VSV antibody. M, magic marker XP (kDa); lanes 1-4, synthesis of VSV-pLHCP without added lipid (lane 1) or in the presence of 0.5, 1, 4 mg/mL DPPG (lanes 2-4 respectively); lanes 5-8, synthesis of VSV-mLHCP without added lipid (lane 5) or in the presence of 0.5, 1, 4 mg/mL DPPG (lanes 6-8 respectively); No added DNA, reaction mixture containing no added DNA template.

(B) The relative intensities of bands in (A) were quantified and plotted. The intensity of *in vitro* synthesized protein without supplemented DPPG (lanes 1 and 5) was set to 100%. The intensity was quantified using ImageJ software (National Institute of Health).

To assure that similar results can be guaranteed, the experiment was repeated. New cell-free reactions were set up for the expression of VSV-pLHCP and VSV-mLHCP. The reactions were supplemented with freshly prepared DPPG SUVs. The final lipid concentration in the 50-µL reaction mixture was set to 0.5, 1, 2 and 4 mg/mL. Standard reactions without the addition of DPPG were also included for the comparison of productivity. Protein synthesis was conducted by incubating the reactions at 30 °C for 90 min. Samples of 5 µL were analyzed. The western blotting analysis and the quantification of the densitometry of the bands were shown in Figure 3.12.

Similar to the first set of results we got above, in this second try, DPPG at 0.5 mg/mL still increased the expression efficiency by ~20% for VSV-pLHCP and ~ 40% for VSV-mLHCP (lanes 2 and 8). However, DPPG at 1 mg/mL became inhibitory to the expression system and resulted in an at least considerably reduced production of both proteins (lanes 3 and 9). Bar diagram in Figure 3.12B showed the densitometry data quantified from western blotting. In the presence of 1 mg/mL DPPG, the productivity of the system dropped ~ two thirds for VSV-pLHCP and ~ one third for VSV-mLHCP, as compared to the productivity of the standard reactions. Further increase of DPPG to 2 mg/mL and 4 mg/mL would completely inhibit general protein synthesis for both proteins (lanes 4-5, 10-11).

The result shown in Figure 3.11 indicated that when the cell-free expression system was supplemented with 4 mg/mL DPPG, the productivity of the system was only fairly affected. While in the second set of reactions, the protein synthesis was completely inhibited when DPPG reached 2 mg/mL in the reaction mixture. Clearly, the coupled wheat germ extract systems used in the second try had a much lower tolerance of supplemented lipids. It is probably because the cell-free system with a different lot number was used. Our colleague also found such lot-to-lot variation with the cell-free expression system based on reticulocyte lysates from the same manufacturer. It has been shown that the concentration of components in wheat germ extract systems is lot-dependent [72]. Other factors that might have impact on the expression efficiency could be: incubation time, incubation temperature, freshly prepared or aged DPPG vesicles, the purity of the DNA template, etc. These factors are more or less under control, but influences coming from these aspects cannot be completely ruled out.

(A)

(B)
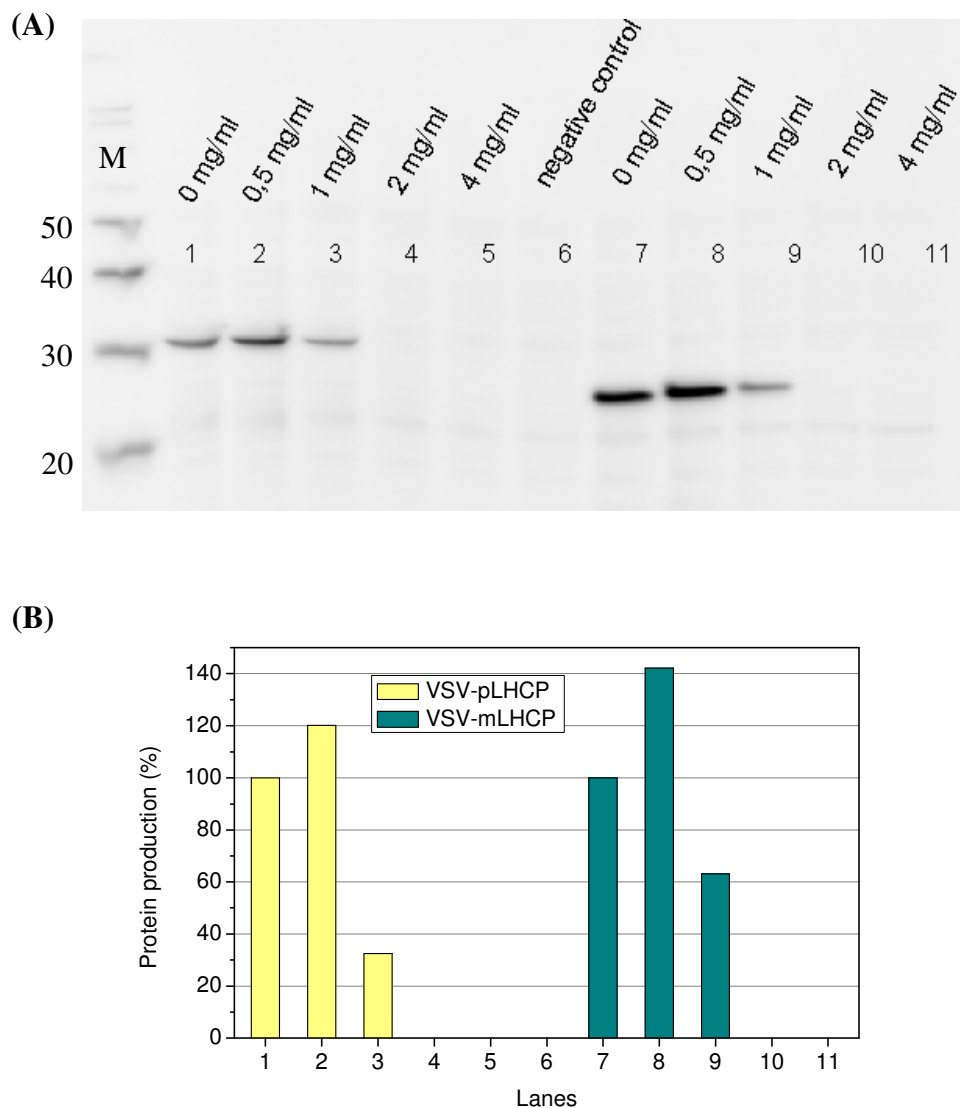
Figure 3.12 Effect of DPPD lipid concentration on the general protein expression efficiency.

(A) *In vitro* synthesis of VSV-pLHCP and VSV-mLHCP in wheat germ extracts with or without supplemented lipids. Samples of 5 µL were analyzed. Western blot was probed with anti-VSV antibody. M, magic marker XP (kDa); lanes 1-5, synthesis of VSV-pLHCP without added lipid (lane 1) or in the presence of 0.5, 1, 2, 4mg/mL DPPG (lanes 2-5 respectively); lane 6, reaction mixture without added DNA template as a negative control; lanes 7-11, synthesis of VSV-mLHCP without added lipid (lane 7) or in the presence of 0.5, 1, 2, 4 mg/mL DPPG (lanes 8-11 respectively).

(B) The protein bands in (a) were quantified by densitometry. The intensity of *in vitro* synthesized protein without supplemented DPPG (lanes 1 and 7) was set to 100%. The intensity was quantified using ImageJ software.

3.3.3.2 Impact of DPPG on the expression of pLHCP-VSV and mLHCP-VSV

The influence of lipid concentration on the expression efficiency of C-terminally VSV-tagged proteins (pLHCP-VSV and mLHCP-VSV) was also investigated. This would be helpful in finding out a 'safe concentration' of DPPG supplemented to the cell-free reaction mixture. Also we could further investigate if the lipid tolerance level of the expression system was lot-dependent, since wheat germ extracts of the same lot number as we used in the second try for the expression of N-terminally VSV-tagged proteins were employed for the synthesis pLHCP-VSV and mLHCP-VSV.

Proteins with VSV tag at C terminus were expressed in coupled wheat germ extracts in the presence of different concentrations of DPPG. DPPG SUVs were always freshly prepared right before the assembly of the reactions. Firstly, the final concentrations of DPPG in the reaction were set to 0.5, 1 and 4 mg/mL, the same as in the first set of experiments for the expression of N-terminally tagged proteins. The western blotting analysis and densitometry quantification of the blotting are shown in Figure 3.13. Then the experiment was repeated, with DPPG concentrations set to 0.5, 1, 2 and 4 mg/mL. The results are shown in Figure 3.14.

For the synthesis of pLHCP-VSV, the addition of lipid DPPG at 0.5 mg/mL was beneficial to the efficiency. Higher concentrations of DPPG would have negative effects or completely inhibit the expression. A band that was slightly smaller than pLHCP-VSV was observed (red arrow). Also a protein band of exact the size of mLHCP-VSV (black arrow) was getting stronger upon the addition of lipids. Since the blotting was probed with anti-VSV antibody, the detected proteins bands should all carry a VSV tag. As the sequence coding VSV tag was placed downstream of the gene sequence, the proteins bands did not seem to be due to premature translational stop. The two unspecific bands were considered be the proteolytic degradation products. During or after protein synthesis, a tiny amount of the precursor protein was processed to mature size. But how the added lipids assisted the processing of precursor proteins is not understood here. Similar bands were also detected in the second gel, as shown in Figure 3.14A.

The addition of DPPG had similar effects on the synthesis of mLHCP-VSV. The only exception is lane 7 in Figure 3.13, which corresponds to the expression of mLHCP-VSV in the presence of 0.5 mg/mL DPPG. The efficiency was slightly decreased for mLHCP-VSV. DPPG at this concentration was always found to be beneficial to the general productivity of the system. In the second test, the productivity of mLHCP-VSV was increased by nearly 10% as compared to that of a standard reaction.

Figure 3.13 Effect of DPPG lipid concentration on the general protein expression efficiency.

(A) *In vitro* synthesis of pLHCP-VSV and mLHCP-VSV in wheat germ extracts with or without supplemented lipids. M, magic marker XP (kDa); lanes 1-4, synthesis of VSV-pLHCP without added lipid (lane 1) or in the presence of 0.5, 1, 4mg/mL DPPG (lanes 2-4 respectively); lane 5, reaction mixture without added DNA template as a negative control; lanes 6-9, synthesis of VSV-mLHCP without added lipid (lane 6) or

in the presence of 0.5, 1, 4 mg/mL DPPG (lanes 7-9 respectively). Samples of 5 µL were analyzed. Western blot was probed with anti-VSV antibody. The black and red arrows indicated two unspecific bands which were considered be the proteolytic degradation products of the full-length proteins.

(B) The relative intensity of bands in (A) was quantified and plotted. The intensity of *in vitro* synthesized protein without supplemented DPPG (lane 1 and lane 6) was set to 100%. The intensity was quantified using ImageJ software.
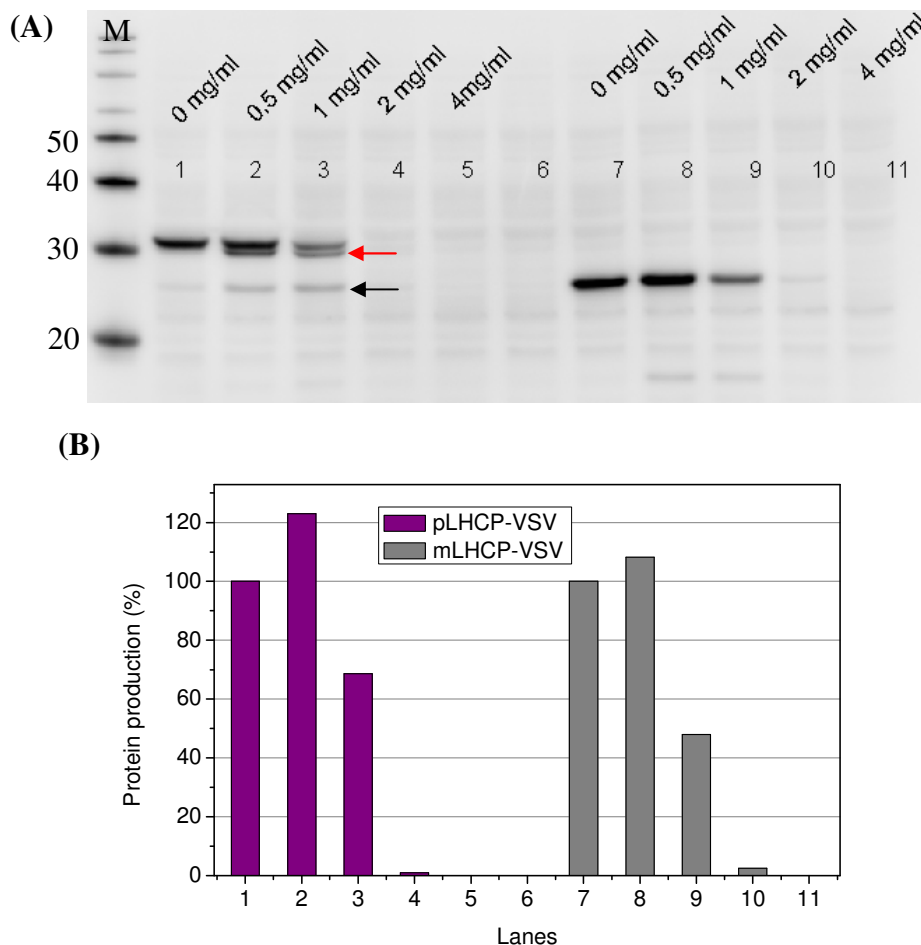
Figure 3.14 Effect of DPPG lipid concentration on the general protein expression efficiency.

(A) *In vitro* synthesis of pLHCP-VSV and mLHCP-VSV in wheat germ extracts with or without supplemented lipids. M, magic marker XP (kDa); lanes 1-5, synthesis of pLHCP-VSV without added lipid (lane 1) or in the presence of 0.5, 1, 2, 4mg/mL DPPG (lanes 2-5 respectively); lane 6, reaction mixture without added DNA template as a negative control; lanes 7-11, synthesis of mLHCP-VSV without added lipid (lane 7) or in the presence of 0.5, 1, 2, 4 mg/mL DPPG (lanes 8-11 respectively). Samples of 5 µL were analyzed. Western blot was probed with anti-VSV antibody.

(B) The relative intensity of bands in (A) was quantified and plotted. The intensity of *in vitro* synthesized protein without supplemented DPPG (lane 1 and lane 7) was set to 100%. The intensity was quantified using ImageJ software.

3.3.3.3   Effect of PG-Chl on the productivity of cell-free protein synthesis

Pigment-containing PG vesicles (PG-Chl) were prepared as described in section 2.2.3. The successful incorporation of pigments into the lipid belayer can be judged by the color or the absorbance spectra of the vesicle solution. The incorporation of pigments into the membranes of giant vesicles was verified with fluorescence microscope. The effect of PG-Chl vesicles on the productivity of cell-free protein synthesis systems is shown in Figure 3.15.

Pigment-containing PG SUVs were added to the coupled wheat germ extract systems for the expression of VSV-pLHCP and VSV-mLHCP, with final lipid concentration set to 0.2 and 0.4 mg/mL. The productivity of the proteins displayed similar tendencies of enhancement and in the presence of different concentrations of lipids. PG of 0.2 mg/mL considerably enhanced the expression efficiency for both VSV-pLHCP and VSV-mLHCP (lanes 2, 4, 7 and 9). It seems that the ions in the buffer have no obvious negative effect on the general productivity of the system. When the lipid concentration was doubled to 0.4 mg/mL in the reaction mixture, the efficiency decreased apparently (lanes 3, 5, 8 and 10), even though still slightly higher than that of standard reactions (lanes 1 and 6).

In order to exclude possible pipetting errors, samples of 5 µL were loaded to a second gel and the western blotting was probed with anti-LHC antibody (Figure 3.15B). The intensities of protein bands as revealed by anti-LHC were consistent with those as revealed by anti-VSV antibody.

Compared with lipid DPPG, the system has a fairly low tolerance of PG-Chl vesicles. This is probably due to the residue chlorophyll aggregates in the mixture. Both DPPG and PG are negatively charged lipids and their effect on the expression efficiency of wheat germ extracts is similar. Bui et al. showed that the lipids with different charge (negative, positive or neutral) affected the GFP expression differently [73]. The thylakoid membranes are composed of mainly non-charged DGDG and MGDG, together with 5-12 % negatively-charged PG. In this work, the effect of lipids on

LHCP expression in wheat germ extract systems was studied with only negatively charged lipids, either synthetic DPPG or PG purified from plant leaves.
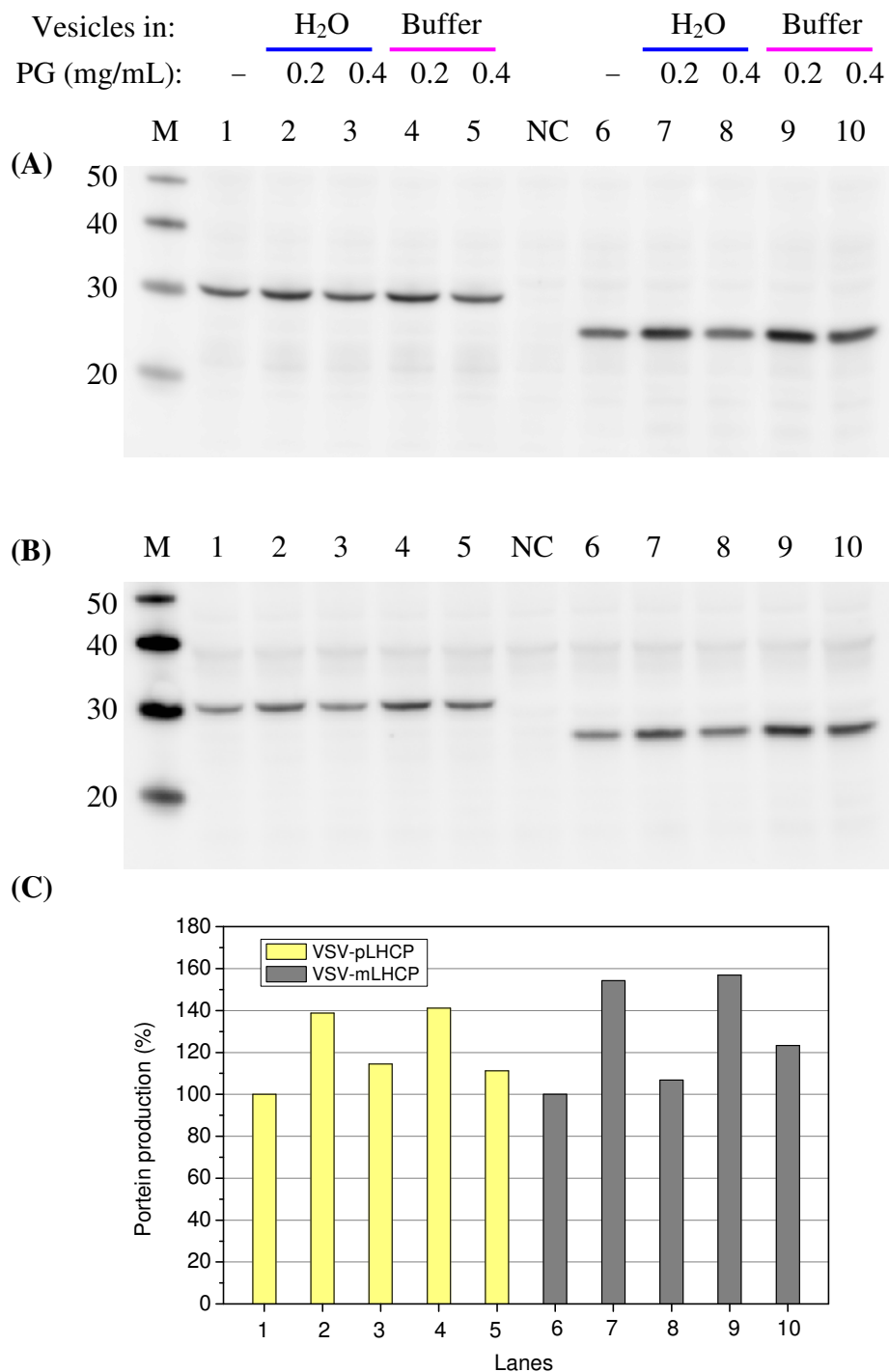
Figure 3.15 Effect of pigment-containing vesicles on the general cell-free expression efficiency.

(A) *In vitro* synthesis of VSV-pLHCP and VSV-mLHCP in wheat germ extracts in the presence or absence of PG-Chl SUVs. Samples of 5 µL were analyzed. The western blot was detected with anti-VSV antibody. M, magic marker XP (kDa); lanes 1-5, synthesis of VSV-pLHCP in a standard reaction (lane 1) or supplemented with 0.2, 0.4 mg/mL lipids (lanes 2-5); lanes 6-10, synthesis of VSV-mLHCP in a standard reaction (lane 6) or supplemented with 0.2 or 0.4 mg/mL lipids (lanes 2-5); NC, reaction mixture without DNA template.

(B) The same samples were loaded to a second gel and the western blot was probed with anti-LHC antibody.

(C) The relative intensity of protein bands in (A) was quantified and plotted. The intensity of *in vitro* synthesized protein in standard reactions (lanes 1 and 6) was set to 100%. The intensity was quantified using ImageJ software.

3.4 Digestion assays of *in vitro* translated proteins

The addition of lipid to coupled wheat germ extracts at certain concentrations had a positive impact on the yield of the synthesized membrane proteins. This repeatable observation naturally brought up this question to us: was there any "interaction" between the lipids and the lipid-assisted synthesized proteins? Did the lipids, which were supplemented in the form of vesicles, provide a suitable hydrophobic environment for the nascent membrane proteins? This question was addressed by digestion assays of the proteins.
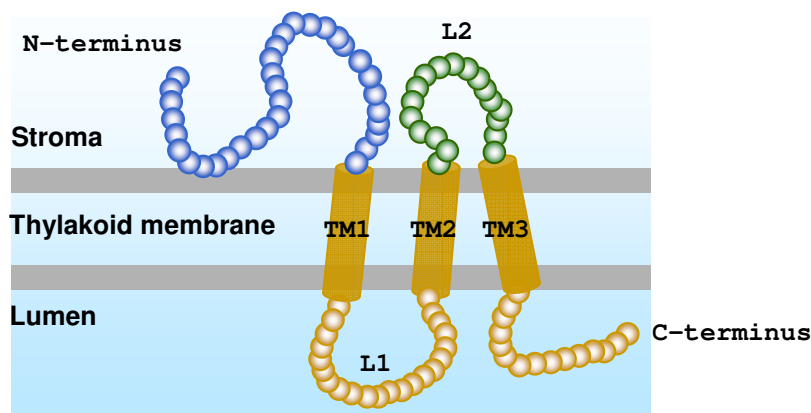
Figure 3.16 Protease digestion assay for the analysis of protein integration.

In vitro reconstitution of LHCP into thylakoid membranes have been extensively investigated [74-76]. And several criteria have been developed to demonstrate the

correct integration of LHCP into the thylakoid membranes: (1) association of imported LHCP exclusively with thylakoids; (2) resistance to extraction with 0.1 M NaOH, a characteristic of integral membrane proteins; and (3) partial protection against protease digestion, an indication that the protein is integrated into the bilayer. The protease digestion assay for membrane insertion was found to be more stringent than the salt wash assay. For successful protein integration, the transmembrane (TM) segments are protected by the membranes against protease treatment, with the parts exposed to the outside of the membranes accessible to protease digestion. In the case of LHCP integration into thylakoid membranes, the major part of inserted polypeptides, except for a 1- or 6-kDa fragment on the N terminus of LHCP or pLHCP, respectively, became protease resistant [76], resulting a largely protected fragment of 24-kDa. In addition to the 24-kDa fragment, a shorter fragment of ~20 kDa was also consistently observed in these digestion assays [77-78]. These two independent digestion fragments were thought to represent two different states of LHCP after its insertion into the thylakoid: LHCII monomers and LHCII trimers. Trimeric LHCII is known to be protected towards protease except about 1 kDa of the N-terminus of the protein where as in monomeric LHCII, about 5 kDa of the N-terminus are susceptible to protease [75]. However, the possibility cannot be ruled out that LHCP inserted into thylakoid but not complexed with pigments may also assume largely-protease-resistant conformation. Based on the resolved structure, the calculated values of the segments of LHCP in Figure 3.16 are: N-terminus, 9.5 and 5.5 kDa for pLHCP and mLHCP, respectively; TM1-L1-TM2, 10 kDa; L2, 2.5 kDa, TM3-C terminus, 7 kDa. The sizes of the segments were calculated using PeptideMass program [79].

3.4.1 Digestion products of LHCP analyzed by western blot

3.4.1.1 Thermolysin treatment results in a 20-kDa fragment

Direct after *in vitro* protein synthesis using the coupled wheat germ extract systems, portion of the reaction mixture was taken out to a new tube. Thermolysin was added to the reaction mixture to a final concentration of 0.1 mg/mL. The mixture was then

incubated at 25°C for 30 min. Digestion assays were terminated by transfer to ice and the addition of LDS buffer. The sample was then heated at 70°C for 10 min before loaded to gels. After separation by SDS-PAGE, the synthesized proteins as well as the digested fragments were detected with polyclonal anti-LHC antibody.
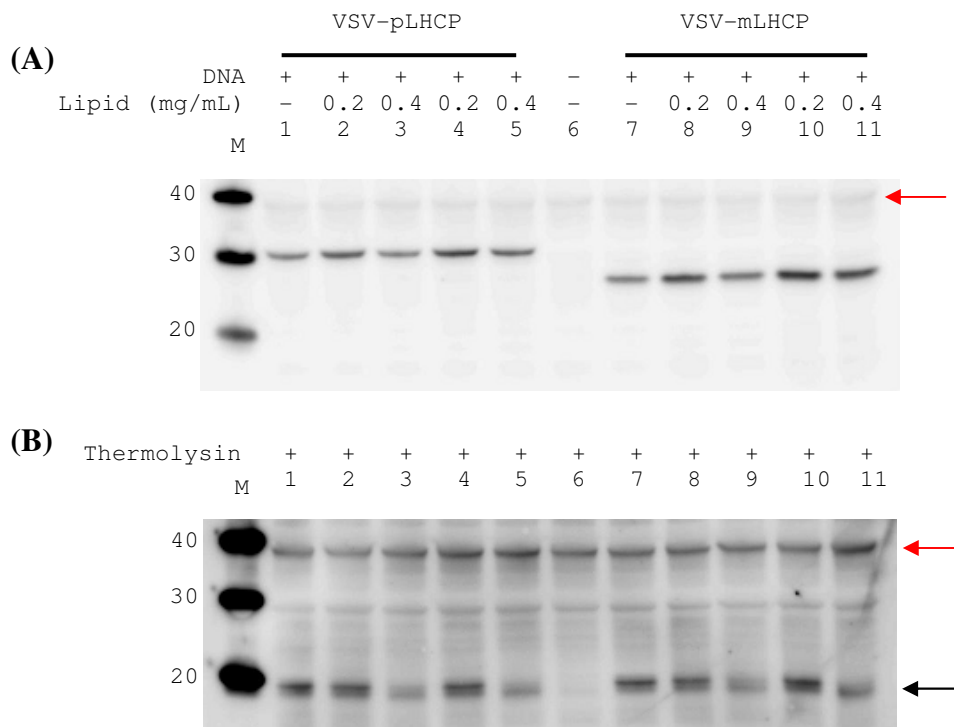
Figure 3.17 Digestion assays of *in vitro* translated proteins. The ~40-kDa band (indicated by the red arrow) was the background signal generating from the system when anti-LHC antibody was used to detect the synthesized proteins. The ~20-kDa fragment (indicated by the black arrow) was the proteolytic fragment.

(A) The proteins were synthesized in coupled wheat germ extracts in the presence or absence of supplemented PG-Chl SUVs. M, magic marker XP (kDa); lanes 1-5, expression of VSV-pLHCP in the presence/absence of PG-Chl SUVs; lane 6, reaction mixture containing no DNA template; lanes 7-11, expression of VSV-mLHCP in the presence/absence of PG-Chl SUVs. Exposure time, 10 min.

(B) The digestion patterns of *in vitro* translated proteins. Lanes 1-11 are corresponding to lanes 1-11 in (A). Exposure time, 40 min. The marker was overexposed. Both of the western blots were probed with anti-LHC antibody. The ~40-kDa band (indicated by the red arrow) was the background signal generating from the system when anti-LHC antibody was used to detect the synthesized proteins. The ~20-kDa fragment (indicated by the black arrow) was the proteolytic fragment.

The protease digestion assays were first carried out with N-terminally VSV-tagged proteins. Western blotting analysis of the expression and digestion patterns of the *in*

vitro translated proteins were shown in Figure 3.17. Pigment-containing PG SUVs prepared in water (lanes 2, 3, 8 and 9) or in buffer solution (lanes 4, 5, 10 and 11) were added to the reaction mixture. The final lipid concentration of samples in lanes 2, 4, 8 and 10 was 0.2 mg/mL, while in lanes 3, 5, 9 and 11 was 0.4 mg/mL. Protein productivity was enhanced with 0.2 mg/mL lipid in the system, but inhibited with higher lipid concentration (Figure 3.17A). After thermolysin treatment, the full-length protein bands disappeared from the blot, indicating that thermolysin at 0.1 mg/mL worked for the system. After digestion, two protein bands were resolved on the blotting as shown in Figure 3.17B. The ~40-kDa band (indicated by the red arrow) appeared in every lane in the digestion assay, including in the negative control (lane 6, Figure 3.17B). Actually a band of similar size can also be observed in Figure 3.17A (red arrow) before the protease treatment. Since the blot in (A) was only exposed for 10 min, while the blot in (B) was exposed for 40 min, the band intensity became much stronger with longer exposure time. And the intensity of this unspecific band in each lane was with similar. Thus this band was considered as the background signal generating from the system when anti-LHC antibody was used to detect the synthesized proteins. Images of the western blotting analysis of the digestion assays shown in the rest of the thesis only focuses on bands of smaller sizes.

The pLHCP and LHCP were digested with thermolysin and the only digested fragment observed in the western blotting was ~20 kDa (indicated by black arrow in Figure 3.17B). This proteolytic fragment showed in every lane where DNA template was added, either encoding VSV-pLHCP or VSV-mLCHP, except in lane 6, where no DNA template was added to the reaction mixture. So this 20-kDa band definitely was resulted from the thermolysin treatment of the synthesized proteins. The intensity of this band in lanes 1-2, 4, 7-8, and 10 was similar. Though the expression level was higher for samples in lanes 2, 4, 8 and 10. The enhanced expression did not generate digestion fragments of enhanced intensity. However the band also appeared in the standard reaction for both proteins, where no lipid was supplemented.

Pigment-containing SUVs prepared plant from lipid mixture of DG/MG/PG (3:3:4, mol%) were also added to coupled wheat germ extract systems for the expression of untagged pLHCP. The final lipid concentration in the reaction mixture was set to 0.1,

0.2 and 0.3 mg/mL. Samples of protein expression and thermolysin treatment were prepared and loaded on the same gel for SDS-PAGE. The western blotting analysis is shown in Figure 3.18. The expression of pLHCP in the presence or absence of lipid was shown in lanes 1-4. No clear increase or decrease in productivity of the system was observed. The expression level was similar with or without supplemented lipids. In the digestion assay, the synthesized proteins disappeared from the blot, generating a fragment of ~20 kDa as observed above. No corresponding bands were observed in the expression part. It has been reported that protease digestion products of LHCP inserted into the thylakoid membranes were of 24 kDa and 20 kDa. The 24-kDa fragment is supposed to be the protease digestion product of LHCII trimer, while the shorter is the protease digestion product of LHCII monomer.
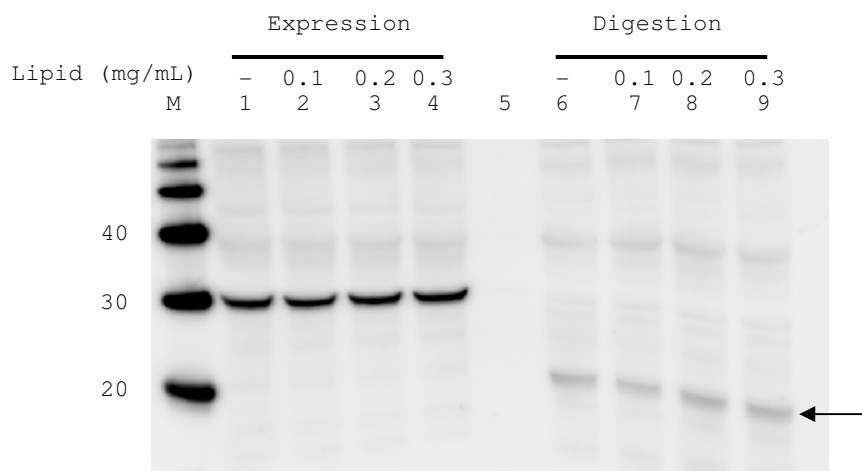
Figure 3.18 The expression and digestion of cell-free synthesized proteins. M, magic marker XP (kDa); lanes 1-4, expression of pLHCP in the presence or absence of supplemented SUVs; lane 5, blank lane; lanes 6-9, thermolysin treatment of samples in lanes 1-4, respectively. Exposure time, 24 min.

3.4.1.2 Treatment of reaction mixture with detergent

The protease digestion of the *in vitro* translated pLHCP or mLHCP in wheat germ extracts all generated a fragment of 20 kDa. The proteins expressed in the standard reactions without supplemented lipids were also protease-resistant. One possibility is that the wheat germ extract system itself comes with meaningful amounts of membrane fragments during preparation, which might provide the hydrophobic

environment for the nascent protein. Treatment of the reaction mixture after protein synthesis with detergent would solubilize the presumed membrane fragments. Studies in the integration of LHCP into thylakoid membranes indicate that it is not so much the membrane environment that is responsible for protection of most of LHCP against protease than it is the pigments bound [76]. Reconstituted LHCII in solution are also protease-resistant, suggesting that the pigments somewhat protect the protein against protease digestion.

The digestion assays were repeated with VSV-tagged protein (pLHCP-VSV and mLHCP-VSV) and non-tagged proteins without a VSV tag (pLHCP and mLHCP). PG-Chl SUVs were supplemented to the system with a final lipid concentration of 0.2 mg/mL. Standard reactions in the absence of added lipid were also set up. Western blotting analysis of the cell-free synthesized proteins is shown in Figure 3.19A. For all of the four proteins included, the productivity of the system with supplied lipids (lanes 2, 4, 8 and 10) was slightly higher than that of the standard reaction without supplemented PG-Chl SUVs (lanes 1, 3, 7 and 9). The expression efficiency of untagged proteins were higher than that of VSV-tagged proteins, by comparing the intensities of lanes 1-2 to lanes 3-4, and intensities of lanes 7-8 to lanes 9-10. These were consistent with the observations before.

Figure 3.19B shows the western blotting analysis of the protease treatment of *in vitro* translated proteins in (A). The digestion generated one major band of ~20 kDa. While for digestion in lanes 3-4, 7-10, there existed a band of higher molecular mass, which might be attributed to incomplete digestion. The intensity of digested band from untagged proteins (lanes 1-2, 7-8) was much stronger than that of VSV-tagged proteins (lanes 3-4, 9-10). For each protein, the digestion of proteins synthesized in the presence or absence of lipids all generated a digestion product of 20 kDa. No perceptible difference can be observed from the digestion patterns, though the expression level was considerably higher in the presence of lipids. In the negative control, where no DNA template was added to the wheat germ extract, no corresponding bands were observed (lanes 5-6).
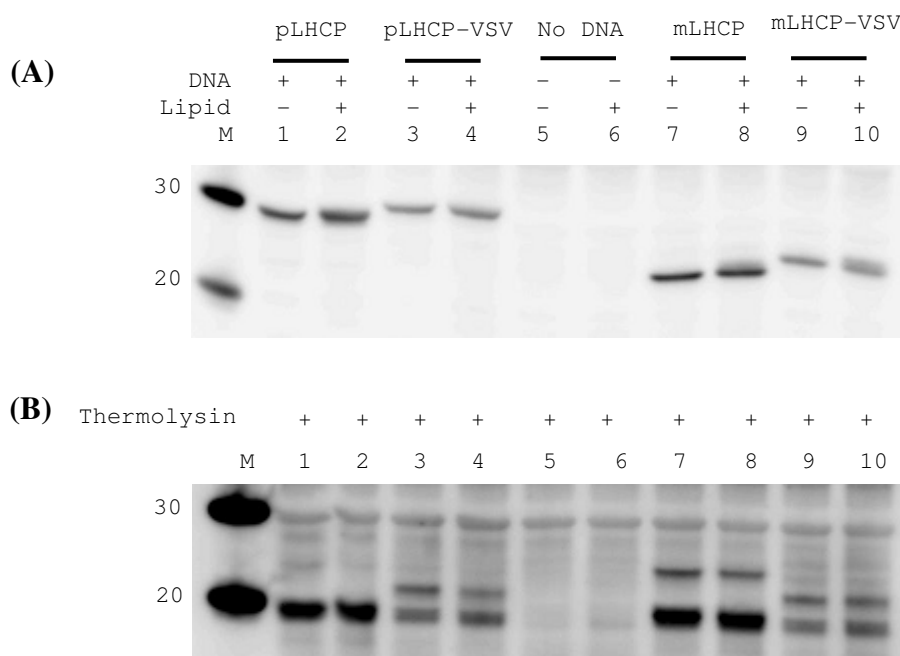
Figure 3.19 Cell-free protein synthesis in coupled wheat germ extracts and protease treatment.

(A) Western blotting of cell-free synthesized proteins. Proteins were expressed in wheat germ extracts, in the presence or absence of 0.2 mg/mL PG-Chl. M, magic marker XP (kDa); lanes 1-2, pLHCP; lanes 3-4, pLHCP-VSV; lanes 5-6, reaction mixture without DNA; lanes 7-8, mLHCP; lanes 9-10, mLHCP-VSV. Exposure time, 12 min.

(B) Western blotting analysis of digestion assays. M, magic mark XP (kDa); lanes 1-10 were corresponding to lanes 1-10 in (A), respectively. Exposure time, 32 min. The marker was overexposed. Both blots were probed with anti-LHC antibody.

The digestion patterns tell no difference from the proteins synthesized in a standard reaction or in the presence of supplemented lipids. Even though, it was clearly shown before that the supplemented lipids at certain concentrations were beneficial to the general productivity of the system. However, the subtle increase in the productivity might be not sufficient to induce a perceptible difference in the digestion patterns. To further discriminate the difference in the digestion patterns between the protein synthesized in the presence or absence of lipids, the reaction mixture was treated with detergent before setting up the digestion assays. Directly after protein synthesis, the reaction mixture was solubilized with 1% OG (octylglucoside) by incubation for 30 min at room temperature followed by digestion assays. Or the reaction mixture was treated with 0.1% SDS. The mixture was cooked at 99°C for 2 min. After the mixture

was cooled down to room temperature, thermolysin was added and the digestion was carried out by incubation at 25°C for 30 min. Western blotting analysis of the digestion assays is shown in Figure 3.20. The reaction mixtures used in this experiment were from the protein synthesis as shown in Figure 3.19A.

Reaction mixtures with or without supplemented lipids were both treated with detergents. Clearly thermolysin worked well in the presence of 1% OG or 0.1% SDS, as the *in vitro* translated protein all disappeared from the blots. No clear digestion products were observed when the reaction mixtures were treated with 0.1% SDS (lanes 5-6, 8-9), no matter the proteins were synthesized in the presence or absence of supplemented lipids. While in the case of 1% OG treatment, the digestion products of 20 kDa were almost gone for VSV-tagged proteins, both synthesized with or without lipids (lanes 2 and 4). However the digestion products of untagged proteins, pLHCP and mLHCP, were still observed in the OG treated samples (lanes 1 and 3).
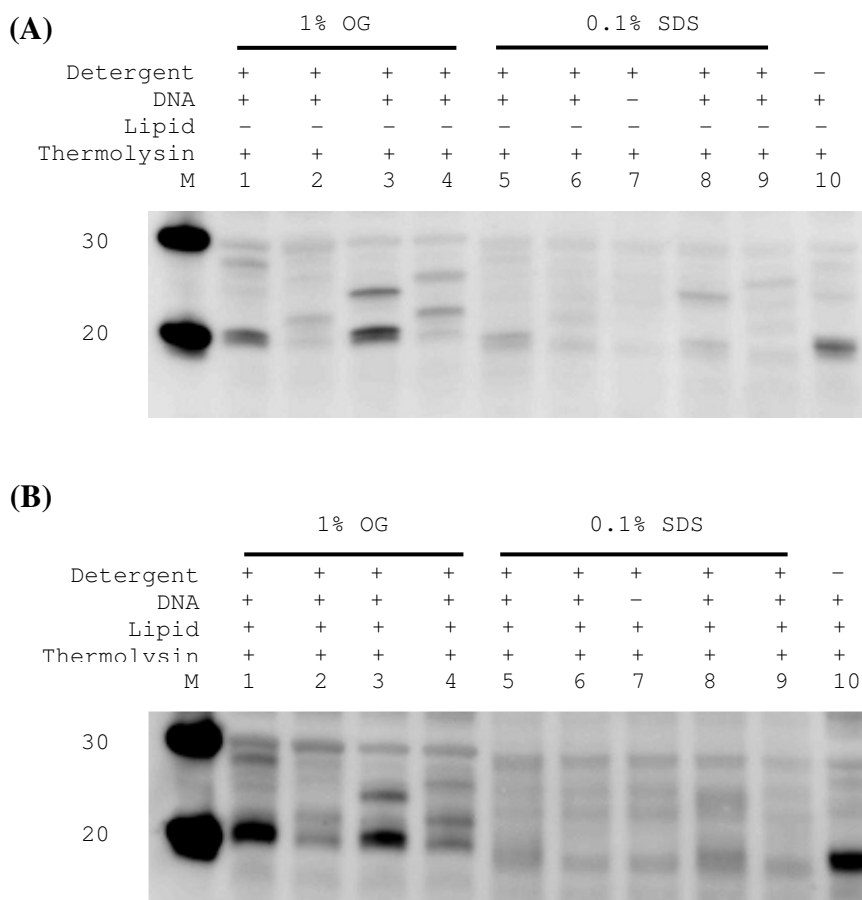
Figure 3.20 Treatment of reaction mixture with detergents before digestion assays.

(A) Western blotting analysis of thermolysin treatment of cell-free translated proteins. Proteins were synthesized in standard reactions. The reaction mixture was treated with detergent and then subject to thermolysin digestion. M, magic marker XP (kDa). The proteins were: lanes 1 and 5, pLHCP; lanes 2 and 6, pLHCP-VSV; lanes 3 and 8, LHCP; lanes 4 and 9, LHCP-VSV; lane 7, reaction mixture containing no DNA template; lane 10, pLHCP. Samples in lane 10 was not treated with detergent. Exposure time, 40 min. The marker was overexposed.

(B) Proteins were synthesized in the presence of lipids. The reaction mixture was treated with detergent and then subject to thermolysin digestion. M, magic marker XP (kDa). The proteins were: lanes 1 and 5, pLHCP; lanes 2 and 6, pLHCP-VSV; lanes 3 and 8, LHCP; lanes 4 and 9, LHCP-VSV; lane 7, reaction mixture containing no DNA template; lane 10, pLHCP. Samples in lane 10 was not treated with detergent. Exposure time, 40 min. The marker was overexposed. Both blots were probed with anti-LHC antibody.

Also 0.1% dodecylmaltoside (DM) was tried and the result is shown in Figure 3.21. The detergent treatment of the reaction mixture before protease digestion only has minor effect on the digestion fragments. The protein was still partially protected against protease digestion. However in the presence of 0.1% SDS, the fragments were gone. But the samples were also heated, so the proteins were supposed to be completely denatured.
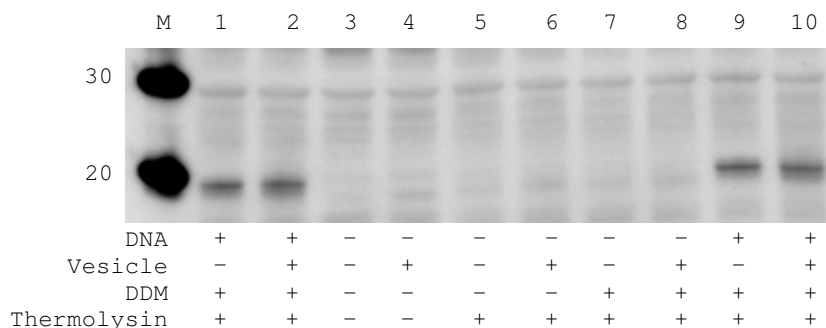
Figure 3.21 The *in vitro* translated mixture was treated with 0.1% DDM before subjected to thermolysin digestion. M, magic marker XP (kDa); lanes 1-2, pLHCP-VSV; lanes3-8, reaction mixture containing no DNA; lanes 9-10, VSV-mLHCP. The reaction mixture was treated with 0.1% DDM before protease digestion. Lane 1-2, VSV-pLHCP; lanes 9-10, VSV-LHCP. Exposure time, 48 min.

3.4.1.3 Partially denaturing gels

To further characterize if the synthesized proteins were integrated into the lipid bilayer and bind to the pigments that were incorporated into the membrane during vesicle preparation, pLHCP synthesized in the presence of pigment-containing SUVs was loaded to partially denaturing gel [71]. LHCII reconstituted from bacterially-expressed LHCP and pigments was used as a standard to determine the detection limit of this method (Figure 3.22A). Proportional amounts of LHCII were loaded to the gel. As low as 20 ng of LHCII was detectable with this method.

Proteins synthesized in coupled wheat germ extracts in the presence of pigment-containing vesicles were then loaded to partially denaturing gel, lanes 2-5 in Figure 3.22B. While only free pigments were observed in the gel, no detectable LHCII monomer. As shown in section 3.3.2, the yield of LHCP synthesized in a typical 50-µL wheat germ reaction was around 100 ng. The efficiency of *in vitro* reconstitution of LHCP into isolated thylakoids was not high. Either the synthesized proteins were not inserted into the supplemented vesicles or only tiny little amount LHCII were formed in the batch reaction. Based on the results of the digestion assays, chances that the proteins were not integrated into added lipids were high.

(A)

(B)
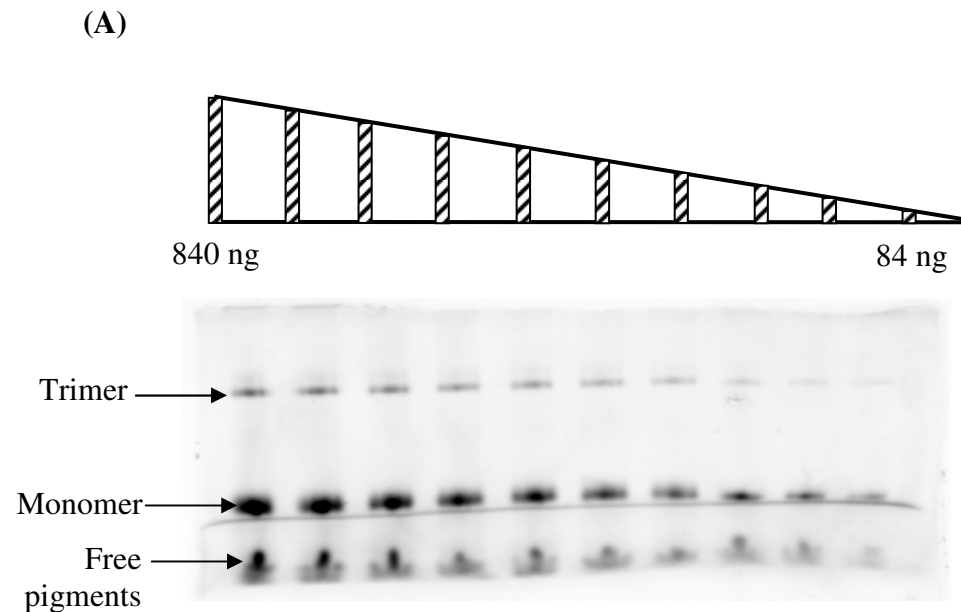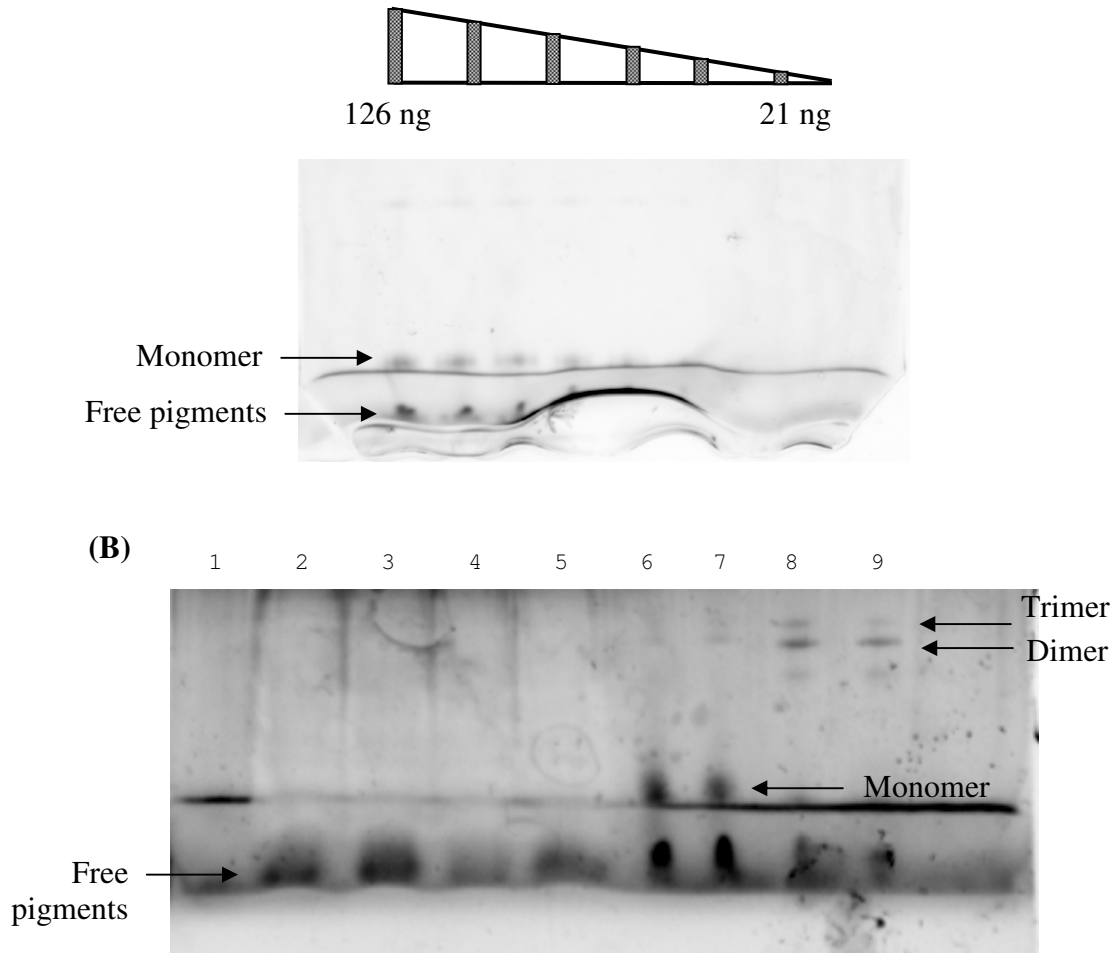
Figure 3.22 Separation of *in vitro* translated proteins by partially denaturing gel.
(A) LHCII reconstituted from bacterially-expressed LHCP and pigments as standards
to determine the detection limit of the method; (B) pLHCP was expressed in coupled
wheat germ extracts in the presence of pigment-containing vesicles. Lanes 2-3,
expression of pLHCP in the presence of 0.2 and 0.4 mg/mL lipid mixture of
DG/MG/PG (3:3:4, mol%), respectively; lanes 3-4, expression of pLHCP in the
presence of 0.2 and 0.4 mg/mL PG, respectively; lanes 6-9, reconstituted LHCII as a
positive control.

3.4.2 Digestion products analyzed by autoradiography

3.4.2.1 Digestion assays of LHCP synthesized in the absence of added lipids

The western blotting analysis of the digestion assays did not reveal any perceptible difference in the proteolytic fragments. A 20-kDa digestion product was observed for both proteins synthesized in the presence and absence of supplemented lipids. Probably there exists membrane fragments or chaperones in the wheat germ extracts, which serve as hydrophobic environments for the protection of the nascent LHCP against protease digestion. Autoradiography, due to its sensitiveness, was employed to analyze the proteolytic fragments of the digestion assays. *In vitro* translated proteins were labeled with [^{35}S]-Methionine as described in section 2.3. The digestion assays started with mLHCP synthesized in the absence of supplemented lipids. After protein synthesis, mLHCP was either treated with thermolysin or trypsin, with protease concentration set to 0.1, 0.2 and 0.5 mg/mL. The digestion was conducted at 25 °C for 30 min.

Figure 3.23 shows the autoradiography analysis of the digestion assays. The treatment of mLHCP with either thermolysin or trypsin generated several digestion bands. While in western blotting analysis, only one band of 20 kDa was observed. The protein bands of lower molecular masses shown in autoradiography were not detectable in western blotting analysis. This is probably because these smaller fragments do not contain any epitopes that can be recognized by anti-LHC antibody. Proteins were less degraded when treated with trypsin. This is not surprising since trypsin has fewer cutting sites in the protein sequence, as analyzed by program PeptideCutter [80]. Though investigations have shown that when the LHCP was correctly integrated into isolated thylakoids, treatment of the protein with either thermolysin or trypsin generated the same digestion products [76,77].

Treating mLHCP with thermolysin led to digestion products mainly around 10 and 7 kDa, together with undefined bands in between 3-6 kDa. Fragment around 20 kDa was observed with 0.1 mg/mL thermolysin. This is consistent with the result from western blotting analysis. When increasing thermolysin concentration, the 20-kDa fragment

was further degraded. Based on the calculation in Figure 3.16, the size of TM1-L1-TM2 is 10 kDa, while TM3-C terminus has a molecular mass of 7 kDa. The loop L2 and N-terminal amino acids are accessible to protease digestion. In the case of protease trypsin, the digestion products had apparently larger molecular masses. Increasing trypsin concentration from 0.1 to 0.5 mg/mL did not affect much of the final proteolytic fragments. The ~20-kDa fragments may correspond to the amino acids of TM1 till C terminus. According to analysis using PeptideCutter program, trypsin doesn't have cutting sites in the amino acid sequence of loop L2.
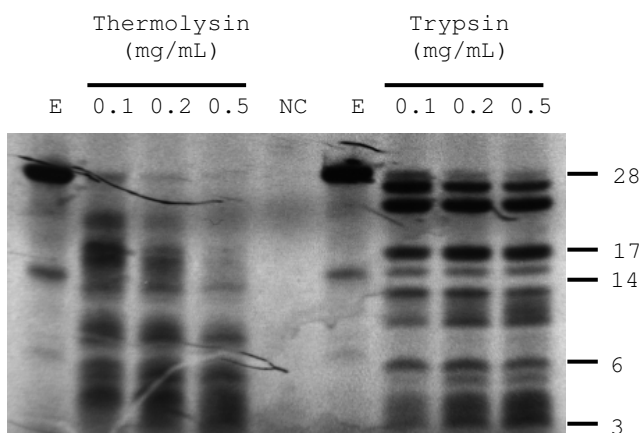
Figure 3.23 Digestion assays of mLHCP expressed in the absence of supplemented lipids. E, mLHCP expressed in wheat germ extrcats; NC, reaction mixture without DNA template.

To investigate the effect of detergent on the digestion assays, reaction mixture was treated with detergent (1% OG, 0.1% or 0.5% DM) before the addition of protease. The detergent treatment was carried at 25°C for 30 min, followed by treatment with thermolysin or trysin. The final concentration of the protease was 0.1 mg/mL. The result is shown in Figure 3.24. Generally, the protease worked well in the presence of detergent, with an exception that the activity of thermolysin was fairly affected with 1% OG (lane 1). A clear difference between the digestion products shown in Figure 3.23 and Figure 3.24 was that fragments smaller than 10 kDa for thermolysin and fragments smaller than 20 kDa for trypsin were decreased when the reaction mixture was treated with detergent prior to protease digestion. These 'detergent-sensitive' fragment were then considered to be associated with lipids that were present in the wheat germ extracts. Upon solubilization of the reaction mixture with detergent, the

lipids no longer protected the proteins against protease digestion. Treating the detergent-solubilized reaction mixture with either protease led to more degradation of the proteins.
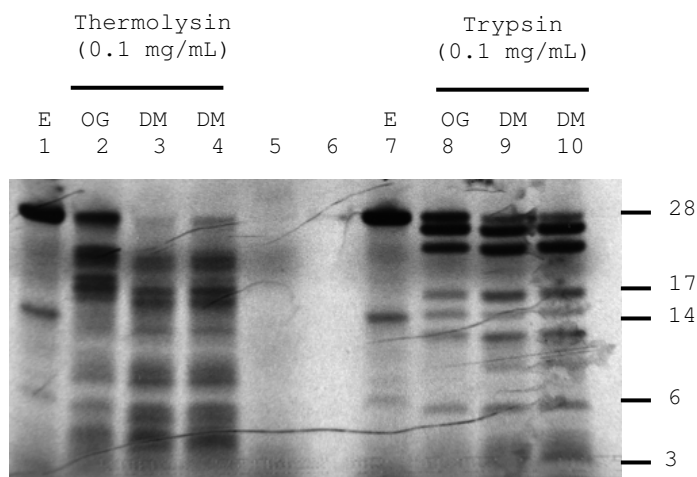
Figure 3.24 Digestion assays of detergent-solubilized mLHCP. mLHCP was synthesized in wheat germ extracts in the absence of added lipids. Lanes 1 and 7, mLHCP expressed in wheat germ extracts; lanes 2-4, thermolysin digestion products of detergent-solubilized mLHCP; lane 5, reaction mixture without added DNA; lane 6, blank; lanes 8-10, trypsin digestion products of mLHCP. The detergents added: lanes 2 and 8, 1% OG; lanes 3 and 9, 0.1% DM; lanes 4 and 10, 0.5% DM.

3.4.2.2 Digestion assays of LHCP synthesized in the presence of added lipids

The digestion assays of proteins translated in the absence of supplemented lipids showed that the proteins were protease-resistant. Western blotting analysis indicated that the addition of DPPG or PG at certain concentration positively affected the productivity of protein expression. However, when subject to protease digestion, the lipid-assisted synthesized protein did not necessarily result in more digestion products. To be more accurate before drawing a conclusion, digestion assays were performed with proteins synthesized in wheat germ extracts in the presence of added lipids. DOPC vesicles were added to the system with final lipid concentration of 0.1 mg/mL. After expression, the protein was treated with trypsin by incubating the mixture at 25°C for 30 min. The result is shown in Figure 3.25.
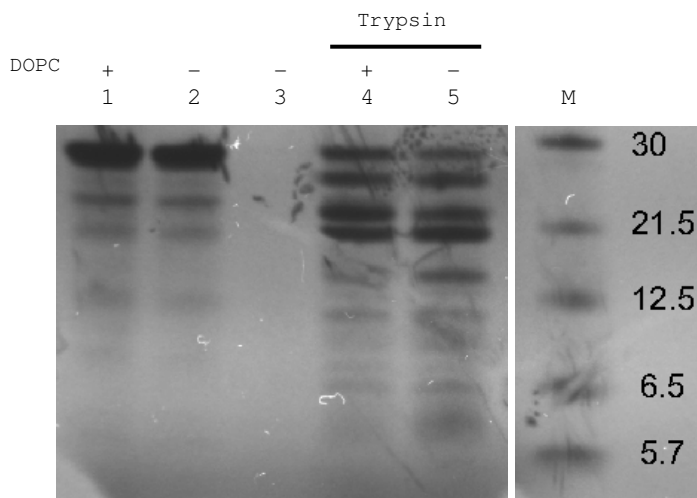
Figure 3.25 Digestion assays of pLHCP expressed in coupled wheat germ extracts with or without DOPC vesicles. Lane 1, pLHCP synthesized in the presence of DOPC; lane 2, pLHCP synthesized in the absence of DOPC; lane 3, reaction mixture without DNA; lanes 4-5, digestion products of samples in lanes 1-2, respectively.

Pigment-containing vesicles, prepared either from PG or a mixture of DG/MG/PG, were added to the reaction mixture, with final lipid concentration set to 0.1 mg/mL. After protein synthesis, the reaction mixture was treated with 0.1 mg/mL trypsin. The digestion products were separated by SDS-PAGE and analyzed by autoradiography. The result is shown in Figure 3.26. The addition of pigment-containing vesicles did not have detectable influence on the digestion products. The proteolytic fragments of pLHCP and mLHCP were of the same molecular masses (only fragments smaller than mLHCP were compared), suggesting that except the amino acids of the transit sequence, pLHCP and mLHCP were protected in a similar way.
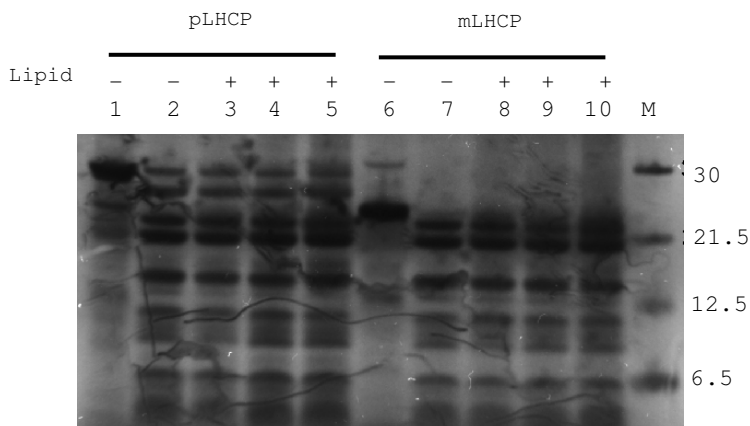
Figure 3.26 Digestion assays of pLHCP/mLHCP expressed in coupled wheat germ extracts with or without pigment-containing vesicles. Lanes 1 and 6, pLHCP and

mLHCP synthesized in the absence of added lipids; lanes 2-6, digestion products of pLHCP synthesized in the presence or absence of lipids; lanes 7-10, digestion products of mLHCP synthesized with or without added lipids; M, protein maker. The pigment-containing vesicles added: lanes 3 and 8, DG/MG/PG (3:3:4, mol%); lanes 4 and 9, DG/MG/PG (2:2:4, mol%); lanes 5 and 10, PG.

3.4.2.3 Proteins in the supernatant were protease-resistant

Proteins were synthesized in coupled wheat germ extracts, with or without supplemented DPPG SUVs. The final lipid concentration in the reaction mixture was 0.5 mg/mL. After cell-free protein synthesis, 5 µL out of the 50-µL reaction mixture was retained for later SDS-PAGE. The rest was centrifuged at 10,000 g for 15 min at room temperature (RT). A pellet could be seen at the bottom of the tube. The supernatant was taken out to a new tube, and the pellet was resuspended with 40 µL water. 18 µL of the supernatant or resuspended pellet solution was mixed with 2 µL thermolysin (1 mg/mL), and the mixture was incubated at 25 °C for 30 min. The procedure is illustrated in Figure 3.27 and the results are shown in Figure 3.28.
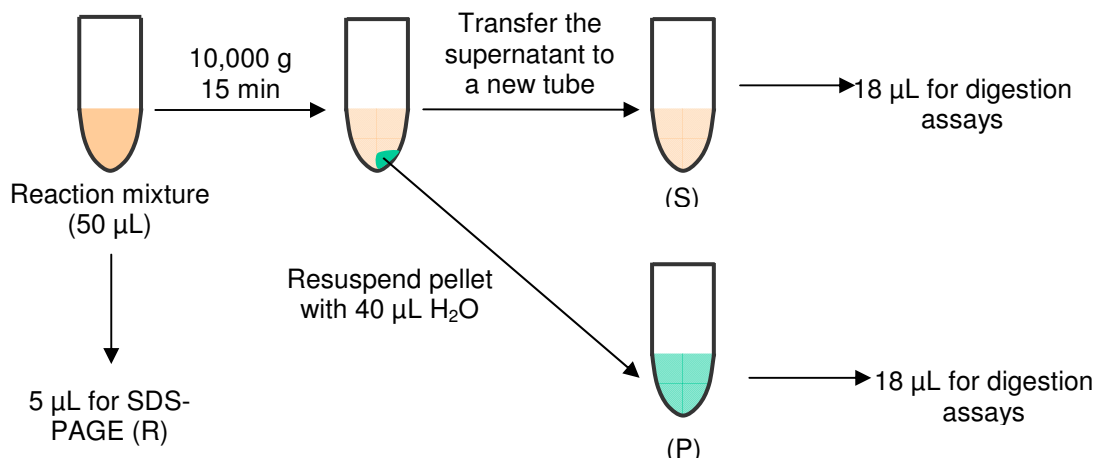
Figure 3.27 Centrifugation of reaction mixture.

After centrifugation, the target proteins were present both in the supernatant and in the resuspended pellet solution. Treating the protein in the pellet part with the protease thermolysin led to the total degradation of both pLHCP and mLHCP as no fragments could be detected (lanes 5 and 11). LHCP in the supernatant, however, was partially protected (lanes 3 and 9). The digestion patterns were consistent with the results above.

A possible explanation for this is, after translation in wheat germ extracts, pLHCP or mLHCP exits in the reaction mixture in two different forms, as precipitates and in soluble form. When treated with protease, the precipitates were completely degraded since there was no hydrophobic environment or chaperones to keep the proteins in a soluble status. While proteins retained in the supernatant was protected against protease digestion. The addition of lipids did not have detectable effect on the digestion products.
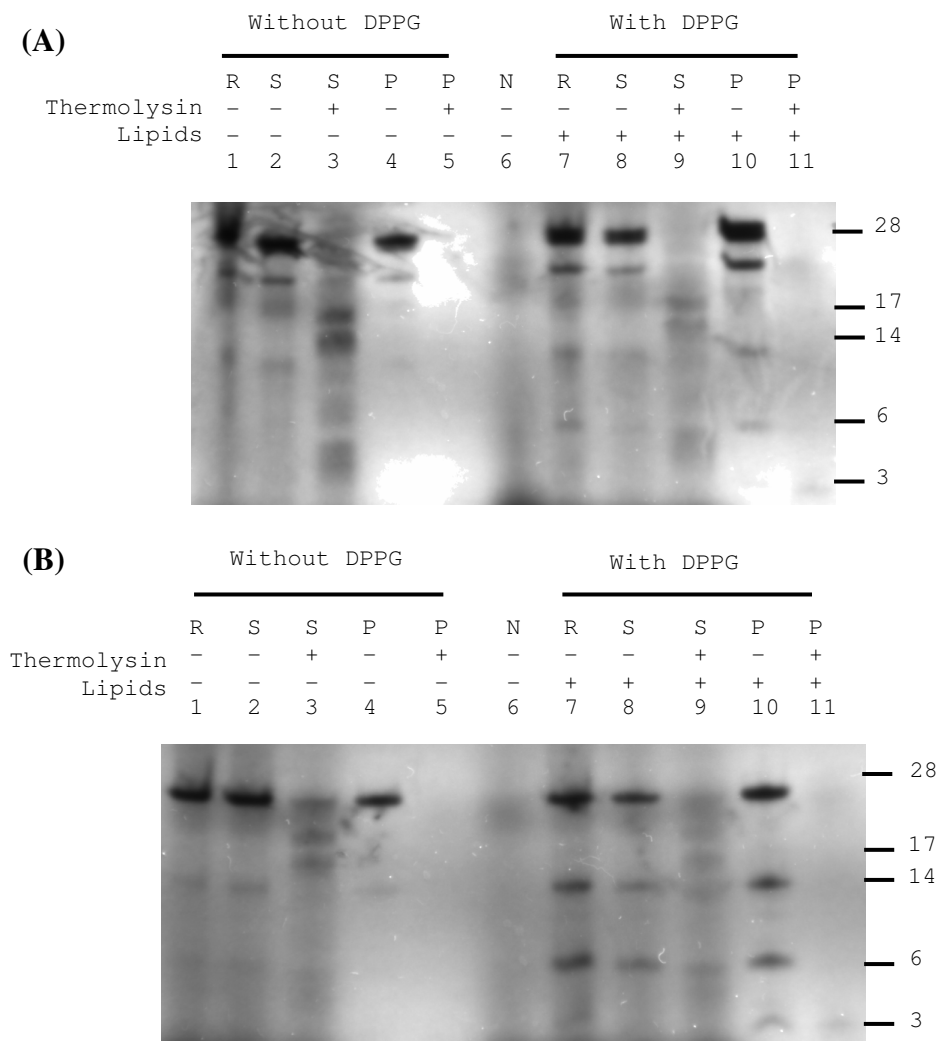
Figure 3.28 Proteins in the supernatant part are protease-resistant.

(A) pLHCP was expressed in the presence or absence of DPPG, and was treated with thermolysin. Lane 1, pLHCP synthesized in the absence of DPPG; lane 2, pLHCP in the supernatant; lane 3, digestion of pLHCP in the supernatant; lane 4, pLHCP in the pellet; lane 5, digestion of pLHCP in the pellet; lane 6, reaction mixture without added DNA; lanes 7-11 .

(B) mLHCP was expressed in the presence or absence of DPPG, and was treated with thermolysin. Lane 1, reaction mixture of pLHCP in the absence of DPPG; lane 2, supernatant of reaction mixture; lane 3, digestion of supernatant; lane 4, pellet; lane 5, digestion of pellet; lane 6, reaction mixture containing no DNA; lane 7, reaction mixture.

3.5 Proteins synthesized by recombinant system "PURExpress"

The PURExpress system is a recombinant cell-free protein synthesis system, which is entirely reconstituted from purified components required for the *E. coli* translation reaction. This flexible system is supposed to be lipid-free. As every component in the kit is recombinant, there should be no meaningful amounts of membrane fragments in such a system. The intension to employ the recombinant expression kit was to see what the proteolytic fragments would look like when the proteins were synthesized in a lipid-free environment. The reactions using the PURE system were assembles according to the protocol. After protein synthesis, the reaction mixture was treated either with thermolysin or trypsin. The final protease concentration was 0.1 mg/mL. The digestion assays were conducted at 25°C for 30 min.

The results of the expression of pLHCP in PURE system and the subsequent treatment with 0.1 mg/mL of thermolysin or trypsin are shown in Figure 3.29. SUVs prepared from either plant lipid PG or mixture of DG/MG/PG (3:3:4, mol%) or DOPC were supplemented to the system, with final lipid concentration of 0.1 mg/mL in the reaction mixture. By comparing the intensity of the synthesized protein band in a reaction minus lipids to that of a reaction plus lipids, it was clear the addition of lipids did not have obvious positive or negative effect on the general productivity of the system. The 6-kDa band is possibly labeled tRNA, which appeared in every lane including the negative control (lane 1).

After the as synthesized proteins were treated with thermolysin ot trypsin, the original protein bands gone, indicating that both proteases worked well in this system. After digestion, no corresponding digestion products can be observed as shown in the digestion assays of proteins synthesized in wheat germ extracts. The membrane protein

synthesized in a lipid-free environment would therefore form precipitates as no substantial amount of hydrophobic environments are present to keep the proteins soluble after translation. The formed precipitates seemed to be accessible to protease digestion since no membranes or chaperones are round to protect the proteins against proteolytic digestion. This is however in consistent with our observations. As shown in Figure 3.28, when proteins were synthesized in wheat germ extract systems, part of the proteins ended up in precipitates, which could be spun down by table-top centrifugation. And the digestion assays of the 'pellet' showed that the proteins were completely digested. While the proteins left in the 'superntant' part were protease-resistant. Unforturenately the supplemented lipids to the PURE system could not serve as suitable hydrophobic environment for the proteins, which provided a hint that special translocation machineries were missing in the system.
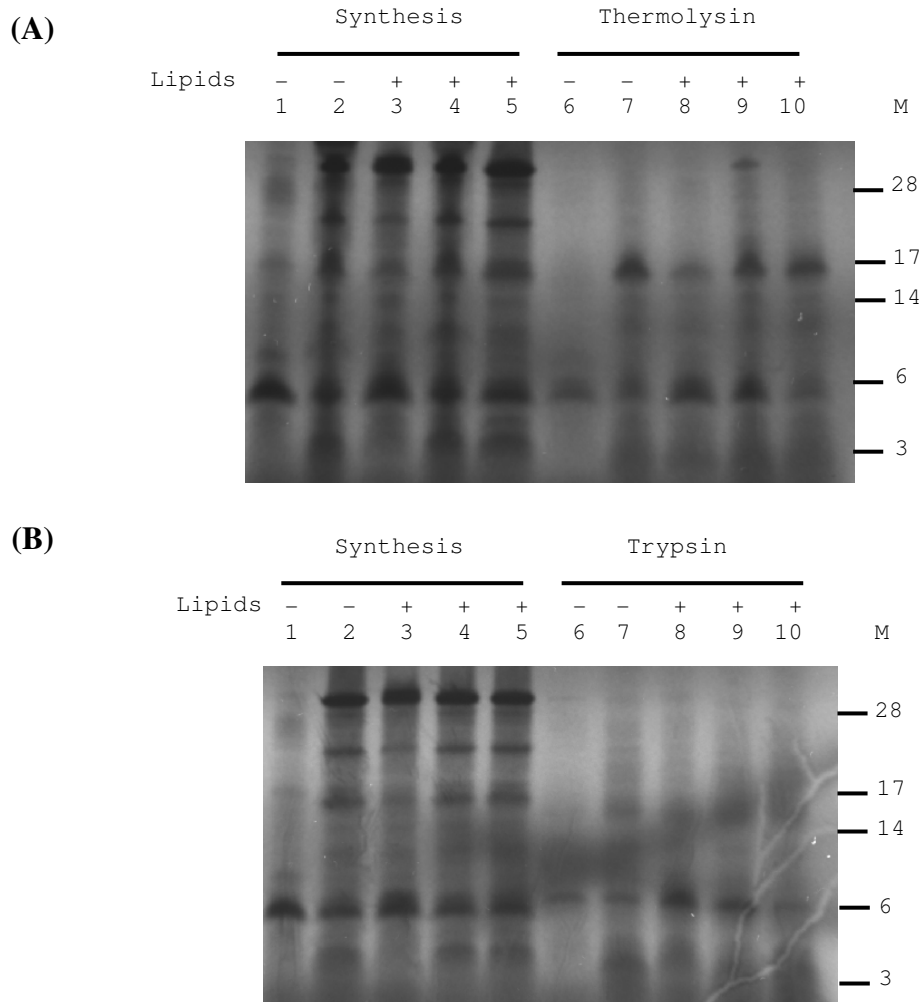
Figure 3.29 The expression of pLHCP in PURE systems in the presence or absence of supplemented lipids and protease treatment.

(A) Lane 1, reaction mixture containing no DNA template; lane 2, protein synthesis without added lipids; lanes 3-5, protein synthesis in the presence of PG (lane 3), mixture of DG/MG/PG (lane 4) and DOPC (lane 5); lanes 6-10, thermolysin treatment of samples in lanes 1-5, repectively. M, protein marker (kDa).

(B) Lanes 1-5 were the same as lanes 1-5 in (A), respectively; lanes 6-10, trypsin treatment of samples in lanes 1-5, respectively.

3.6 Rehydration of lipid film with reaction mixture

3.6.1 Parallel protein synthesis and vesicles formation

As shown in Figure 3.3, the incubation of the wheat germ extract reaction system with giant vesicles prepared in 200 mM sucrose led to the collapse of the vesicles, probably due to the osmotic pressure difference between outside and inside of the vesicles. Alternatively, the giant vesicles were introduced to the system by the direct hydration of lipid film using cell-free reaction mixtures as depicted in Figure 3.30. Firstly, a lipid film was deposited to the bottom of a glass tube (35×12 mm, Schuett Biotec GmbH), dried with a stream of nitrogen, and put in a desiccator for 1.5 h to remove residual organic solvent; then the freshly-assembled 50-µL reaction mixture in a plastic tube was transferred to the glass tube; (3) then the glass tube was capped and incubated at 30°C for 2 h (Hera Cell). During incubation, the protein synthesis and vesicles formation performed parallel. The giant vesicle would stay stable since there was supposed to be no obvious difference in the osmotic pressure outside and inside of the vesicles.
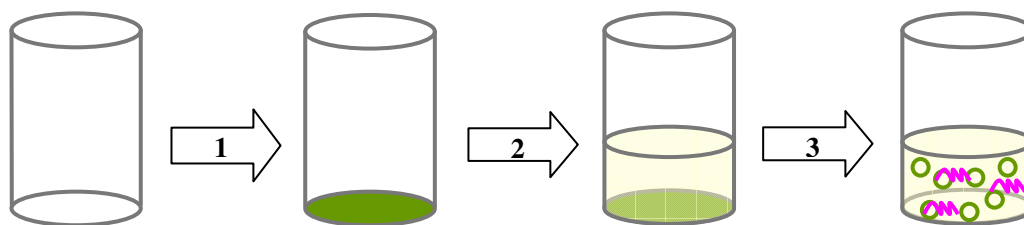
Figure 3.30 Direct rehydration of lipid film with cell-free protein synthesis reaction mixture. (1) deposition of lipid film on the bottom of glass tubes; (2) rehydration of lipid film with reaction mixture and (3) protein synthesis (purple lines) and vesicles formation (green circles) during incubation.

Either 2 µL or 4 µL of lipid PG (5 mg/mL in chloroform) were deposited on the bottom of glass tubes. So the final lipid concentration in the reaction mixture was 0,2 or 0,4 mg/mL. The glass tubes were then put in a desiccator for at least 1.5 h to remove residual chloroform. The lipid film was then rehydrated with 50-µL reaction mixture of wheat germ extract systems. As a control, 50-µL reaction mixture was also added to a glass tube without deposited lipid film. After incubation at 30°C for 2 h (Hera Cell), the reaction mixture was transferred to plastic tubes. 5 µL of the reaction mixture from each sample was diluted with 200 µL PBS in a plastic chamber (ibidi, 80821) for the observation under microscope. 5 µL of each sample were retained for SDS-PAGE and western blotting analysis. The rest of the reaction mixture was centrifuged at 10,000 g for 15 min with a table-top centrifuge at room temperature. The supernatant (S, ~40 µL) was transferred to a new tube, while the pellet (P) was resuspended with water or desired buffer. 5 µL of supernatant or pellet were diluted with PBS in hydrophobic chambers for microscopy observation.

3.6.2 Characterization of the giant vesicles

Figure 3.31 shows the microscopy images of the crude reaction mixture after incubation at 30°C for 2 h (a), the supernatant (b) and the resuspended pellet after centrifugation (c). The white arrows in (a) indicate the formed PG giant vesicles, showing a different morphology as compared to the giant PG vesicles prepared by spontaneous swelling of lipid film using water as rehydration buffer (Figure 3.2c). Probably the components in the crude wheat germ extract bind to the formed vesicles. Also the ions in the extract may influence the formation of giant vesicles.

After centrifugation at 10,000 g for 15 min, the vesicles were mainly found in the supernatant part (b). However, the attempt to use immunofluorescence to detect the presence of *in vitro* translated LHCP in the giant vesicles failed. The unspecific binding of the secondary antibody to the giant vesicles made it difficult to tell any difference of the fluorescence in the positive and negative controls. As an alternative,

GFP could be fused to the either N- or C-terminus of the protein and used as a built-in fluorescence marker for the expression of LHCP. The unspecific antibody binding can therefore be avoided. It has been shown that fusion with GFP at the N-terminus did not seriously interfere with LHCP insertion into thylakoids *in vitro* [76]. Though a different strategy is employed here, it might be worth a try for future reference.
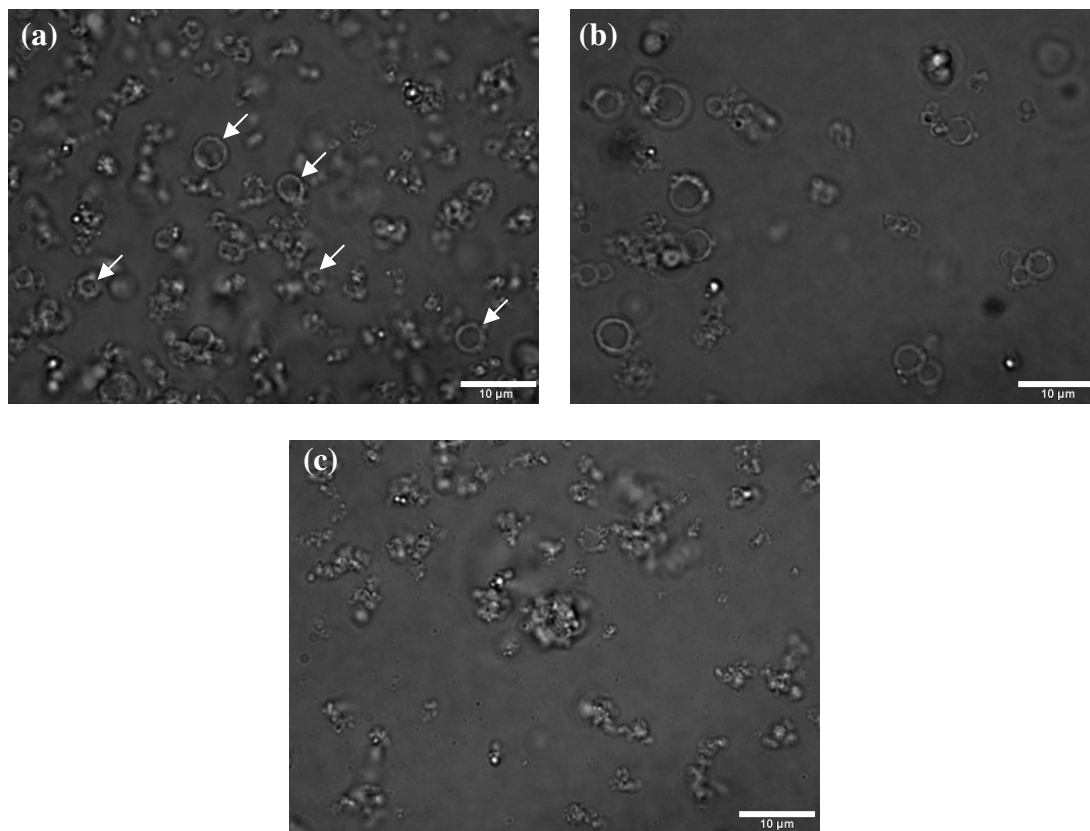
Figure 3.31 Microscopy images of the crude reaction mixture (a), supernatant after centrifugation at 10,000 g for 15 min (b), and pellet resuspended with PBS (c). The reaction mixture was used to rehydrate the lipid film of 4 µL of PG (5 mg/mL). The arrows in (a) indicate the formed giant vesicles during incubation. Scale bar, 10 µm.

3.6.3 Western blotting analysis of the proteins

The protein productivity in this kind of expression format was analyzed by western blotting as shown in Figure 3.32. The proteins were expressed in all three samples. After centrifugation at 10,000 g for 15 min, the proteins were present in both the

supernatant part and pellet part. The expression level was slightly higher in the presence of lipids. In the pellet part, more proteins were observed when the reaction mixture containing supplemented lipids (compare the intensity of P2 and P3 to that of P1).
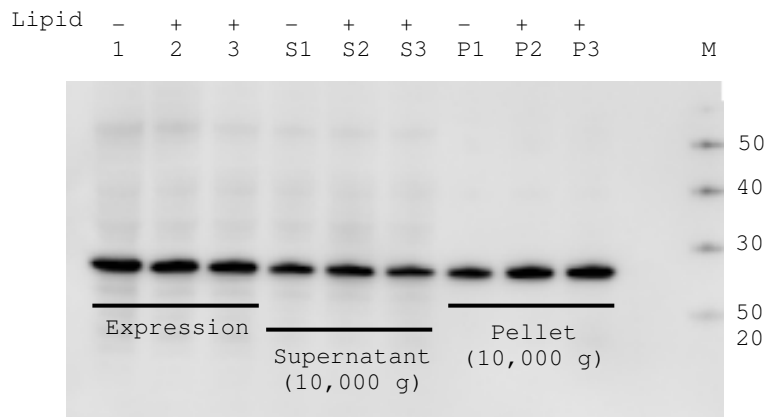
Figure 3.32 Western blotting analysis of VSV-mLHCP synthesized in coupled wheat germ extracts in glass tubes. Lane 1, reaction mixture of standard reaction containing no supplemented lipid; lanes 2 and 3, reaction mixture containing 0.2 and 0.4 mg/mL lipid, respectively. S1-S3, supernatant of reactions in 1-3, respectively; P1-P3, pellet of reaction in 1-3, respectively. The blot was probed with anti-VSV antibody. Exposure time, 14 min.

To further isolate the vesicles in the supernatant, ultracentrifugation was performed. 25 µL of the supernatant was diluted with 25 µL PBS and centrifuged at 100,000 g for 1 hr at room temperature (Beckman Coulter Optima231). After ultracentrifugation, the upper 25 µL was collected into a new tube as USx, and the lower 25 µL was vortexed (UPx). Samples of 5 µL from USx or UPx were prepared for SDS-PAGE and western blotting analysis. The procedure and nomenclature of samples are schematically illustrated as shown in Figure 3.33.
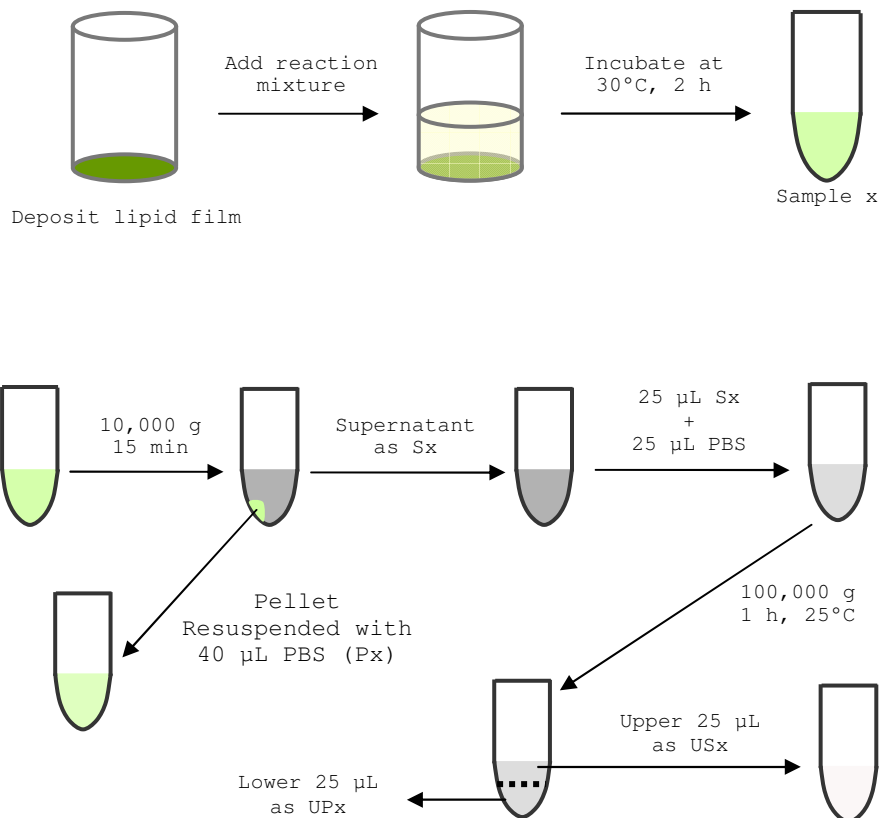
Figure 3.33 Schematic illustration of the centrifugation procedure used for the separation of aggregated LHCP and lipid-associated LHCP. After ultracentrifugation, the upper 25 µL was transferred to a new tube and the lower 25 µL was vortexed.

The first result of ultracentrifugation is shown in Figure 3.34. The supernatant of samples in Figure 3.32 after table-top centrifugation were analyzed. 25 µL of the supernatant were diluted with 25 µL PBS and then ultracentrifuged. Also cell-free expression in plastic tubes without supplemented lipids was included as controls (lanes 4-5). After protein synthesis, reaction mixtures were first centrifuged with table-top centrifuge; 25 µL out of the supernatant part were diluted to 50 µL and went to ultracentrifugation as those samples in the glass tubes. Western blotting analysis showed that after ultracentrifugation, the protein that was present in the supernatant part after table-top centrifugation was found mainly in the lower 25 µL (lanes 1-5). One exception was sample in lane 7. The tube containing sample 7/2 was dropped to the ground by accident after ultracentrifugation, so a weak protein band appeared in the upper 25 µL of the sample.
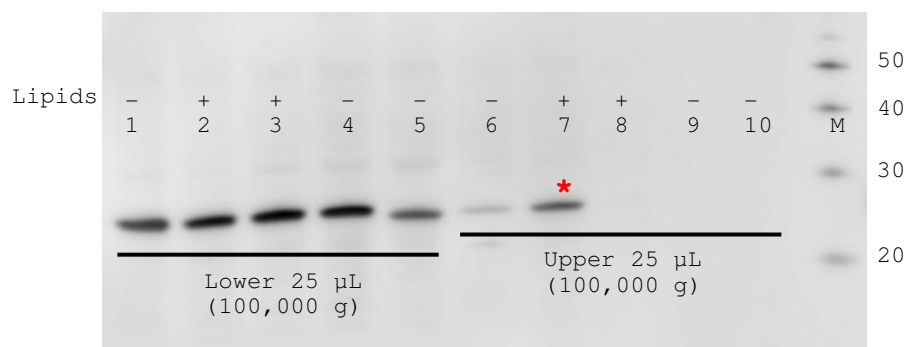
Figure 3.34 Centrifugation of VSV-mLHCP synthesized in the wheat germ extracts. After centrifugation at 10,000 g for 15 min, the supernatant of cell-free proteins synthesis in glass tubes with or without deposited lipid films were ultracentrifuged. The lower 25 µL (lanes 1-3) and upper 25 µL (lanes 6-8) were analyzed by western blotting. Supernatant of reaction mixtures of protein synthesis in plastic tubes without added lipids was also ultracentrifuged and analyzed (lanes 4-5, 9-10). M, magic marker XP (kDa). The blot was detected with anti-VSV antibody. Exposure time, 12 min.

The experiments were repeated. 4×50-µL standard cell-free reactions containing plasmids encoding VSV-mLHCP were assembled in plastic tubes on ice. The reactions were added to glass tubes which were deposited beforehand without or with 2/4/8 µL of lipid PG (5 mg/mL in chloroform). The four samples were named 1-4, respectively. The final lipid concentration in the reaction mixture was 0, 0.2, 0.4 and 0.8 mg/mL for samples 1-4, respectively. After incubation at 30 °C for 2 h, the crude reaction mixture was transferred from the glass tubes to new plastic tubes. 5 µL of each sample was retained for western blotting analysis. The rest of reaction mixture was centrifuged at 10,000 g for 15 min at RT. The resuspended pellet solution of samples 1-4 were labeled as P1-P4, respectively; the supernatant as S1-S4. The ultracentrifugation was carried out as illustrated in Figure 3.33. The upper 25 µL after ultracentrifugation was collected and names US1-US4, while the lower 25 µL as UP1-UP4. 5 µL of each sample during the whole procedure were retained for western blotting analysis. The result is shown in Figure 3.35.

Lanes 1-4 are the crude reactions mixtures. As we observed before, the presence of lipids at 0.2 and 0.4 mg/mL were beneficial to the expression efficiency (lanes 2 and 3); while when the lipid concentration reached 0.8 mg/mL, the productivity decreased considerably (lane 4). So the addition of lipids to the system either in the form of

vesicles or by direct rehydration of lipid film with reaction mixture have affected the general expression efficiency in a similar way. After centrifugation at 10,000 g, the pellet was resuspended (P1-P4). The expression level was higher for sample 2 and 3, with more protein expressed in the reaction mixture. But the 'extra' part of the protein seemed to end up in precipitates, which could be centrifuged down together with other components in the wheat germ extract. The intensities of band for P2 and P3 were higher than that of P1, where no lipid was added. While for P4, the initial expression was inhibited, so a weaker band was shown as expected. For the protein left in the supernatant part (S1-S4), the intensity of S1 was higher than those of S2 and S3, indicating that without the addition of lipids, more of the synthesized proteins remained in the supernatant part. As demonstrated in the digestion assays, proteins in the supernatant were protease-resistant, while in the pellet were not protected against protease digestion. After centrifugation, the proteins were found in the lower 25 µL part. The intensities of UP1-UP4 should be corresponding to those of S1-S4, respectively, since no clear bands were shown in US1-US4. The intensity of UP3 was much higher that those of UP1 and UP4.
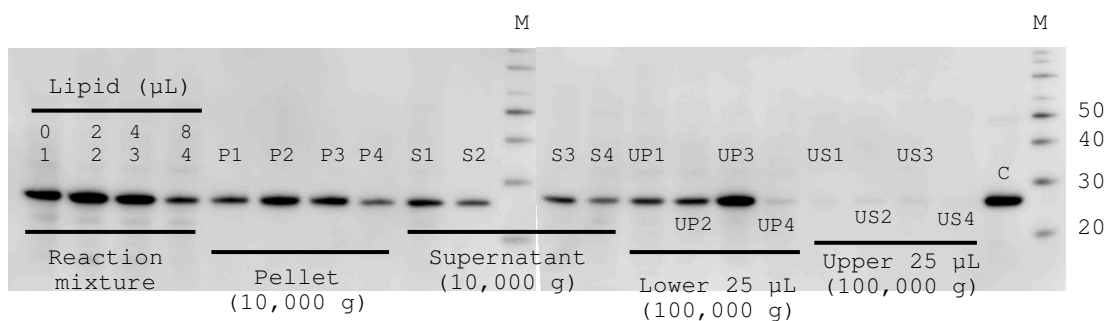
Figure 3.35 Cell-free expression of VSV-mLHCP in coupled wheat germ extracts. Lanes 1-4, reaction mixtures; P1-P4, pellet resuspended after centrifugation at 10,000 g, 15 min; S1-S4, supernatant part after centrifugation at 10,000 g, 15 min; UP1-UP4, lower 25 µL after ultracentrifugation; US1-US4, upper 25 µL after ultracentrifugation. C, VSV-mLHCP synthesized in tube. The blot was detected with anti-VSV antibody. Exposure time, 10 min.

To exclude the possibility of pipetting errors, the experiment was repeated again. Two reactions were prepared: sample 1, 50-µL reaction mixture were added to a glass tube without deposited lipid film; sample 2, 50-µL reaction mixture were added to a glass tube which was deposited with 4-µL lipid PG (5 mg/mL). So the final lipid concentration in sample 2 was 0.4 mg/mL. The reaction was incubated and centrifuged

as before. The western blotting analysis is shown in Figure 3.15. The expression efficiency was enhanced in the presence of lipids (lane 2), while more protein was found as precipitates (P2). The supernatant part of standard reaction contained more synthesized protein (S1) than that of lipid-assisted reaction (S2).
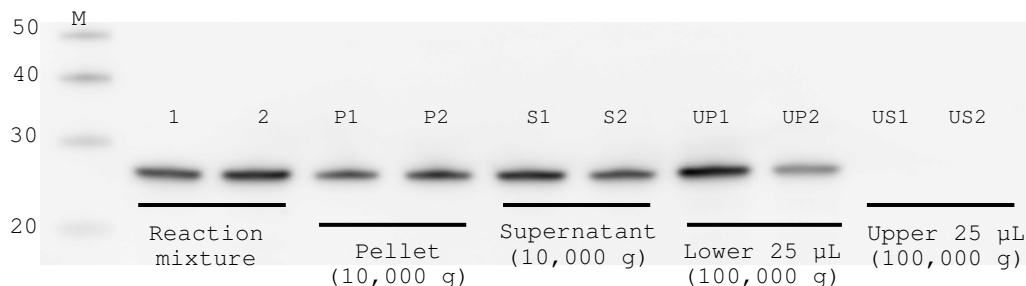
Figure 3.36 Cell-free expression of VSV-mLHCP in coupled wheat germ extracts. Lanes 1-2, reaction mixtures; P1-P2, pellet resuspended after centrifugation at 10,000 g, 15 min; S1-S2, supernatant part after centrifugation at 10,000 g, 15 min; UP1-UP2, lower 25 µL after ultracentrifugation; US1-US2, upper 25 µL after ultracentrifugation. The blot was detected with anti-VSV antibody. Exposure time, 28 min.

3.7 Topological studies by SPR and SPFS measurements

3.7.1 The principle

The idea to employ SPR/SPFS as a tool to measure the topography of the protein in the membranes is based on the principle as depicted in Figure 3.37. The orientation of *in vitro* translated OP5, a member of G-protein coupled receptor family, into artificial membranes has been verified using this method by Robelek et al [22]. Taking LHCP as an example, after successful integration of proteins into the lipid bilayers, the N-terminus is exposed to the outside of the membrane, which is accessible to the binding of antibody that recognizes the N-terminal sequence. The C-terminus, however, on the inside of the membranes, is not available to antibody binding. Taking advantage of the engineered VSV tag at either N- or C-terminus of LHCP, the orientation of proteins in the membranes can be investigated.
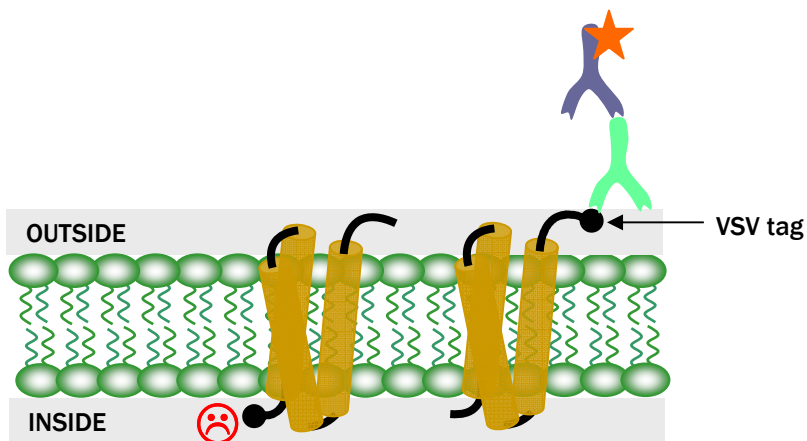
Figure 3.37 Principle of employing SPR and SPFS measurement for the topological study of proteins integrated into membranes.

3.7.2 Build up the surface

The experiment started with the biotinylated thiol monolayer already on the gold substrate in the SPR flow cell, which was described in section 2.2.5. Streptavidin (0.5 µM in PBS) was injected into the flow cell. A typical binding curve of streptavidin to the biotinyl thiol-coated gold surface is shown in Figure 3.38, in which the substrate was incubated with streptavidin for ~30 min, followed by a buffer rinsing for ~15 min. The thickness of the streptavidin layer was calculated to be ~4 nm.
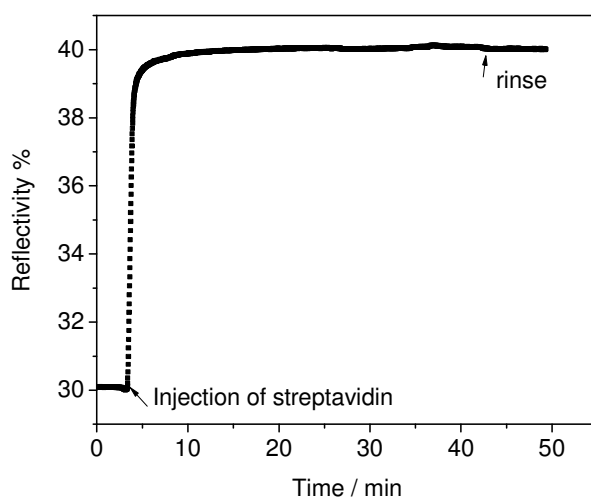
Figure 3.38 Typical binding curves of streptavidin on the mixed biotin-thiol/thiol layer on gold surface.

Biotinylated SUVs were prepared as described in 2.2.2. After rinsing, freshly prepared SUVs in PBS were injected to the flow cell. The SPR response for a typical experimental sequence to study biotinylated vesicles binding to streptavidin on gold surface is shown in Figure 3.39 (blue). The addition of biotinylated vesicles resulted in an obvious change in the reflectivity of SPR scan. The vesicles were incubated on the surface for 90 min and then the surface was rinsed with PBS for 10 min. Two control experiments were performed to demonstrate that the vesicles were attached to the surface *via* biotin-streptavidin interaction, but not physisorption. In one control experiment, the gold surface was coated with biotinylated thiol and then incubated with streptavidin; following rinsing, vesicles containing no biotin groups were injected to the flow cell. The SPR scan is shown in Figure 3.39 (red). Only minor change in reflectivity was observed. In the other control, biotinylated vesicles were directly injected onto the surface of biotiny thiol-coated gold substrates (purple). Without streptavidin acting as a linker between the vesicles and the surface, the biotinylated vesicles were not attached to the surface.
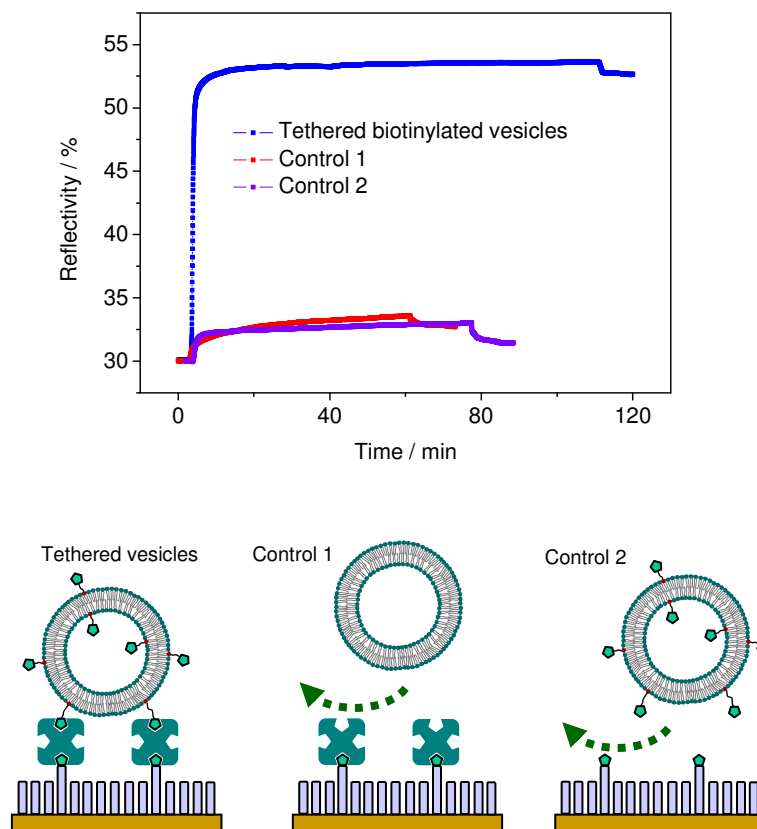
Figure 3.39 Kinetic scan of biotinylated vesicles binding to streptavidin modified gold surface. In control experiments, vesicles without biotinylated PE lipid were also

incubated on the streptavidin-coated gold surface (red); or biotinylated vesicles were directly incubated on biotin thiol-coated gold surface without streptavidin as a linker (purple).

3.7.3 Incubation of *in vitro* mixture

A typical 50-µL reaction was assembled on ice in plastic tubes right after the surface with tethered vesicles was ready. The reaction mixture was injected to the flow cell and incubated at ~30°C for 90 min. The temperature of the flow cell is not controlled. A lamp was placed closed to the flow cell to heat up the reaction mixture. The temperature was monitored with a thermometer. After incubation, the reaction mixture was collected and the surface was rinsed with PBS for 10 min. Problem with this procedure was that the expression efficiency was not as controllable as that of batch reactions, which were incubated in heating blocks.

Alternatively, the biotinylated vesicles were added directly to the reaction mixture. Biotinylated vesicles were prepared in PBS from a lipid mixture composed of DG/MG/PG (3:3:4, mol%). The vesicles were added to cell-free protein synthesis system at a lipid concentration of 0.1 mg/mL. Protein synthesis was conducted by incubating the reaction mixture at 30°C for 90 min. After protein synthesis, the 50-µL reaction mixture containing the biotinylated vesicles were injected into the flow cell and incubated at RT for 30 min. After incubation, the reaction mixture was collected and the surface was rinsed with PBS for 10 min. The surface was blocked with 1% western blocking reagent (Roche) for 30 min. Following rinsing, primary antibody, anti-VSV, was injected and incubated on the surface for 1 hour. The unbound antibody was rinsed with PBS for 10 min. The kinetic of the reflectivity change upon the injection of the reaction mixture till the rinsing of primary antibody with PBS was recorded. The SPR spectroscopy is shown in Figure 3.40. Then the secondary antibody, Cy5-labeled goat-anti-mouse IgG was injected into the flow cell and incubated for 30 min. The fluorescence kinetic of the binding of the secondary antibody was recorded. The surface was then rinsed with PBS for 10 min. The SPR reflectivity and the fluorescence angular scan were recorded (Figure 3.41).
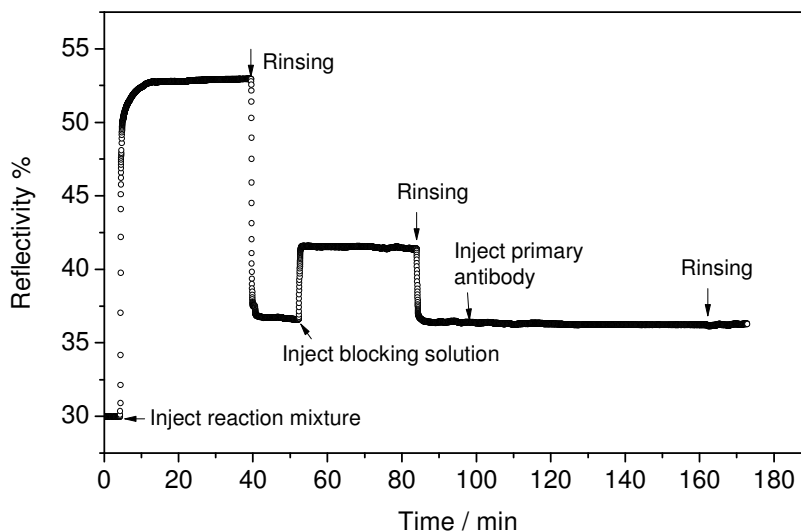
Figure 3.40 A typical kinetic curve of reflectivity change upon injection of reaction mixture till the rinsing of primary antibody with PBS.
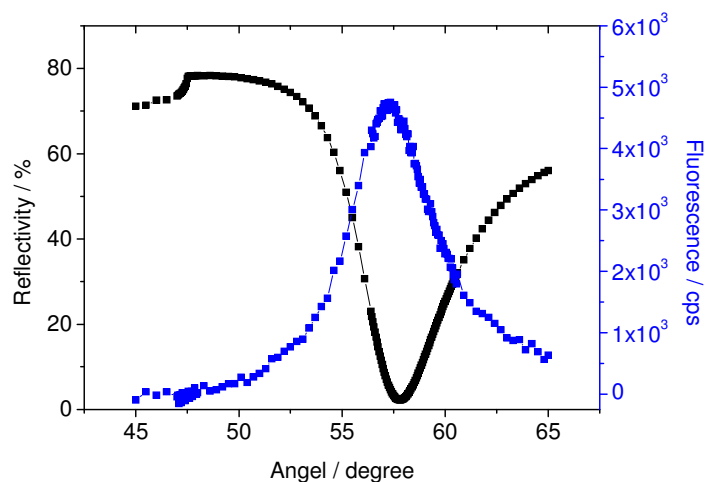
Figure 3.41 Typical SPR reflectivity and the corresponding fluorescence angular scan (background signal subtracted) after the binding of Cy5-labeled antibody. Reaction mixture containing plasmid encoding VSV-pLHCP.

One set of experiments included three cell-free proteins synthesis reactions, containing the plasmid encoding pLHCP with VSV tag at either N- or C-terminus, or reaction containing no DNA template. The fluorescence angular scan after the binding of Cy5-labeled secondary antibody was recorded for each sample and compared. VSV-pLHCP or pLHCP-VSV was synthesized in coupled wheat germ extract systems in the

presence of biotinylated vesicles. After protein synthesis, the reaction mixture was injected into flow cell and incubated on the surface for 30 min. Reaction mixture without added DNA template was included as negative control. The fluorescence angular scan of the as stated three separate experiments was plotted as shown in Figure 3.42. The fluorescence signal of sample containing VSV-pLHCP was considerably higher than that of negative control, where no DNA template was added, indicating that certain amount of synthesized protein were retained on the surface after rinsing. However the fluorescence signal from the sample containing pLHCP-VSV can not be neglected.

There were several possibilities for the proteins to be attached to the surface: (a), proteins were integrated into the lipid bilayer of the supplemented biotinylated vesicles, which could be tethered on the gold surface via streptavidin. However, based on the results of digestion assays and ultracentrifugation assays, the chance for protein integration was low; (b), proteins were associated with other components in the wheat germ extracts, which could be retained on the surface after thorough rinsing. The VSV tag at the terminal site of the proteins was still available for antibody binding, resulting in the positive fluorescence signals. And since the proteins had no uniform orientation on the surface, the VSV tag at either N- or C-terminus was able to be recognized by anti-VSV antibody; (c)
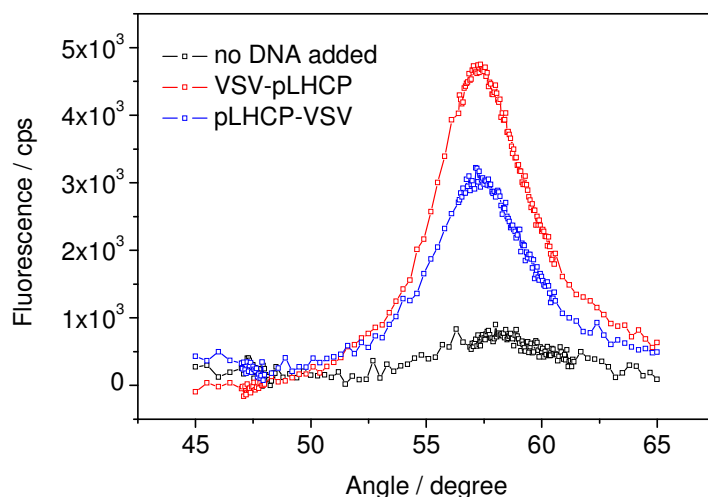
Figure 3.42 Fluorescence angular scan (background signal subtracted) after the binding of Cy5-labeled antibody.

3.7.4 Control experiments

A control experiment was performed to investigate if the positive fluorescence signal in Figure 3.42 was coming from proteins that were associated with the supplemented biotinylated vesicles. VSV-pLHCP was synthesized in the wheat germ extract systems in the absence of biotinylated vesicles. The 50-µL reaction mixture was assembled in plastic tubes and incubated at 30 °C for 90 min. After protein synthesis, the reaction mixture was injected into the flow cell and incubated on the gold surface for 30 min at RT. The gold substrate was coated with biotinyl thiol and streptavidin beforehand as described above. As shown in Figure 3.43, certain amounts of synthesized proteins were still retained to the surface in the absence of biotinylated vesicles. The fluorescence intensity from sample containing VSV-pLHCP was similar to that as shown in Figure 3.42, indicating that the proteins were not integrated into supplemented vesicles, but rather associated with other components present in the wheat germ extract systems. These proteins were randomly oriented, with both N- and C-terminus were accessible to antibody binding.
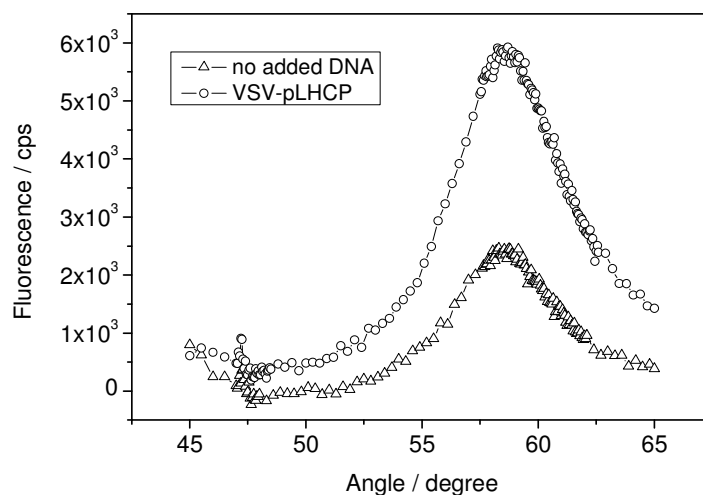
Figure 3.43 Fluorescence angular scan (background signal subtracted) after the binding of Cy5-labeled antibody.

3.8   A close look at the wheat germ extracts

A standard cell-free expression reaction is devoid of substantial amounts of membranes or lipids. Most membrane fragments originating from the lysed cells have been removed by centrifugation steps. However, lipids are not completely depleted [72] and residual amounts of approximately 50–100 µg/mL of extract can be detected. Those lipids might be associated with other proteins and it is not clear whether they are organized in membranes or vesicles [2]. Actually the crude extracts always come with a lot of membrane fragments. Microscopy image as shown in Figure 3.44 clearly indicates the presence of membrane fragments in the wheat germ extract used in this study. The fragments of large sizes sink to the bottom of the chamber in a couple of hours, while lipids in the form of vesicles might also present in the extract, but cannot be viewed with microscope.
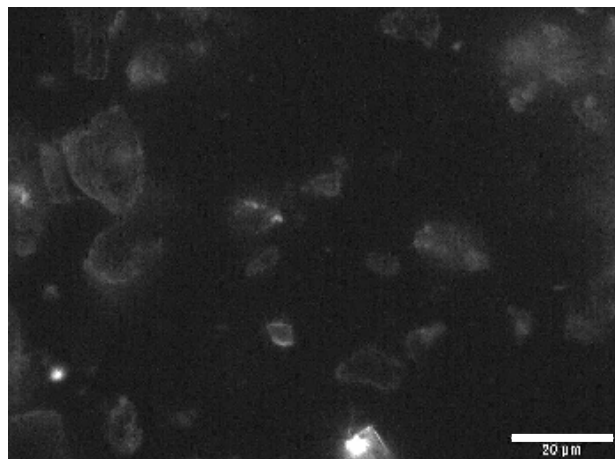
Figure 3.44 Microscopy picture of the rich membrane fragments in wheat germ extracts. The membranes are stained with lipophilic tracer DiD (Invitrogen). Scale bar, 20 µm.

The system is capable of protein synthesis. The membrane fragments may serve as the hrdrophobic environment for the nascent membrane proteins. Results in the digestion assays in section 3.4 clearly showed that proteins synthesized in coupled wheat germ extract systems without added lipid were protected against thermolysin or trypsin treatment. After protein synthesis, the reaction mixture was treated with detergent (OG or DM) before subject to protease treatment. After detergent treatment, the reaction

mixture turned from turbid to clear solution (only judged by naked eye). Digestion of detergent-solubilized reaction mixture generated similar patterns as those of untreated reaction mixture, but with decreased intensity of digestion products. These proteolytic fragments were attributed to the protection of the synthesized proteins by the membranes present in the cell-free expression system.

4 Conclusions

In this thesis, cell-free protein synthesis systems were employed to study the incorporation of the light-harvesting chlorophyll a/b protein (LHCP) into artificial membranes. Closely mimicking the *in vivo* situation, the approach started merely from the genetic information of the protein, so the difficult and time-consuming procedures of conventional protein expression and purification could be avoided. The open nature of cell-free systems allowed the direct supplementation of artificial membranes to the reaction mixture at anytime.

A pea LHCP gene (AB80) was cloned into a suitable vector backbone (pTNT vector) for *in vitro* transcription and translation. Three plasmids encoding precursor LHCP (pLHCP) and three plasmids encoding mature LHCP (mLHCP) were constructed. A VSV epitope tag was engineered to either amino (N-) or carboxyl (C-) terminus of the protein to create a molecular handle for the synthesized protein. The VSV-tagged proteins were mainly detected with western blotting analysis using anti-VSV antibody, while non-tagged proteins were detected with autoradiography. The yield of mLHCP synthesized in a standard 50-µL wheat germ cell-free reaction was determined to be ~100-150 ng.

Synthetic lipid DPPG or purified plant leaf lipids were mainly used to prepare small unilamellar vesicles or giant vesicles as cell membrane mimics. The vesicles or pigment-containing vesicles were added to cell-free protein synthesis reactions in an attempt to provide hydrophobic environment for the nascent proteins. The effect of lipids on the general productivity of the wheat germ expression system was investigated. The addition of DPPG at 0.5 mg·mL^{-1} in the reaction mixture was found to be beneficial to the expression efficiency of both pLHCP and mLHCP. The addition of pigment-containing PG vesicles also promoted the protein yield of wheat germ cell-free protein synthesis. The lipid tolerance level of wheat germ extract system was found to be lot-dependent. The amounts of proteins synthesized in the presence of lipids were promoted to 20%-40% higher than those synthesized in the absence of supplemented lipids. Further increasing the lipid concentration would inhibit the

protein expression of the system. Centrifugation assays indicated that the lipid-assisted synthesized proteins formed precipitates in the expression system. The above results implied that the addition of lipids mainly affect the transcription/translation of the gene, but not the folding of the polypeptide. Without the supplement of required translocation machineries governing the insertion of proteins into membranes such as cpSRP and Alb3, translocation of the synthesized proteins might be hindered.

Proteins expressed *in vitro* with or without supplemented lipids were treated with either thermolysin or trypsin. The digestion products were analyzed by western blotting and autoradiography. After protein synthesis, the reaction mixture was centrifuged at 10,000 g for 15 min. Target proteins were found to be present in both the supernatant and resuspended pellet solution. Proteins in the supernatant part were protease-resistant, while those in the pellet were totally degraded when treated with thermolysin or trypsin. This was not surprising since proteins formed precipitates in the absence of suitable hydrophobic environment and the precipitates were not protease-resistant. A close look of wheat germ extracts under microscope showed that the system came with rich membrane fragments. The effect of detergents on the digestion products was investigated. Proteins were less protected when they were treated with detergents before subject to protease digestion, implying that the proteins were protected by lipids against protease treatment. The digestion assays of proteins synthesized in lipid-free recombinant expression system resulted in total proteins degradation, implying that proteins were not protease-resistant without hydrophobic environment present in the system, which was consistent with the results from wheat germ extract systems.

5 Appendix

5.1 Vector NTI maps of the plasmids

pLHCP-expression plasmids:
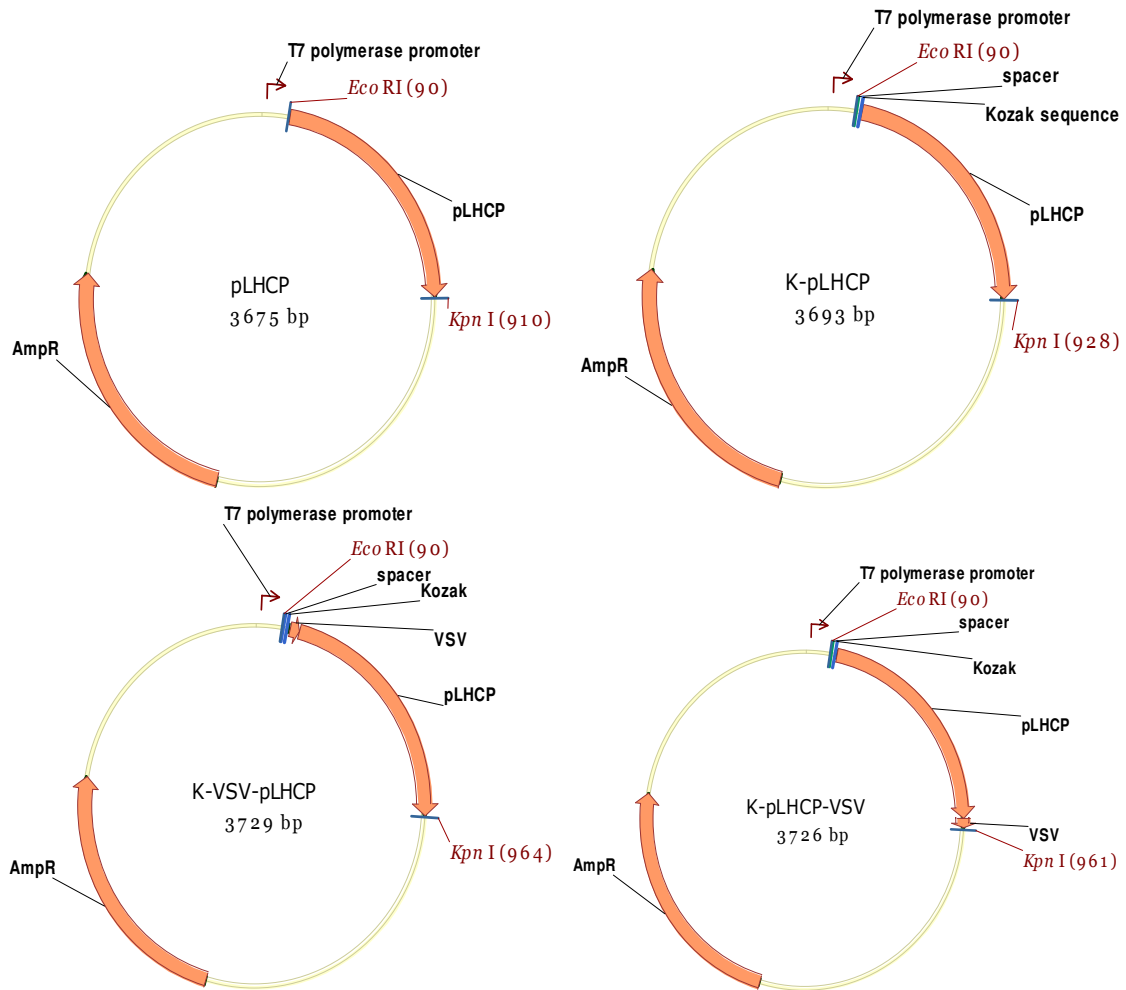
pLHCP (pTNT-insert②): encoding precursor LHCP

K-pLHCP (pTNT-insert③): encoding precursor LHCP

K-VSV-pLHCP (pTNT-insert④): encoding precursor LHCP carrying a VSV tag at N-terminus

K-pLHCP-VSV (pTNT-insert⑤): encoding precursor LHCP carrying a VSV tag at C-terminus

K: Kozak sequence used in place of the ATG start codon

LHCP-expression plasmids:
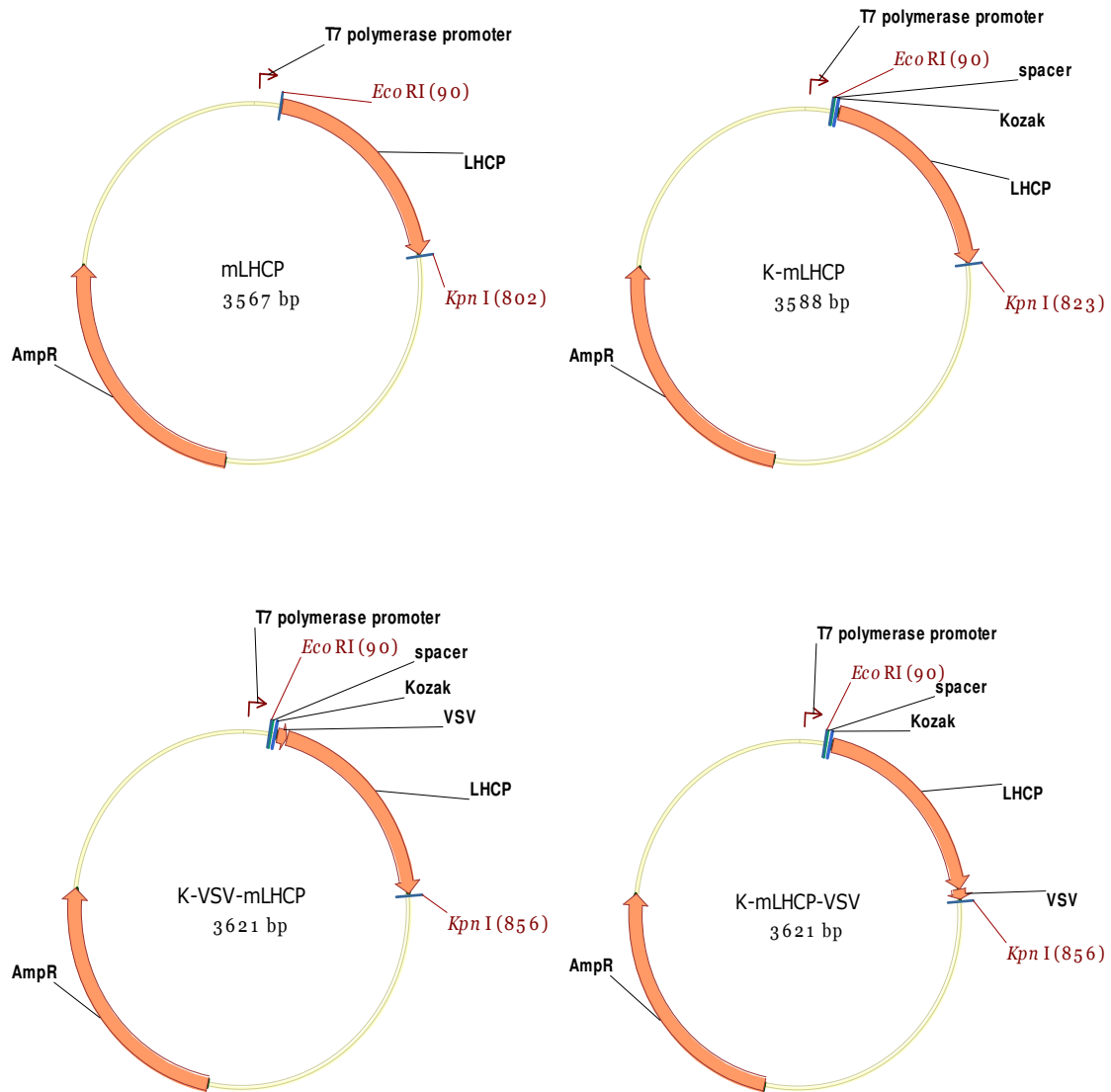
mLHCP (pTNT-insert⑦): encoding mature LHCP

K-mLHCP (pTNT-insert⑧): encoding mature LHCP

K-VSV-mLHCP (pTNT-insert⑨): encoding mature LHCP carrying a VSV tag at N-terminus

K-mLHCP-VSV (pTNT-insert⑩): encoding mature LHCP carrying a VSV tag at C-terminus

K: Kozak sequence used in place of the ATG start codon

5.2 Nucleotide sequence of AB80

```
TCCATGAACG GATTCTAGAA TTGCAAAGAA AATCTCCAAC TAGCCATAGC TTTAGATAAC
ACACGATAAG AGCATCTGCA TTATAAATAC AGACTCATAT TCATCTTACA AAATCACCAT
TGATAAGGAT ACAATTATCA AAAGCATAAC AATCTTTTCA ATTTCATTGC AATATAATAC
ACG ATG GCCG CATCATCATC ATCATCCATG GCTCTCTCTT CTCCAACCTT GGCTGGCAAG
CAACTCAAGC TGAACCCATC AAGCCAAGAA TTGGGAGCTG CAAGGTTCAC C ATG AGGAAG
TCTGCTACCA CCAAGAAAGT AGCTTCCTCT GGAAGCCCAT GGTACGGACC AGACCGTGTT
AAGTACTTAG GCCCATTCTC CGGTGAGTCT CCATCCTACT TGACTGGAGA GTTCCCCGGT
GACTACGGTT GGGACACTGC CGGACTCTCT GCTGACCCAG AGACATTCTC CAAGAACCGT
GAGCTTGAAG TCATCCACTC CAGATGGGCT ATGTTGGGTG CTTTGGGATG TGTCTTCCCA
GAGCTTTTGT CTCGCAACGG TGTTAAATTC GGCGAAGCTG TGTGGTTCAA GGCAGGATCT
CAAATCTTTA GTGAGGGTGG ACTTGATTAC TTGGGCAACC CAAGCTTGGT CCATGCTCAA
AGCATCCTTG CCATATGGGC CACTCAGGTT ATCTTGATGG GAGCTGTCGA AGGTTACCGT
ATTGCCGGTG GGCCTCTCGG TGAGGTGGTT GATCCACTTT ACCCAGGTGG AAGCTTTGAT
CCATTGGGCT TAGCTGATGA TCCAGAAGCA TTCGCAGAAT TGAAGGTGAA GGAACTCAAG
AACGGTAGAT TAGCCATGTT CTCAATGTTT GGATTCTTCG TTCAAGCTAT TGTAACTGGA
AAGGGTCCTT TGGAGAACCT TGCTGATCAT CTTGCAGACC CAGTCAACAA CAATGCATGG
TCATATGCCA CCAACTTTGT TCCCGGAAAA TAA ACACTCT TATATTTATA TGTTTTTGTG
ATAGTAATCT TCTTCCCAAT TCAATGTGAA TTATTATCAT TATCATTATC ATGTGGGTAT
GCATAGGTTC ACTAATACAA GATGATGGAT GCTTTTTTTT TACCAAATTT TAAATTTTAT
GTTTCATGCT TTCCATTGCT AGACAT
```

5.3 Protein sequence of precursor LHCP and LHCP

Signal sequence – 1-36 aa in red

```
         10         20         30         40         50         60
MAASSSSSMA LSSPTLAGKQ LKLNPSSQEL GAARFTMRKS ATTKKVASSG SPWYGPDRVK

         70         80         90        100        110        120
YLGPFSGESP SYLTGEFPGD YGWDTAGLSA DPETFSKNRE LEVIHSRWAM LGALGCVFPE

        130        140        150        160        170        180
LLSRNGVKFG EAVWFKAGSQ IFSEGGLDYL GNPSLVHAQS ILAIWATQVI LMGAVEGYRI

        190        200        210        220        230        240
AGGPLGEVVD PLYPGGSFDP LGLADDPEAF AELKVKELKN GRLAMFSMFG FFVQAIVTGK

        250        260
GPLENLADHL ADPVNNNAWS YATNFVPGK
```

5.4 List of figures

5.5   List of tables

Bibliography

[1]   Nirenberg, M.W., Matthaei, J.H. (1961) The dependence of cell-free protein synthesis in E. coli upon naturally occurring or synthetic polyribonucleotides. Proc. Natl. Acad. Sci. 47, 1588-1602.

[2]   Schwarz, D., Dotsch, V., Bernhard, F. (2008) Production of membrane proteins using cell-free expression systems. Proteomics. 8, 3933-3946.

[3]   Spirin, A.S., Baranov, V.I., Ryabova, L.A., Ovodov, S.Y., Alakhov Y.B. (1988) A Continuous Cell-Free Translation System Capable of Producing Polypeptides in High Yield. Science. 242, 1162-1164.

[4]   Kim, D.M., Choi, C.Y. (1996) A semicontinuous prokaryotic coupled transcription/translation system using a dialysis membrane. Biotechnol. Prog. 12, 645-649.

[5]   Kigawa, T., Yabuki, T., Matsuda, N., Matsuda, T., Nakajima, T., Tanaka, A., Yokoyama, S. (2004) Preparation of Escherichia coli cell extract for highly productive cell-free protein expression. J. Struct. Funct. Genomics. 5, 63–68.

[6]   Sawasaki, T., Ogasawara, T., Morishita, R., Endo, Y. (2002) A cell-free protein synthesis system for high-throughput proteomics. Proc. Natl. Acad. Sci. USA. 99, 14652-14657.

[7]   Spirin, A.S., Swartz, J.R. (2008) Cell-free protein synthesis: methods and protocols. Wiley-VCH Verlag GmbH & Co.

[8]   Shimizu, Y., Inoue, A., Tomari, Y., Suzuki, T., Yokogawa, T., Nishikawa, K., Ueda, T. (2001) Cell-free translation reconstituted with purified components. Nat. Biotechnol. 19, 751-755.

[9]   Jackson, A.M., Boutell, J., Cooley, N., He, M.Y. (2004) Cell-free protein synthesis for proteomics. Brief Funct. Genomic. Proteomic. 2. 308-319.

[10]   Trbovic, N., Klammt, C., Koglin, A., Lohr, F., Bernhard, F., Dotsch, V. (2005) Efficient strategy for the rapid backbone assignment of membrane proteins. J. Am. Chem. Soc. 127, 13504-13505.

[11]   Katzen, F.; Chang, G.; Kudlicki, W. (2005) The past, present and future of cell-free protein synthesis. Trends Biotechnol. 23, 150-156.

[12]   Klammt, C., Lohr, F., Schafer, B., Haase, W., Dotsch, V., Ruterjans, H., Glaubitz, C., Bernhard, F. (2004) High level cell-free expression and specific labeling of integral membrane proteins. Eur. J. Biochem. 271, 568-580.

[13]   Klammt, C., Schwarz, D., Fendler, K., Haase, W., Dotsch, V., Bernhard, F. (2005) Evaluation of detergents for the soluble expression of alpha-helical and beta-barrel-type integral membrane proteins by a preparative scale individual cell-free expression system. FEBS J. 272, 6024-6038.

[14]   Seddon, A.M., Curnow, P., Booth, P.J. (2004) Membrane proteins, lipids and detergents: not just a soap opera. BBA-Biomembranes. 1666, 105-117.

[15]   Katzen, F., Peterson, T.C., Kudlicki, W. (2009) Membrane protein expression: no cells required. Trends Biotechnol. 27, 455-460.

[16]   Wuu, J.J., Swartz, J.R. (2008) High yield cell-free production of integral membrane proteins without refolding or detergents. BBA-Biomembranes. 1778, 1237-1250.

[17]   Kalmbach, R., Chizhov, I., Schumacher, M.C., Friedrich, T., Bamberg, E., Engelhard, M. (2007) Functional cell-free synthesis of a seven helix membrane protein: in situ insertion of bacteriorhodopsin into liposomes. J. Mol. Biol. 371, 639–64.

[18] Nozawa, A., Nanamiya, H., Miyata, T., Linka, N., Endo, Y., Weber, A.P.M., Tozawa, Y. (2007) A cell-free translation and proteoliposome reconstitution system for functional analysis of plant solute transporters. Plant Cell Physiol. 48, 1815-1820.

[19] Moritani, Y., Nomura, S.M., Morita, I., Akiyoshi, K. (2010) Direct integration of cell-free-synthesized connexin-43 into liposomes and hemichannel formation. FEBS J. 277, 3343-3352.

[20] Nomura, S.I.M., Kondoh, S., Asayama, W., Asada, A., Nishikawa, S., Akiyoshi, K. (2008) Direct preparation of giant proteo-liposomes by in vitro membrane protein synthesis. J. Biotechnol. 133, 190-195.

[21] Kaneda M, Nomura SM, Ichinose S, Kondo S, Nakahama K, Akiyoshi K, Morita I. (2009) Direct formation of proteo-liposomes by in vitro synthesis and cellular cytosolic delivery with connexin-expressing liposomes. Biomaterials. 30, 3971-3977.

[22] Robelek, R., Lemker, E.S., Wiltschi, B., Kirste, V., Naumann, R., Oesterhelt, D., Sinner, E.K. (2007) Incorporation of in vitro synthesized GPCR into a tethered artificial lipid membrane system. Angew. Chem. Int. Ed., 46, 605-608.

[23] Dreyfuss, B.W., Thornber, J.P. (1994) Assembly of the light-harvesting complexes (LHCs) of photosystem II. Monomeric LHCIIb complexes are intermediates in the formation of oligomeric LHCIIb complexes. Plant Physiol. 106, 829-839.

[24] Kuhlbrandt, W., Wang, D.N., Fujiyoshi, Y. (1994) Atomic model of plant light-harvesting complex by electron crystallography. Nature. 367, 614-621.

[25] Liu, Z.F., Yan, H.C., Wang, K.B., Kuang, T.Y., Zhang, J.P., Gui, L.L., An, X.M., Chang, W.R. (2004) Crystal structure of spinach major light-harvesting complex at 2.72 angstrom resolution. Nature. 428, 287-292.

[26] Standfuss, J., van Scheltinga, A.C.T., Lamborghini, M., Kuhlbrandt, W. (2005) Mechanisms of photoprotection and nonphotochemical quenching in pea light-harvesting complex at 2.5Å resolution. EMBO J. 24, 919-928.

[27] Allen, J.F. (2003) State transitions – a question of balance. Science. 299, 1530-1532.

[28] Mullet, J.E. (1983) The amino acid sequence of the polypeptide segment which regulates membrane adhesion (grana stacking) in chloroplasts. J. Biol. Chem. 258, 9941-9948.

[29] Abdallah, F., Salamini, F., Leister, D. (2000) A prediction of the size and evolutionary origin of the proteome of chloroplasts of Arabidopsis. Trends Plant Sci. 5, 141-142.

[30] Di Cola, A., Klostermann, E., Robinson, C. (2005) The complexity of pathways for protein import into thylakoids: it's not easy being green. Biochem. Soc. T. 33, 1024-1027.

[31] Schunemann, D. (2007) Mechanisms of protein import into thylakoids of chloroplasts. Biol. Chem. 388, 907-915.

[32] Keegstra, K., Cline, K. (1999) Protein Import and Routing Systems of Chloroplasts. Plant Cell. 11, 557-570.

[33] Jarvis, P., Robinson, C. (2004) Mechanisms of protein import and routing in chloroplasts. Curr. Biol. 14, 1064-1077.

[34] Sundberg, E., Slagter, J.G., Fridborg, I., Cleary, S.P., Robinson, C., Coupland, G. (1997) ALBINO3, an Arabidopsis nuclear gene essential for chloroplast differentiation, encodes a chloroplast protein that shows homology to proteins present in bacterial membranes and yeast mitochondria. Plant Cell. 9, 717-730.

[35] Plumley, F.G., Schmidt, G.W. (1987) Reconstitution of chlorophyll a/b light-harvesting complexes: xanthophylls-dependent assembly and energy transfer. Proc. Natl. Acad. Sci. USA. 84, 146-150.

[36] Paulsen, H., Rümler, U., Rüdiger, W. (1990) Reconstitution of pigment-containing complexes from light-harvesting chlorophyll a/b-binding protein overexpressed in Escherichia coli. Planta. 181, 204–211.

[37] Booth, PJ; Paulsen, H. (1996) Assembly of light-harvesting chlorophyll a/b complex in vitro. Time-resolved fluorescence measurements. Biochemistry. 35, 5103-5108.

[38] Horn, R., Grundmann, G., Paulsen, H. (2007) Consecutive binding of chlorophylls a and b during the assembly in vitro of light-harvesting chlorophyll-a/b protein (LHCIIb). J. Mol. Biol. 366, 1045-1054.

[39] Heinemann, B., Paulsen, H. (1999) Random mutations directed to transmembrane and loop domains of the light-harvesting chlorophyll alb protein: Impact on pigment binding. Biochemistry. 38, 14088-14093.

[40] Mick V, Eggert K, Heinemann B, Geister S, Paulsen H. (2004) Single amino acids in the lumenal loop domain influence the stability of the major light-harvesting chlorophyll alb complex. Biochemistry. 43, 5467-5473.

[41] Hobe, S., Fey, H., Rogl, H., Paulsen, H. (2003) Determination of relative chlorophyll binding affinities in the major light-harvesting chlorophyll a/b complex. J. Biol. Chem. 278, 5912-5919.2003

[42] Cline, K. (1986) Import of proteins into chloroplasts – membrane integration of a thylakoid precursor protein reconstituted in chloroplast lysates. J. Biol. Chem. 261, 4804-4810.

[43] Schmidt, G.W., Bartlett, S. G., Grossman, A.R., Cashmore, A.R., Chua, N.H. (1981) Biosynthetic pathways of two polypeptide subunits of the light-harvesting chlorophyll a/b protein complex. J. Cell Biol., 91, 468-478.

[44] Field, J., Nikawa, J., Broek, D., macDonald, B., Rodgers, L., Wilson, I.A., Lerner, R.A., Wigler, M. (1988) Purification of a Ras-responsive adenylyl cyclase complex from saccharomyces-cerevisiae by use of an epitope addition method. Mol. Cell Biol. 8, 2159-2165.

[45] Kreis, T.E., Lodish, H.F. (1986) Oligomerization is essential for transport of vesicular stomatitis viral glycoprotein to the cell-surface. Cell, 46, 929-937.

[46] Robelek, R., Lemker, E. S., Wiltschi, B., Kirste, V., Naumann, R., Oesterhelt, D, Sinner, E. K. (2007) Incorporation of in vitro synthesized GPCR into a tethered artificial lipid membrane system. Angew. Chem. Int. Ed., 46, 605-608.

[47] Technical bulletin for pTNTTM Vector (Promega, L5610).

[48] Cashmore, A. R. (1984) Structure and expression of a pea nuclear gene encoding a chlorophyll a/b-binding polypeptide. Proc. Natl. Acad. Sci., 81, 2960-2964.

[49] Kozak, M. (1987) An analysis of 5'-noncoding sequences from 699 vertebrate messenger RNAs. Nucleic Acids Res., 15, 8125-8148.

[50] Douce, R., Joyard, J. (1996) Biosynthesis of thylakoid membrane lipids. In Advances in photosynthesis, vol 4. Oxygenic photosynthesis: the light reactions. Edited by Ort DR, Yocum CF. Dordrecht: Kluwer Academic Publishers; 69-101.

[51] Lipid in photosynthesis: essential and regulatory functions. (2009) Edited by Wada, H., Murata, N. Springer.

[52] Podo, F., Cain, J.E., Blasie, J.K. (1976) Structural and dynamical studies of mixed chlorophyll/phosphatidylcholine bilayers via X-ray diffraction, absorption polarization spectroscopy and nuclear magnetic resonance. Biochimica et Biophysica Acta. 419, 19-41.

[53] Murata, N., Sato, N. (1978) Studies on the absorption spectra of chlorophyll a in aqueous dispersions of lipids from the photosynthetic membranes. Plant Cell Physiol., 19, 401-410.

[54] Rodriguez, N., Pincet, F., Cribier, S. (2005) Giant vesicles formed by gentle hydration and electroformation: A comparison by fluorescence microscopy. Colloids Surf. B, 42, 125-130.

[55] Walde, P., Cosentino, K., Engel, H., Stano, P. (2010) Giant vesicles: preparation and applications. ChemBioChem, 11, 848-865.

[56] Schwille, P., Diez, S. (2009) Synthetic biology of minimal systems. Crit. Rev. Biochem. Mol., 44, 232-242.

[57] Stamou, D., Duschl, C., Delamarche, E., Vogel, H. (2003) Self-assembled microarrays of attoliter molecular vessels. Angew. Chem. Int. Ed., 42, 5580-5583.

[58] Lohse, B., Bolinger, P.-Y., Stamou, D. (2008) Encapsulation Efficiency Measured on Single Small Unilamellar Vesicles. J. Am. Chem. Soc. 130, 14372-14373.

[59] Jung, L. S., Shumaker-Parry J. S., Campbell, C. T., Yee, S. S., Gelb, M. H. (2000) Quantification of tight binding to surface-immobilized phospholipid vesicles using surface plasmon resonance: binding constant of phospholipase A2. J. Am. Chem. Soc. 122, 4177-4184.

[60] Spinke, J., Liley, M., Schmitt, F. J., Guder, H. J., Angermaier, L., Knoll, W. (1993) Molecular recognition at self-assembled monolayers - optimization of surface functionalization. J. Chem. Phys., 99, 7012-7019.

[61] Yu, F. (2004) Surface plasmon fluorescence spectroscopy and surface plasmon diffraction in biomolecular interaction studies. PhD dissertation. Max-Planck Institute for polymer Research, Mainz.

[62] Instruction Manual of PURExpress™ *In Vitro* Protein Synthesis kit (NEB, E6800S).

[63] Laskey, R.A. Review 23: Efficient detection of biomolecules by autoradiography, fluorography or chemiluminescence. Amersham Life Science.

[64] Circolo, A., Gulati, S. (2002) Autoradiography and Fluorography of Acrylamide gels. The protein protocols handbook, part II, second edition. Gumana Press.

[65] Knoll, W. (1998) Interfaces and thin films as seen by bound electromagnetic waves. Annu. Rev. Phys. Chem. 49, 569–638.

[66] Barnes, W. L., Dereux, A., Ebbesen, T. W. (2003) Surface plasmon subwavelength optics. Nature. 424, 824-830.

[67] Kambhampati, D. K., Knoll, W. (1999) Surface-plasmon optical techniques. Curr. Opin. Colloid In., 4, 273-280.

[68] Liebermann, T., Knoll, W. Surface-plasmon field-enhanced fluorescence spectroscopy. (2000) Colloid Surface A. 171, 115-130.

[69] Yu, F., Yao, D., Knoll, W. (2003) Surface plasmon field-enhanced fluorescence spectroscopy studies of the interaction between an antibody and its surface-coupled antigen. Anal. Chem. 75, 2610-2617.

[70] Christensen, S.M.; Stamou, D. (2007) Surface-based lipid vesicle reactor system: fabrication and applications. Soft Matter. 3, 828–836.

[71] Kosemund, K., Geiger, I., Paulsen, H. (2000) Insertion of light-harvesting chlorophyll a/b protein into the thylakoid – topographical studies. Eur. J. Biochem. 267, 1138-1145.

[72] Goren, M. A, Fox, B. G. (2008) Protein Express. Purif. 62, 171-178.

[73] Bui, H.T., Umakoshi, H., Ngo, K.X., Nishida, M., Shimanouchi, T., Kuboi, R. (2008) Lipsome membrane itself can affect gene expression in the Escherichia coli cell-free translation system. Langmuir. 24, 10537-10542.

[74] Cline, K. (1986) Import of proteins into chloroplasts – membrane integration of a thylakoid precursor protein reconstituted in chloroplast lysates. J. Biol. Chem. 261, 14804-14810.

[75] Fulson, D.R., Cline, K. (1988) A soluble protein factor is required in vitro for membrane insertion of the thylakoid precursor protein, pLHCP. Plant Physiol. (1988) 88, 1146-1153.

[76] Kuttkat, A., Grimm, R., Paulsen, H. (1995) Light-harvesting chlorophyll a/b-binding protein inserted into isolated thylakoids binds pigments and is assembled into trimeric light-harvesting complex. Plant Physiol., 109, 1267-1276.

[77] Cline, K. (1988) Light-harvesting chlorophyll a/b protein. Membrane insertion, proteolytic processing, assembly into LHCII, and localization to appressed membranes occurs in chloroplast lysates. Plant Physiol. 86, 1120-1126.

[78] Reed, J.E., Cline, K., Stephens, L.C., Bacot, K.O., Viitanen, P.V. (1990) Early events in the import assembly pathway of an integral thylakoid protein. Eur J Biochem., 194, 33-42.

[79] URL: www.expasy.ch/tools/peptide-mass.html

[80] URL: www.expasy.org/tools/peptidecutter/